Cloning and functional characterization of seven novel members of the peptide gated sodium channel family (HyNaC) in *Hydra magnipapillata*

Von der Fakultät für Mathematik, Informatik und Naturwissenschaften der RWTH Aachen University zur Erlangung des akademischen Grades eines Doktors der Naturwissenschaften genehmigte Dissertation

vorgelegt von

Master of Science
Marc Christopher Assmann
aus Gießen

Berichter:

Universitätsprofessor Dr. rer. nat. Stefan Gründer
Universitätsprofessor Dr. rer. nat. Marc Spehr

Tag der mündlichen Prüfung: 15.07.2014

Diese Dissertation ist auf den Internetseiten der Hochschulbibliothek online verfügbar.

Contents

List of Figures

List of Tables

Summary

The peptide gated sodium channel (HyNaC) from the freshwater polyp *Hydra magnipapillata* forms a heterotrimeric ion channel consisting of the subunits HyNaC2/3/5. It is directly activated by the endogenously expressed neuropeptides Hydra-RFamide I and II. HyNaC belongs to the DEG/ENaC ion channel superfamily, a group of ion channels that all share highly conserved structures and a selectivity for sodium. In addition, HyNaC2/3/5 has been found to be highly permeable for calcium.

This work describes cloning and characterization of seven novel members of the HyNaC subfamily, HyNaC6 - HyNaC12. A phylogenetic analysis illustrated that all HyNaC subunits, except HyNaC12, show a high degree of sequence homology. Furthermore HyNaC2 - HyNaC11 are closely related to ASIC and BASIC, forming a monophyletic group inside the DEG/ENaC superfamily. Similar to HyNaC2/3/5, the newly cloned HyNaC subunits 6 - 11 formed functional heterotrimers. Based on sequence homology the HyNaC subunits can be divided into two subgroups. HyNaC3, HyNaC4 and HyNaC8 - HyNaC11 form the first subgroup, whereas HyNaC2 and HyNaC5 - HyNaC7 form the second one. HyNaC2 is the crucial subunit, which is part of every functional heterotrimer. In addition to HyNaC2, one representative of each of the two subgroups is needed to form a functional heterotrimeric ion channel. HyNaC12 is isolated from the other HyNaC subunits and so far has not been shown to form a functional ion channel. Despite the close phylogenetic distance between HyNaCs, ASICs and BASICs, no functional homotrimeric HyNaC could be identified. Every HyNaC was activated by Hydra-RFamides I and II and by lowering the extracellular calcium concentration. Hydra-RFamides III to V failed to activate HyNaCs, as it had been described previously for HyNaC2/3/5. Interestingly all HyNaCs formed unselective cation channels, which showed a high permeability for calcium. *In situ* hybridizations showed that HyNaC subunits are expressed at the tentacle basis, the penduncle region and, for HyNaC8 and HyNaC9, along the whole body column of *H. magnipapillata*. An expression at the tentacle basis was previously described for HyNaC2 - HyNaC5, suggesting a role in tentacle movement.

Most of the new HyNaCs revealed an up to hundred-times higher affinity for Hydra-RFamide I than HyNaC2/3/5. Since HyNaC2/3/7 showed an about twenty times higher apparent ligand affinity than HyNaC2/3/5, the subunit HyNaC7 must be responsible for the increased ligand affinity. By systematically swapping parts between HyNaC5 and HyNaC7, the second transmembrane domain and adjacent amino acids were identified

to cause the higher affinity of HyNaC2/3/7.

A hallmark of the DEG/ENaC ion channel superfamily is the inhibition by the diuretic amiloride. But the affinity of HyNaC2/3/5 for amiloride is low with an IC_{50} at 120 μM. In this work it could be demonstrated that the diarylamidine diminazene inhibits HyNaCs in the nanomolar range. In previous *in vivo* experiments an application of amiloride inhibited the feeding response in *H. magnipapillata*, presumably by inhibiting HyNaC activity. Taking the expression pattern of HyNaC2/3/5 into account this finding suggested that HyNaCs are expressed in neuromuscular cells involved in feeding reaction. *In vivo* experiments in this work showed that diminazene also inhibits the feeding response, supporting the previous findings.

Taken together, HyNaCs form a variety of peptide gated cation channels with a high permeability for calcium. Considering the expression pattern, HyNaCs might not exclusively play a role in tentacle movement but also in other physiological processes.

Zusammenfassung

Der peptid-aktivierte Natriumkanal (HyNaC) aus dem Süßwasserpolypen *Hydra magnipapillata* bildet heterotrimere Ionenkanäle aus den Untereinheiten HyNaC2/3/5. Dieser Kanal wird direkt aktiviert durch die endogen exprimierten Neuropeptide Hydra-RFamid I und II. HyNaC gehört zu der Ionenkanal Superfamilie DEG/ENaC, die sich durch eine hoch konservierte Struktur und eine selektive Leitfähigkeit für Natrium auszeichnet. Es konnte zudem gezeigt werden, dass HyNaC hoch permeabel für Calcium ist.

Diese Arbeit beschreibt die Klonierung und Charakterisierung sieben weiterer Mitglieder der HyNaC Subfamilie, HyNaC6 - HyNaC12. Mittels phylogenetischer Analyse konnte gezeigt werden, dass alle HyNaC Untereinheiten, mit Ausnahme von HyNaC12, ein hohes Maß an Sequenz-Homologie aufweisen. Zudem zeichnet sich die Subfamilie HyNaC durch einen hohen Verwandtschaftsgrad zu den Subfamilien ASIC und BASIC aus. Innerhalb der DEG/ENaC Superfamilie formen HyNaCs, ASICs und BASICs eine monophyletische Gruppe. Entsprechend zu HyNaC2/3/5 bildeten die neu klonierten HyNaC Untereinheiten 6 - 11 heterotrimere Ionenkanäle. Basierend auf den Ergebnissen dieser Arbeit lassen sich die Untereinheiten der HyNaC Subfamilie in zwei Untergruppen unterteilen. Die erste Untergruppe beinhaltet die Untereinheiten HyNaC3, HyNaC4 und HyNaC8 - HyNaC11, die zweite Untergruppe wird durch HyNaC2 und HyNaC5 - HyNaC7 gebildet. Die Anwesenheit von HyNaC2 ist zwingend erforderlich um einen funktionalen heterotrimeren Kanal zu bilden. Für einen funktionalen Kanal muss zusätzlich zu HyNaC2 je ein Mitglied aus einer der beiden Untergruppen vertreten sein. HyNaC12 hingegen ist isoliert von den anderen HyNaC Untereinheiten und die Bildung eines funktionalen Ionenkanals konnte für HyNaC12 bisher nicht gezeigt werden. Die Entstehung homotrimerer Kanäle durch eine der neuen HyNaC Untereinheiten konnte, trotz der nahen Verwandtschaft zu ASICs und BASICs, nicht gezeigt werden. Alle HyNaCs konnten durch Hydra-RFamid I und II sowie durch eine Reduktion der extrazellulären Calcium-Konzentration aktiviert werden. Hydra-RFamid III bis V hingegen aktivierten HyNaCs nicht, wie es bereits für HyNaC2/3/5 beschrieben worden war. Es konnte zudem gezeigt werden, dass ebenso wie HyNaC2/3/5 alle weiteren HyNaCs unselektive Kationenkanäle mit einer hohen Permeabilität für Calcium bilden. Eine *in situ* Hybridisierung in *H. magnipapillata* ergab, dass HyNaC Untereinheiten sowohl in der Tentakelregion als auch dem Pedunkel exprimiert werden. Weiterhin konnte eine Expression für HyNaC8 und HyNaC9 entlang der gesamten Körperachse gezeigt werden. Eine Expression von HyNaC2/3/5 an der Tentakelbasis wurde

bereits in früheren Arbeiten gezeigt. Damit eröffnet der Nachweis neuer HyNaC Expressionsmuster weitere physiologische Bedeutungen für HyNaCs *in vivo*. Der Großteil der neu klonierten HyNaC Untereinheiten bildete Ionenkanäle mit einer bis zu hundertfach höheren Affinität für Hydra-RFamid I als HyNaC2/3/5. Da HyNaC2/3/5 und HyNaC2/3/7 sich nur in einer Untereinheit unterscheiden, HyNaC2/3/7 jedoch eine zwanzig-fach höhere Ligandenaffinität zeigt, wurde HyNaC7 für diesen Effekt verantworlich gemacht. Ein systematischer Austausch von Sequenzen zwischen HyNaC5 und HyNaC7 zeigte, dass die zweite Transmembrandomäne sowie angrenzende Aminosäuren die höhere Ligandenaffinität von HyNaC7 hervorrufen.

Ein Markenzeichen der DEG/ENaC Ionenkanal Superfamilie ist die Inhibition durch Amilorid. Die Affinität für Amilorid von HyNaC2/3/5 ist jedoch gering mit einem IC_{50} im Bereich von 120 μM. In dieser Arbeit konnte gezeigt werden, dass das Diarylamidin Diminazen HyNaCs bereits im nanomolaren Bereich inhibiert. In früheren *in vivo* Experimenten konnte bereits gezeigt werden, dass Amilorid den Beutefangreflex von *H. magnipapillata*, vermutlich durch die Inhibition von HyNaC Aktivität, unterdrückt. *In vivo* Experimente, die im Rahmen dieser Arbeit mit Diminazen durchgeführt wurden, zeigten ebenso eine Inhibition des Beutefangreflexes. Dies bestätigt frühere Erkenntnisse aus den Amilorid-Versuchen.

Zusammenfassend lässt sich sagen, dass HyNaCs eine Vielzahl Peptid-aktivierter Kationenkanäle mit einer hohen Permeabilität für Calcium bilden. Betrachtet man das Expressionsmuster, dürften HyNaCs nicht nur an der Tentakelbewegung sondern auch an anderen physiologischen Prozessen beteiligt sein.

Danksagung

Zuallererst möchte ich meinem Doktorvater Prof. Dr. Stefan Gründer danken: für die Bereitstellung dieses spannenden Themas, für die sehr gute wissenschaftliche Betreuung und dass du immer ein offenes Ohr für mich hattest, falls mal etwas nicht so lief, wie geplant. Die letzten drei Jahre in deinem Labor waren eine sehr schöne Zeit, in der ich viel lernen konnte und an die ich mit Sicherheit in meiner weiteren beruflichen Laufbahn sehr gerne zurückdenken werde.

Auch unserem Kooperationspartner Prof. Dr. Holstein und seinem Team möchte ich für die Bereitstellung von Material sowie für die *in situ* Hybridisierungen danken. Aus Ihrem Team möchte ich namentlich vor allem Frau Anne Kuhn hervorheben, da sie die sehr schönen *in situ* durchgeführt hat.

Herrn Prof. Dr. Spehr aus der AG Chemosensorik gebührt mein besonderer Dank dafür, dass er sich als Zweitgutachter meiner Doktorarbeit zur Verfügung gestellt hat und dass er mir im Laufe meiner Doktorarbeit mit konstruktiver Kritik stets ein gutes Feedback gegeben hat.

Weiterhin bedanken möchte ich mich natürlich bei meinen wissenschaftlichen Kollegen, Cati, Heike, Pia, Stefan, Katrin, Axel, Daniel, Barbara, Niko, Verena, Silke, Anna und Georg sowie unseren TA's Steffi, Hilde, Rosi, Hannelore, Adrienne und Monika. Dominik, dir gilt mein besonderer Dank, da du mir stets mit konstruktiver Kritik weitergeholfen hast und dich bereit erklärt hast meine Dissertation Korrektur zu lesen. Es war wirklich eine schöne Zeit mit euch und ich bin froh so tolle Kollegen wie euch gehabt zu haben.

Ganz besonderer Dank gilt jedoch meiner Familie und meiner Freundin Katharina. Kathi, ich danke dir dafür, dass du immer für mich da warst. Durch dich habe ich die nötige Kraft gefunden, die letzten Jahre meiner Doktorarbeit so gut zu meistern. Meinen Eltern Volkmar und Renate, meiner Schwester Mirjam sowie meiner Großmutter Erika möchte ich dafür danken, dass ihr mir stets das Gefühl von Heimat bewahrt habt. Nach Hause zu kommen gab mir immer wieder Kraft und Zuversicht, sowohl zu Schulzeiten, im Studium als auch während meiner Doktorarbeit. Ohne euch wäre ich sicher nicht dort wo ich heute stehe.

1. Introduction

1.1. The cell and its connection to the environment

1.1.1. An isolated system: The cell

All cells, prokaryotic as well as eukaryotic, are compartments surrounded by a lipid bilayer, which separates them from their environment. This bilayer is formed by phospholipids that contain a hydrophilic head and a hydrophobic tail. The lipid bilayer is impermeable for polar substances like ions or charged molecules. The impermeability of the lipid bilayer for charged substances allows an imbalance of substances across the cell membrane. Under physiological conditions, a high concentration of potassium is found inside the cell, whereas sodium, chloride and calcium are found in high concentrations outside the cell.

This imbalance of ions generates a chemical gradient for each ion across the cell membrane. Together with negatively charged proteins and the DNA inside the cell, this imbalance of ions also generates an electric gradient, resulting in a negatively charged cell. Cells are living organisms and thus rely on transport processes between the extracellular space and the cytoplasm. But since the cell membrane is impermeable for charged substances, specified transport proteins are necessary in the cell membrane.

1.1.2. Transport proteins, gates through the cell membrane

To overcome the problem of impermeability, every cell synthesizes transport proteins that are integrated into the cell membrane. These proteins span the cell membrane and form a gate between the intracellular cytoplasm and the extracellular space. Two types of transmembrane transport processes can be distinguished: active and passive transport.

The active transport is an energy consuming process because it acts against electrical and/or chemical gradients. One of the most prominent active transporters is the Na/K-ATPase. While consuming ATP, this protein transports sodium out of the cell and

potassium into the cell. Active transporters are required to create the imbalance of ions across the cell membrane. The chemical and electric gradient generated by this imbalance is the driving force for the passive transport.

The passive transport describes the diffusion of charged substances through passive transport proteins following a chemical and/or electric gradient. Passive transport proteins are gates that allow the passive migration across the cell membrane by forming a pore. One type of passive transporters are ion channels. Ion channels play a crucial role in cell physiology.

1.1.3. The biophysical properties of ion channels

Ion channels can be divided into different subtypes: (I) constitutively open ion channels that continously conduct ions across cell membranes and (II) gated channels that have to be activated by a stimulus. The stimulus that leads to the opening of an ion channel can be a mechanic activation, an electric activation by a change in membrane potential, ligand binding, phosphorylation by an inctracellular kinase and other post-translational modifications.

Many ion channels have a certain permeability for only one type of ion, others are permeable for two or more ions. Moreover, some ion channels show current rectification. Inwardly rectifying channels show a greater conductance for inward currents (influx of cations or outflow of anions) than outward currents. For outwardly rectifying channels it is the other way round.

Sodium channels normally conduct sodium ions into the cell, resulting from the high chemical and electric gradient for sodium from the extracellular space to the cytoplasm. The influx of positively charged sodium into the negatively charged cell causes depolarization of the cell and reduces the electric driving force. Additionally, the influx of sodium increases the intracellular sodium concentration reducing the chemical driving force. At a certain membrane potential, the direction of the ion flow changes. This is called the reversal potential.

1.1.4. The physiological role of ion channels

Ion channels are necessary for a broad range of physiological processes and only two aspects will be discussed here, because they are associated with the ion channel family this work is based on. Ion channels are crucial for osmotic balance in the single cell as well as for whole multicellular organisms. The permeation of ions across epithelial

cells is involved in the generation of an osmotic gradient that regulates the movement of water across epithelia [70], for example in the colon or the kidney.

Furthermore ion channels are crucial for the generation and transmission of electric signals in neuronal cells. The signal transmission of the nervous system is based on voltage-controlled ion channels, whereas the signal transduction at the neuronal synapse is generated by ligand gated ion channels. In the peripheral nervous system (PNS) ion channels are necessary for the perception of environmental stimuli like taste, smell, touch, sound and sight. These signals are transported to the central nervous system, called afferent neuronal signalling. In contrast, efferent signals from the central nervous system are transmitted to the neuromuscular junction, where it controls muscle contractions by depolarization of the muscle cell postsynaptic membrane [65].

A family of ion channels that is present in epithelia as well as in the nervous system is the degenerin/epithelial Na^+ channel (DEG/ENaC) ion channel family.

1.2. The DEG/ENaC ion channel family

The DEG/ENaC ion channel family is a large family formed by a group of ion channels that share conserved molecular structures and biophysical properties. They are found in different phyla of the animal kingdom ranging from insects over birds, molluscs and fishes to mammals (figure 1.1). It is a family of voltage independent cation channels that mainly conduct sodium, and as a hallmark are blocked by amiloride [70]. Members of the DEG/ENaC ion channel family are exclusively found in multicellular metazoan organisms. This ion channel family contains seven subfamilies: the epithelial sodium channel **ENaC**, the acid sensing ion channels **ASIC**s and the bile acid sensitive ion channel **BASIC** from vertrebrates, the **PPK** (pickpocket) channel from *Drosophila spp.*, the **degenerins** from the worm *Caenorhabditis elegans*, the FMRFamide activated sodium channel **FaNaC** from snails and the peptide gated sodium channel **HyNaC** from *Hydra magnipapillata* [70]. Members of the DEG/ENaC ion channel family show a variety in expression patterns, physiological roles and activating stimuli. This ion channel family includes constitutively open as well as gated channels. Gated DEG/ENaC channels are activated by different mechanisms, like mechanical stimuli and ligand binding. Members of this ion channel family are expressed in epithelial cells, muscle cells and neurons and are responsible for mechanosensation, salt reabsorption, chemosensation, nociception and neuronal function [70].

In humans, some members of this ion channel family are linked to severe diseases,

like the Liddle's syndrome or psychiatric and neuronal disorders [97] illustrating the importance of the DEG/ENaC ion channel family for multicellular organisms.

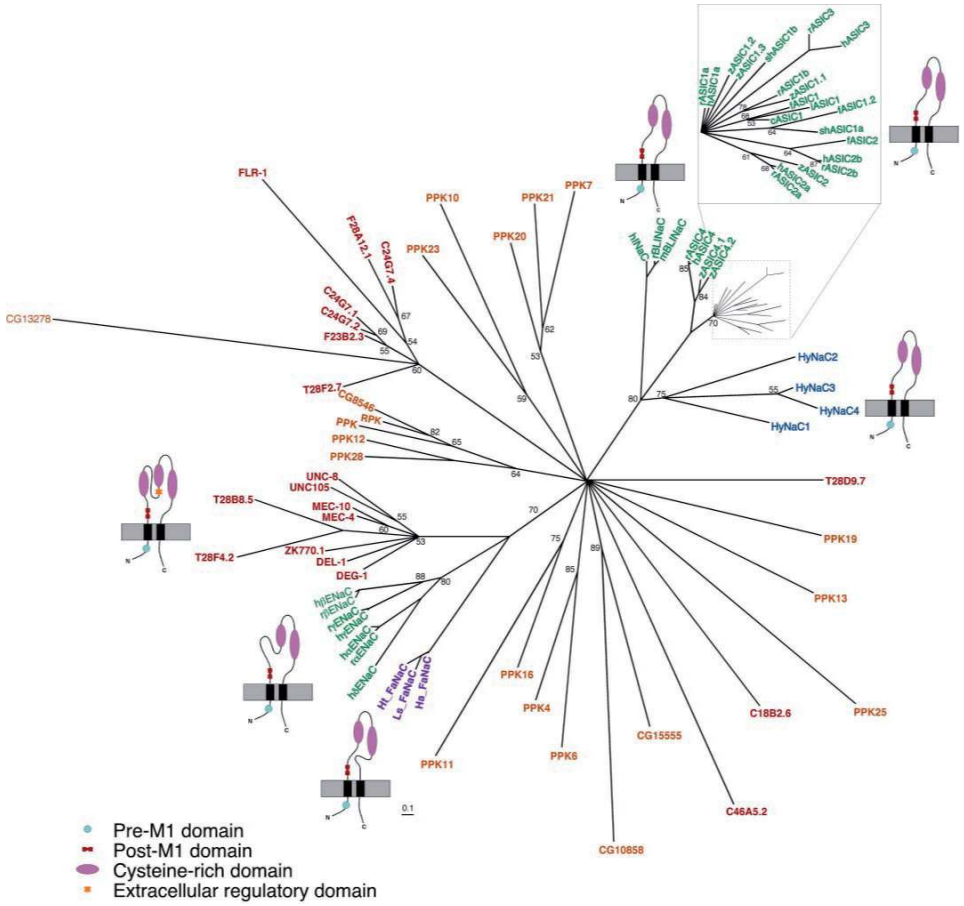

Figure 1.1.: **Phylogenetic tree of the DEG/ENaC ion channel family from Golubovic et al. 2007.**

1.2.1. Structure of the DEG/ENaC ion channel family based on the crystal structure of cASIC1

The DEG/ENaC ion channel family shows a diverse range of biophysical features and physiological roles but all DEG/ENaC ion channels share a common structure and conserved protein motifs. The tertiary structure of DEG/ENaC ion channels reveals short intracellular N- and C-termini, two transmembrane domains (TMDs) and a large extracellular domain (ECD). Proteins of this superfamily form multimeric ion channels. TMD2 of the individual subunits form the ion pore across the cell membrane [70].

In primary structure, members of the DEG/ENaC ion channel family share highly conserved sequences. At the N-terminal domain, the his-gly (HG) motif is a highly conserved amino acid sequence in the DEG/ENaC ion channel family. In all DEG/ENaC channels it is located about 15 amino acids N-terminal of TMD1 and is crucial for channel gating as described for the epithelial sodium channel ENaC [50, 52]. The selectivity filter, which is responsible for the sodium selectivity of the DEG/ENaC ion channel family, is located at the narrowest part of the ion pore in TMD2 and formed by the so called Gly/Ser-X-Ser motif [67, 70].

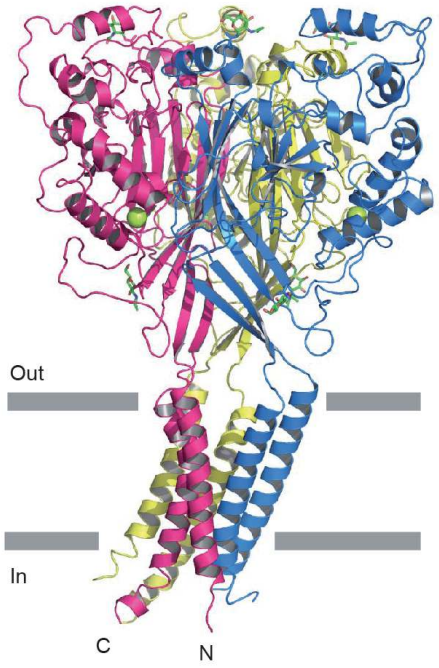

Figure 1.2.: **Crystal structure of cASIC1 in the desensitized state.** From Jasti et al. 2007.

Two conserved cysteine rich domains are found in the ECD. Cysteins form disulfide bonds and are crucial for the three-dimensional folding of a protein [37]. This reveals a comparable three dimensional structure of DEG/ENaC proteins [70]. The intracellular N- and C-terminal domains of the DEG/ENaC ion channels are targets for modification by kinases and other enzymes like ubquitin ligases [1, 34, 56, 58, 59, 64, 107, 122]. These modificiations alters channel activity, surface expression and biophysical properties, supposed mainly to be mediated by conformational changes in the ion channel structure.

A recently published crystal structure of chicken ASIC1 by Jasti et al., 2007, with a resolution of 1.9 Å (figure 1.2) reveals a better understanding of the molecular structure of the ECD of DEG/ENaC channels. In this study it was demonstrated that ASICs form trimeric ion channels. Since DEG/ENaC ion channel family members show a high sequence identity in the range of 20% [70], all members of this superfamily might assemble into trimers. The authors compared the ECD to a clenched hand, which is connected to the TMDs. This connection is flexible allowing movement of the ECD. The hand comprises five subdomains: palm, finger, thumb, knuckle and a β-ball domain [21, 62]. It has been shown that the cysteine bonds that are supposed to be associated with three-dimensional folding, are located mainly in the thumb-domain. The thumb-

domain is connected to TMD2 and thus is supposed to transmit conformational changes from the ECD to the ion pore. The authors further described that this clenched hand structure comprises an acidic pocket formed by acidic amino acids located distant from TMD2. This acidic pocket has been hypothesized to be bound by divalent cations like Ca^{2+}. Another possible binding site for calcium was hypothesized by Paukert et al., at the entrance of the pore at an aspartate located directly N-terminal of TMD2 (figure 1.3 A) [91].

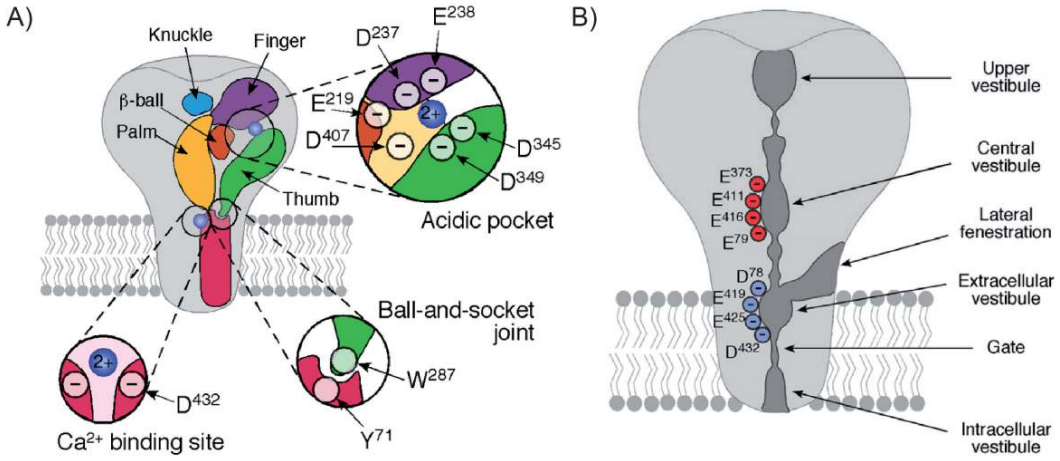

Figure 1.3.: **Two dimensional model of subdomains of the ECD revealing ion permeation pathways.** A) The five subdomains of the ECD of cASIC1 show two binding sites for extracellular calcium. B) Two pathways contributing to ion permeation across the ECD of cASIC1. From Chen and Gründer, 2010.

Finally, the crystal structure of cASIC1 revealed two candidates for the ion permeation pathways across the ECD. The first pathway is formed by two vestibules that are connected by a narrowed tunnel and that span across the central axis of the channel (figure 1.3). The crystal structure by Jasti et al., 2007, was derived from a cASIC1 in the desensitized state. The connections of the vestibules of the first pathway are too narrow in the desensitized state to allow permeation of ions. When activated, this pathway might be widened. The second pathway is formed by so called lateral fenestrations [21, 62] above the TMDs at the connection to the clenched hand. But permeation of ions through this pathway is also not possible during the desensitzed state, because in this state TMD2 of the three channel subunits form a physical blockade to the ion pore (figure 1.3 B). It is hypothesized by Jasti et al. that ligand binding causes conformational

changes in the ECD. These changes are mediated to TMD2, opening the pathways to the ion pore and thus induce ion permeation through the channel [62].

1.2.2. The epithelial sodium channel, ENaC

In 1993 and 1994, the group of Rossier et al. cloned three subunits of the epithelial sodium channel, α, β and γ, from cDNA of a rat colon library, which showed homology to degenerins from *C. elegans.* [15, 16]. One year later, in 1995, the group of Lazdunski et al. cloned a fourth subunit from human kidney cDNA, the δENaC [19]. ENaC subunits form two different combinations of heterotrimers, $\alpha/\beta/\gamma$ENaC [16] and $\delta/\beta/\gamma$ENaC [19].

The physiological role of $\alpha/\beta/\gamma$ENaC is the passive transport of sodium across the apical side of polarized epithelia into the epithelial cells in salt reabsorbing tissues. There it is involved in water and sodium homeostasis across epithelia, like in the the lung, the distal colon or the cortical collecting duct in the kidney. $\alpha/\beta/\gamma$ENaC is a constitutively open ion channel that shows a high selectivity for sodium and barely conducts potassium. ENaC has a high affinity in the micromolar range for the DEG/ENaC blocker amiloride [16, 70].

$\alpha/\beta/\gamma$ENaC is mainly expressed in the colon, the kidney and the lung. δENaC in contrast is mainly found in pancreas, ovary and the central nervous system, where its physiological role remains unclear [19, 42]. Since α, β, and γENaC are also abundant in neuronal tissue [5, 11], it is likely that *in vivo* ENaC also forms the functional heterotrimer $\delta/\beta/\gamma$ENaC.

Since ENaC is a constitutively active ion channel, it is regulated by different mechanisms. Ubiquitin ligases ubiquitinate ENaC proteins causing protein internalization and degradation. The ubiquitination counteracts the synthesis and integration of new ENaC proteins into the cell membrane [1, 70]. Further mechanisms have been described for the regulation of ENaC activity like proteolytic cleavage of the ECD of ENaC subunits or shear forces. Both mechanisms increase ENaC activity [4, 13, 14, 17, 24, 96, 98]

1.2.3. The acid sensing ion channels, ASICs

In contrast to the constitutively active ENaCs, the ASIC subfamily is a group of gated ion channels activated by protons. The ASIC subfamily consists of six members: ASIC1a, ASIC1b, ASIC2a, ASIC2b, ASIC3 and ASIC4, encoded by four genes. ASIC1a and 1b are splice variants of the gene ACCN2, ASIC2a and 2b are splice variants of the gene ACCN1 [70].

ASIC1a, 2a and 2b are expressed in the whole brain and show an increased concentration in areas like the hippocampus and the cerebellum [113]. ASIC4 is expressed in the central nervous system, too, and in some cases co-expresses with ASIC1a, 2a and 2b. Furthermore ASIC4 is expressed in the pituitary gland [51]. In addition to the CNS, the acid sensing ion channels are also expressed in the PNS.

In the PNS, ASICs are mainly found in sensory neurons, where they were reported to be crucial for pain sensation, especially ASIC3, which is activated by inflammatory processes [32]. Furthermore ASICs have been shown to be involved in the sensation of touch. Eventhough ASICs are not activated directly by mechanical forces, they have been shown to be involved in the perception of cutanous mechanical stimuli [66].

ASICs are sodium channels, which are closed at rest and are activated by an extracellular increase in H^+ concentration (figure 1.4). Activation by acidic pH leads to a fast transient inward current followed by a smaller sustained component. After activation, ASICs switch to a non-conducting desensitized state and require time to recover. In contrast to other ASICs, ASIC4 is not activated by protons [51].

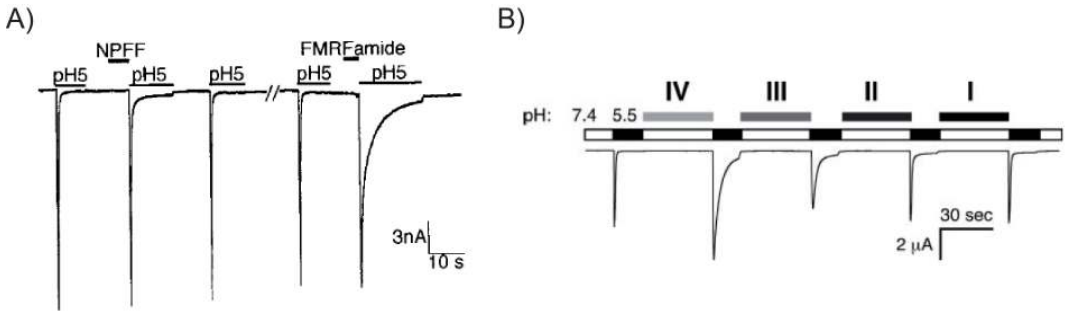

Figure 1.4.: **ASIC currents and their alteration by RF- and FFamides.** A) Activation of ASIC current in DRG neurons by acidic pH. Modulation of ASIC current by FMRFamide and FFamide (50 μM). From Askwith et al. 2000. B) Modulation of acid evoked ASIC3 currents by Hydra-RFamides I - IV (50 μM) in *Xenopus* oocytes. From Golubovic et al. 2007.

The activation of ASICs by protons competes with the binding of calcium ions that block the permeation of cations through the ASIC pore. The blocking site in ASICs that keeps the channels inactive is bound by Ca^{2+} and an exchange of Ca^{2+} by H^+ activates the ion channel [7, 90].

ASICs form homotrimers as well as heterotrimers. The combination of ASIC subunits influences the biophysical properties like the apparent proton affinity or the desinsitiza-

tion time of the transient current [41, 70]. All ASIC trimers show a high permeability for Na^+ and a low permeability for K^+. Furthermore ASIC1a ($P_{Ca^{2+}}/P_{Na^+} = 0.06$ to 0.3, [9, 113, 120]) and human ASIC1b homomers ($P_{Ca^{2+}}/P_{Na^+} = 0.5$, [57]) as well as ASIC1a/2b heteromers ($P_{Ca^{2+}}/P_{Na^+} = 0.25$, [104]) are slightly permeable for Ca^{2+}.

A phylogenetic tree of the DEG/ENaC ion channel family published by Golubovic et al., 2007, demonstrated ASIC, BASIC and HyNaC to form a monophyletic group within this superfamily. HyNaC that will be described in more detail later, is activated by endogenous neuropeptides of the Hydra-RFamide family from *Hydra magnipapillata*. Interestingly, these invertebrate neuropeptides together with other neuropeptides like the FMRFamide from molluscs alter ASIC channel activity [6, 45]. It has also been found that FFamides from vertebrates have an effect on ASIC currents. A simultaneous application of either RF- or FFamides during ASIC activation by H^+ results in a potentiated acid response. RF- and FFamides increase the desensitization time of the transient current and also increase the sustained current of ASICs in dorsal root ganglia of the rat (figure 1.4) [6, 45]. An evidence for the regulation of ASICs by neuropeptides *in vivo* is still missing. The physiological role of ASICs has not been fully understood yet. But since neuropeptides are found in the whole nervous system of vertebrates, it seems possible that small neuropeptides *in vivo* modify ASIC activity.

1.2.4. BASIC, a DEG/ENaC ion channel sensing bile acid

Besides ASIC and ENaC, BASIC is the third DEG/ENaC subfamily found in vertebrates. The bile acid sensing ion channel (BASIC) is a cation channel originally cloned from rat and mouse in 1999 [100]. One year later, the human BASIC was cloned from a genomic DNA library [101]. In mouse and rat, BASIC is mainly expressed in the brain, liver, small intestine and testis whereas the human BASIC mainly is expressed in the small intestine. In addition rBASIC is also expressed in epithelial cells of the bile duct [119]. Interestingly, hBASIC is not expressed either in the brain or in the liver, which has been shown to be the predominant expression pattern of rBASIC and mBASIC [100, 101, 119].

rBASICs and hBASIC show only a small basal activity [100, 101], mBASIC in contrast is a constitutively open ion channel [117]. Like ASIC, rBASIC and hBASIC are also blocked by calcium. This calcium block is not observed in mBASIC, which explains why rBASIC and hBASIC are mostly inactive at rest and mBASIC is not [74, 117, 119]. Natural activators of rBASIC and hBASIC are bile acids, while they are no ligands for mBASIC. An application of bile acids induces a fast and reversible inward sodium

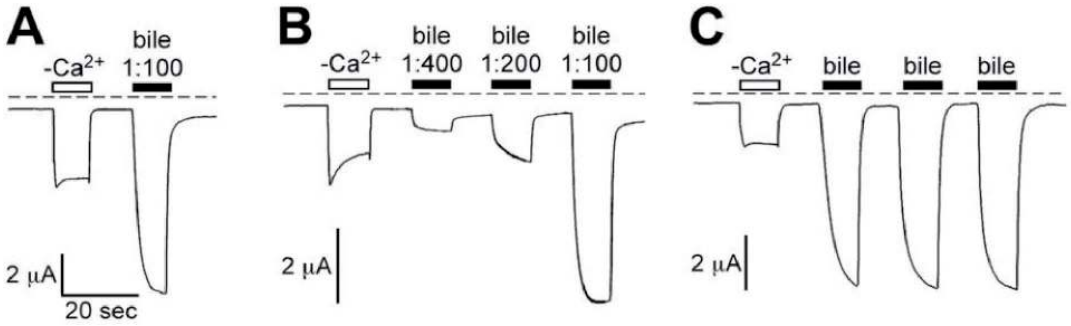

Figure 1.5.: **BASIC is activated by bile.** A) and B) Activation of rBASIC by bile. C) Successive activation of rBASIC by bile demonstrates that the channel does not desensitize. From Wiemuth et al. 2012.

current [74, 119]. Only little is known about the physiological role of BASIC. But since it is expressed in epithelial cells of the bile duct and activated by bile acids, BASIC might play a role in Na^+ transport in the bile duct, like it has been reported for ENaC in other polarized epithelia.

1.2.5. Pickpocket, a DEG/ENaC subfamily from *Drosophila spp*

Members of the DEG/ENaC ion channel family are not only found in vertebrates but also in invertebrate organisms. Pickpocket is the largest subgroup within the DEG/ENaC ion channel family and is found in *Drosophila spp.*: so far 31 different PPK proteins have been found in *Drosophila melanogaster*. Comparable to ASIC, BASIC and ENaC from vertebrates, the physiological role of PPKs, which already have been studied in more detail, are linked to water homeostasis, mechanosensation and chemosensation [121]. Regarding the expression pattern of PPK channels, mRNA coding for PPK proteins was found in neuronal as well as non-neuronal cells like the ovary or the fatbody and in different stages of animal development [121].

PPK1 is expressed in peripheral mechanosensory neurons of *Drosophila* in all developmental stages, but fails to generate currents when heterologously is expressed in *Xenopus* oocytes. Ripped pocket (RPK), another member of the PPK channels, is only expressed in early developmental stages and its expression is not limited to a specific cell type. Heterologous expression of RPK generates a constitutively open Na^+ selective ion channel that is impermeable for K^+ and that can be blocked by amiloride [2].

In *Drosophila spp.* PPK channels play an important role in mechanical nociception in

multidendritic neurons [123] and alveolar clearance in the tracheal system of *Drosophila* larvae [79]. The male courtship of *Drosophila spp.* is evoked by female pheromones. PPKs are expressed in gustatory neurons and are associated with mating of *Drosophila*. It remains unclear whether a heteromer of those three PPK proteins is gated directly by the pheromones or if it alters the sensitivity for other pheromone receptors in gustatory neurons [79, 80, 108, 112].

1.2.6. The degenerins in *Caenorhabditis elegans*

The first cloned DEG/ENaC ion channel was the degenerin-1 (DEG-1) channel from *Caenorhabditis elegans* [18]. The group of Chalfie cloned and described this channel in 1990 from animals showing touch-insensitivity. They found that DEG-1 is expressed in neuronal cells of the animals and when mutated results in touch-insensitive animals showing neuronal degeneration. Ion channels of this subfamily were named degenerins due to their phenotype of degeneration of neurons. The degenerins contain a variety of mechanically activated ion channels [18, 33, 60]. In the following year, the same group cloned two further degenerins from *C. elegans*, MEC-4 and MEC-10 that when mutated caused the same phenotype as the DEG-1 mutants. This mutation is caused by an amino acid exchange of a conserved glycine located shortly N-terminal of TMD2, called the DEG-mutation [18, 33, 60].

Different studies showed that the degenerin channels are part of a mechanotransduction complex that contains also other proteins that are not part of the DEG/ENaC ion channel family [47, 60]. The mechanotransducing complex mediates the opening of the two DEG/ENaC ion channels MEC-4 and MEC-10 that are linked to the cytoskeleton and/or the extracellular matrix. The deformation of the cytoskeleton or the extracellular matrix during stretch induces the direct mechanical opening of the ion channel. Isolated from this mechanotransducing complex, for example when heterologously expressed in *Xenopus* oocytes, the degenerins are insensitive to mechanical stimuli [47, 60]. The neurodegenerative phenotype of the mutations DEG-1, MEC-4 and MEC-10 presumably is the effect of hyperactive and hypersensitive ion channels. This hyperactivity causes increased influx of sodium and for MEC-4 also of calcium into the neurons, causing cell swelling and cell death [55].

1.2.7. The FMRFamide activated ion channel, FaNaC

The FMRFamide activated ion channel (FaNaC) was cloned from the garden snail *Helix aspersa* in 1995 by the group of Lazdunski. FaNaC was the first ion channel, which had been shown to be directly activated by a neuropeptide and until now is the only known peptide gated ion channel together with HyNaC. In *Helix aspersa* (*H.a.*) FaNaC is expressed in neuronal cells and the pedal muscle [25, 78]. In the following years three further FaNaCs were cloned from *Helisoma trivolvis* (*H.t.*) [63], *Lymnea stagnalis* (*L.s.*) [94] and *Aplysia kurodai* (*A.k.*) [38]. Consistently FaNaCs were found to be expressed in neuronal cells of the respective snail species [29, 38, 63, 78, 94]. Additionally *L.s.* FaNaC has been shown to be also expressed in the pedal muscle and the heart [94].

FaNaCs form homotrimeric sodium channels that are activated by FMRFamide [25, 38, 63, 78, 94]. For *H.a.* FaNaC and *H.t.* FaNaC it has been demonstrated that these two channels show a high selectivity for sodium over potassium but do not conduct calcium [48, 63, 78]. Similar to ASIC and BASIC, *H.t.* FaNaC and *A.k.* FaNaC are blocked by extracellular calcium [38, 63].

Activation by FMRFamide induces a desensitizing inward current. It was excluded that FaNaC is activated by a G-protein coupled intracellular signalling cascade induced by binding of a metabotropic FMRFamide receptor. Rather FaNaC is directly activated by FMRFamide [63, 78].

Amino acids that are associated with apparent ligand affinity for FMRFamide are located at the proximal ECD. The affinity of FaNaC for its ligand is rather low with an

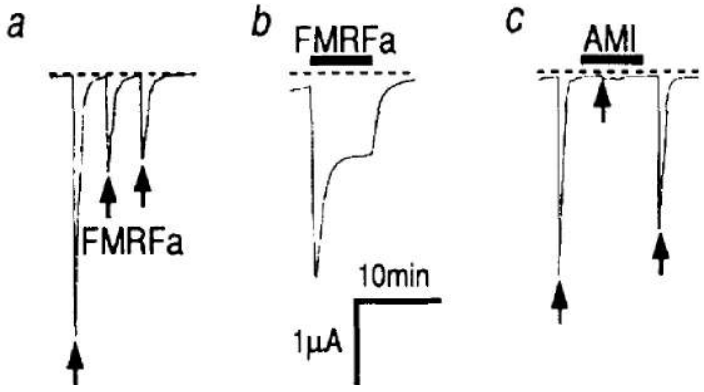

Figure 1.6.: **FaNaC, a peptide gated ion channel from molluscs.** A) Succesive short time and b) long time activation of *H.t.* FaNaC by 30 μM FMRFamide. C) Block with 100 μM amiloride. From Lingueglia et al. 1995.

EC_{50} in the range of 2 μM for *H.a.* FaNaC and 70 μM for *H.t.* FaNaC [26, 27, 63, 78]. An exchange of these amino acids between *H.a.* FaNaC and *H.t.* FaNaC also exchanges their apparent affinity for FMRFamide [26, 27].

1.3. The peptide gated sodium channel from the fresh water polyp *Hydra magnipapillata*

1.3.1. Taxonomy and anatomy of *Hydra magnipapillata*

Hydra magnipapillata belongs to the phylum cnidaria and the class hydrozoa and is exclusively found in fresh water. It is one of the evolutionary oldest known multicellular animals and it is presumed that *Hydra magnipapillata* is one of the first animals that evolved a nervous system. It shows a radial symmetry and is closely related to jelly fish. Cnidaria can reproduce in two ways, the sexual and the asexual way. For the sexual reproduction, the animals undergo a life cycle containg two major stages, the medusa stage and the polyp stage. During the medusa stage, the animals produce gametocytes that are released into the water. Fertilized eggs then adhere to the ground where they grow up to mature polyps. The mature polyp produces new medusa buds that are released from the parental body, restarting the life cycle. The sexual reproductive pathway is induced when the nutrition situation is insufficient. In contrast, the asexual reproduction occurs only in the polyp stage and under a good nutrition. For this reproductive way, the polyp forms buds that fall off and grow up to new polyps. In contrast to other hydrozoa, *Hydra magnipapillata* does not change between medusa and polyps, but remains as a polyp for its complete life span. Since commonly the medusae produce the gametocytes, in *H. magnipapillata* this is done by the polyps [43].

The body plan of *H. magnipapillata* is simple: it has no apparent organs and its tube-like shaped body consists only of two layers of tissue. Between these two tissue layers, multipotent stem cells are found that can differentiate into four different celltypes: neurons, cnidocytes (also called nematocytes), gametes and secretory cells [43, 111].

The head region of *H. magnipapillata* is formed by tentacles surrounding the hypostome, the mouth region of the animal. The aboral end of the animal is formed by a basal disc and a foot that adheres to the ground (figure 1.7). *Hydra magnipapillata* is carnivourus and captures its prey with its tentacles, which carry cnidocytes containing cnidocysts. Cnidocytes are cells that are limited to the phylum cnidaria. Those cells contain a cnidocyst, a subcellular compartiment that produces a condensed, toxin loaded

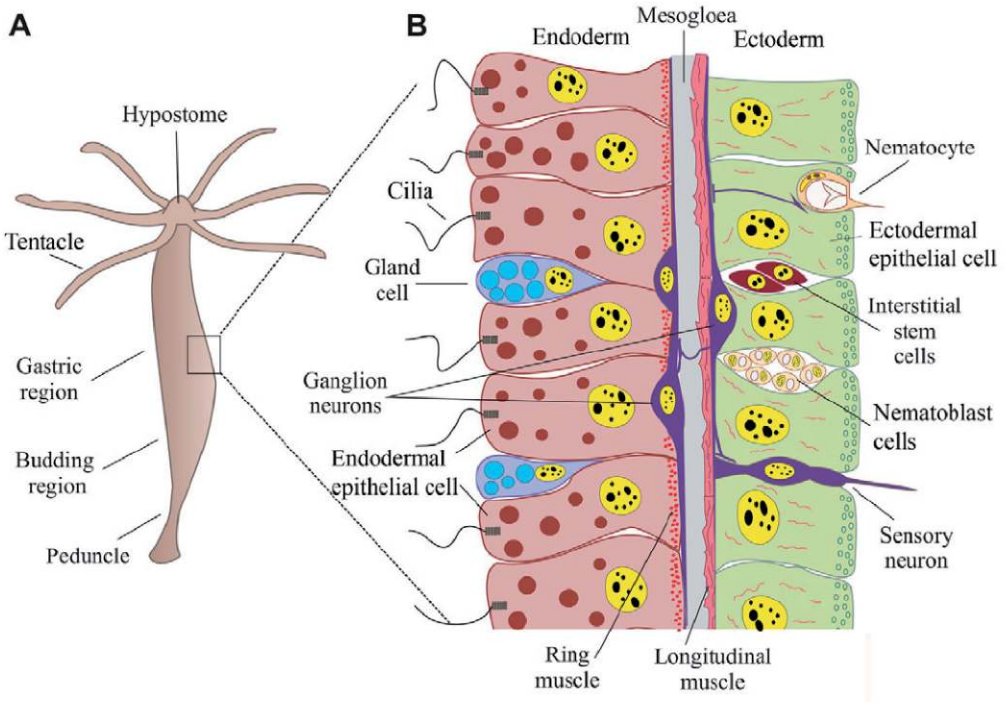

Figure 1.7.: **Body plan of *Hydra magnipapillata*.** A) Anatomical overview of *Hydra magnipapillata*. B) Cell types within the two layers of the endoderm and ectoderm forming the *Hydra* bodywall. From Technau et al. 2012.

filament. When the cnidocyte is touched, the condensed filament expands explosively and penetrates the skin of prey or foe animals where it injects the toxins. Thus cnidocysts are used for defense and prey capturing by cnidaria. The tentacles then transport the prey to the mouth [43, 116].

Hydra magnipapillata is an interesting model for developmental biology, because it has a strong ability to regenerate. Even a disintegration of the complete body of the adult animal to single cells can be regenerated to complete and healthy animals [43].

1.3.2. The peptide gated sodium channel from *Hydra magnipapillata* (HyNaC)

HyNaC has been cloned in 2007 from cDNA of *Hydra magnipapillata* by homology to other DEG/ENaC ion channel family members by the group of Gründer et al. [45]. The phylum cnidaria is very old and at the basal level of metazoan development, thus *Hydra* is the oldest known genus expressing members of the DEG/ENaC ion channel

family. Due to its age, DEG/ENaC channels from *Hydra* are supposed to show ancestral features of the DEG/ENaC ion channel family [43, 45]. So, studying HyNaC might reveal ancient properties of the DEG/ENaC ion channel family that give insights into "younger" DEG/ENaC ion channel family members like ASIC and BASIC.

Four different HyNaC subunits have been cloned from the fresh water polyp *Hydra magnipapillata* so far: HyNaC2 - HyNaC5. HyNaC1 is a pseudogene since it lacks a starting methionine [36, 45].

As the phylogenetic tree in figure 1.1 illustrates, the closest relatives of HyNaCs are BASICs and ASICs. Unexpectedly, FaNaC, the only other known peptide gated ion channel, is not a direct orthologue of HyNaCs.

HyNaC2, 3 and 5 form a functional heterotrimer, HyNaC2/3/5, which is activated by the endogenously expressed neuropeptides Hydra-RFamide I and II [36, 45]. HyNaC2 and HyNaC3 can also form a functional channel in the abscence of HyNaC5, but since HyNaC2/3 shows a considerably lower expression than HyNaC2/3/5, the heterotrimer consisting of HyNaC2/3/5 is supposed to be the physiological subunit combination [36].

Although HyNaC2/3/5 is activated directly by neuropeptides like FaNaC, the phylogenetic distance suggests an independent evolution of peptide gating in FaNaC and HyNaC. Moreover, the DEG/ENaC superfamily could have evolved from a peptide gated ancestor and only in HyNaC2/3/5 and FaNaC peptide activation has been conserved. HyNaC4 can not form a functional channel with the other HyNaC subunits that is activated either by Hydra-RFamide I or by Hydra-RFamide II to IV [36, 45]. HyNaCs are closed at rest and when activated show a slight selectivity for $Na^+ > Li^+ > K^+$. Besides

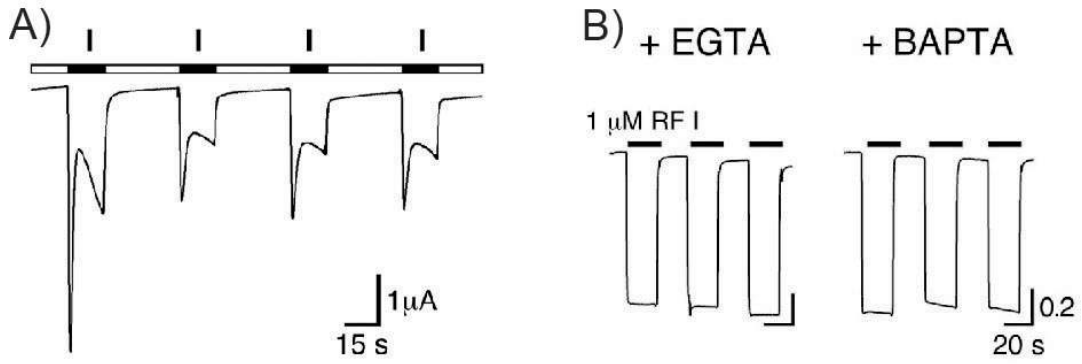

Figure 1.8.: **Activation of the *Hydra* sodium channel.** HyNaCs activated by Hydra-RFamide I A) without and B) with injecton of a Ca^{2+} chelator. From Dürrnagel et al. 2012.

Hydra-RFamides I and II, a removal of extracellular Ca^{2+} opens the channel, revealing a block by extracellular calcium [36].

Interestingly, HyNaCs not only conduct monovalent cations but also the divalent cation calcium with a permeability ratio $P_{Ca^{2+}}/P_{Na^+} = 3.85$ [35] (figure 1.8). In contrast, ASIC1a and human ASIC1b homomer as well as ASIC1a/2b heteromer show a calcium permeability ratio $P_{Ca^{2+}}/P_{Na^+}$ lower than 0.5 [9, 57, 104, 120]. As far as it is known, ASIC and HyNaC2/3/5 are the only calcium permeable ion channels in the DEG/ENaC ion channel family. Only MEC-4(d) also shows calcium permeability with a $P_{Ca^{2+}}/P_{Na^+}$ of 0.22 when modified with the deg-mutation [10].

Before HyNaC was shown to be permeable for calcium, the peptide activation was described as a biphasic current with a transient and a sustained component. Successive activation of HyNaC2/3/5 led to a desensitization of the channel [36]. However, the finding of calcium permeability of HyNaC2/3/5 revealed that the biphasic current as well as the desensitization result from an overlay of currents produced by HyNaC2/3/5 and an endogenously expressed calcium activated chloride channel (CaCC) in *Xenopus* oocytes. When a calcium chelator, which binds influxing calcium, is injected into the oocytes before whole cell measurements, an application of Hydra-RFamide I and II evokes a non-desensitizing current with a typical on-off-characteristic [8, 35].

HyNaC2 - HyNaC5 have been shown by *in situ* hybridization to be expressed at the basis of the tentacles of *Hydra magnipapillata* (figure 1.9) [36, 45]. HyNaC2 and HyNaC3 are expressed at the oral as well as the aboral side of the tentacle basis. In contrast, HyNaC5 is expressed only at the oral side, whereas HyNaC4 is expressed only at the aboral side of the tentacle basis, suggesting that HyNaC4 and HyNaC5 play different roles *in vivo*. HyNaCs not only differ in their expression pattern but also in their appearance in different developmental stages of the animal. All HyNaCs are expressed in adult animals but only HyNaC5 is also present in early buds. A first expression of HyNaC2 and HyNaC3 is observed when the tentacles begin to develop. HyNaC4 instead is only found in adult animals.

HyNaCs are supposed to be involved in the feeding reaction of *Hydra magnipapillata*. Glutathione (GSH) is a substrate that is a component of prey animals. GSH is bound by a specific metabotropic GSH receptor in sensory cells of *Hydra magnipapillata*. When bound, this metabotropic receptor induces the curling of tentacles that transports the prey to the mouth of the animal. This mechanism is called feeding reaction [95]. When amiloride, an inhibitor of HyNaCs, is applied together with GSH, the feeding reaction is inhibited significantly [36]. Regarding the expression pattern of HyNaC subunits and

the inhibition of the feeding reaction by amiloride, HyNaC2/3/5 likely is expressed in neuromuscular cells at the tentacle basis, possibly inducing tentacle curling [36, 45].

1.3.3. The nervous system of *Hydra magnipapillata* and its role for studying the DEG/ENaC ion channel family

Although *Hydra sp.* lacks a central nervous system, it has a so called nerve net. This nerve net is built by neuronal cells located between the two tissue layers of endoderm and ectoderm and along the whole oral-aboral body axis. The nerve net is characterized by a diffuse organization pattern without cephalization, as it is found in higher animals. The nervous cells of *Hydra sp.* already show an early stage of specialization, since sensory cells are found in the tentacles and a neuronal plexus is found in the foot region [116].

Grimmelikhuijzen could show that neuronal cells in *Hydra* express peptides containing an RFamide sequence. RFamide expressing neuronal cells form a nerve ring surrounding the hypostome and are also found frequently at the hypostome and at low frequency along the body axis of *Hydra*. In addition, RFamide positive neuronal cells form a plexus at the peduncle, the foot region of *Hydra* [49] (figure 1.10). Cnidaria are an

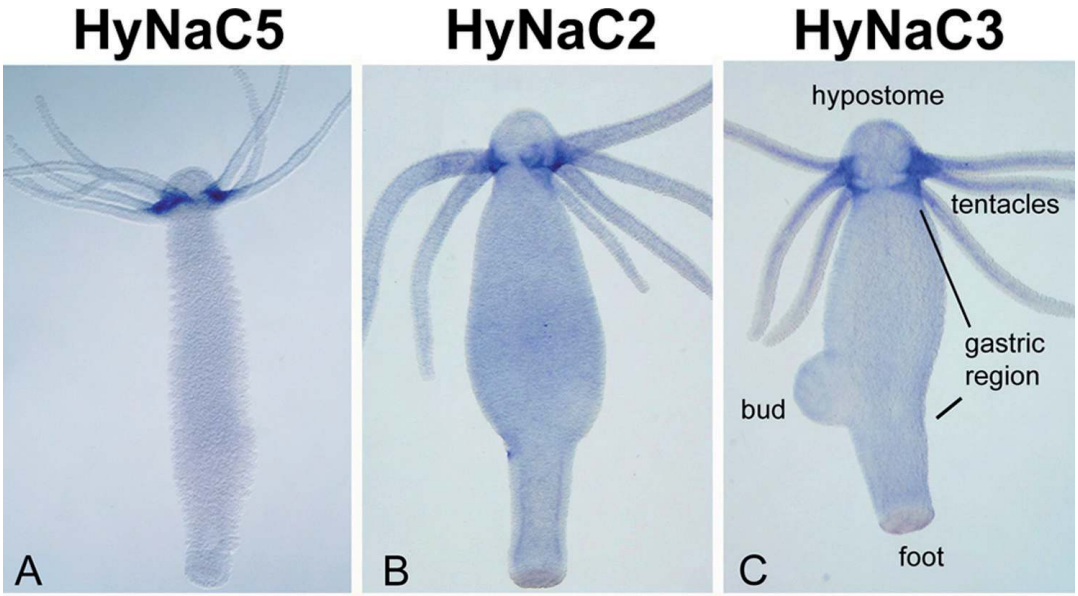

Figure 1.9.: **Expression pattern of the *Hydra* sodium channel in *Hydra magnipapillata*.** Whole mount *in situ* hybridization against HyNaC 2, 3 and 5. From Dürrnagel et al. 2010.

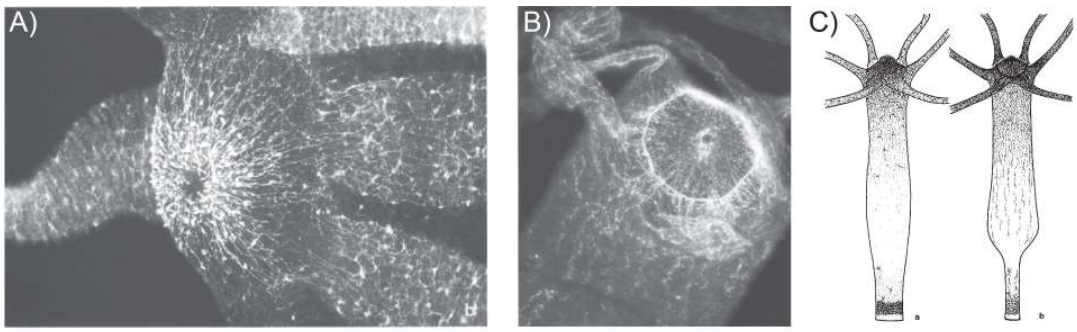

Figure 1.10.: **The nerve net of *Hydra sp.*** Whole mount anti- RFamide staining. A) *Hydra attenuata*. B) *Hydra oligactis*. C) Drawing of RFamide positive regions in both species. From Grimmelikhuijzen 1985.

evolutionary very old phylum suggesting that the nervous system in cnidaria is also at a very basic level of evolutionary development. However, ligand gated ion channels that are found in all higher animals and activated by neurotransmitters are already present in *Hydra magnipapillata*. Receptors for neurotransmitters of excitatory neurons, like acetylcholine- and glutamate-receptors, as well as of inhibitory neurons like the $GABA_A$ receptor have been found in the nervous system of *Hydra magnipapillata* [95].

1.3.4. Hydra-RFamides, a family of neuropeptides from the freshwater polyp *Hydra*

RFamide neuropeptides expressed in the nervous system of *Hydra magnipapillata* are derived from three different preprohormones, called preprohormone A-C. Preprohormone A is expressed in the head as well as the foot region. In contrast, preprohormones B and C are expressed exclusively at the head region. All cDNAs coding for the three preprohormones comprise an open reading frame in the range of 160 amino acids for A and B and of 397 amino acids for C [28].

Preprohormone A codes for Hydra-RFamides I - VI. Preprohormone B codes for I, II, V and VII to IX, preprohormone C codes for Hydra-RFamide I (figure 1.11) [28]. Hydra-RFamides I and II [85], as described above, are known to activate the *Hydra* sodium channel while Hydra-RFamides III and IV do not [36, 45, 85]. Since Hydra-RFamides V to IX are putative peptides that have not been confirmed yet to be expressed *in vivo*, those peptides have not been tested on HyNaC activity.

Interestingly the expression pattern of Hydra-RFamides I and II does not completely

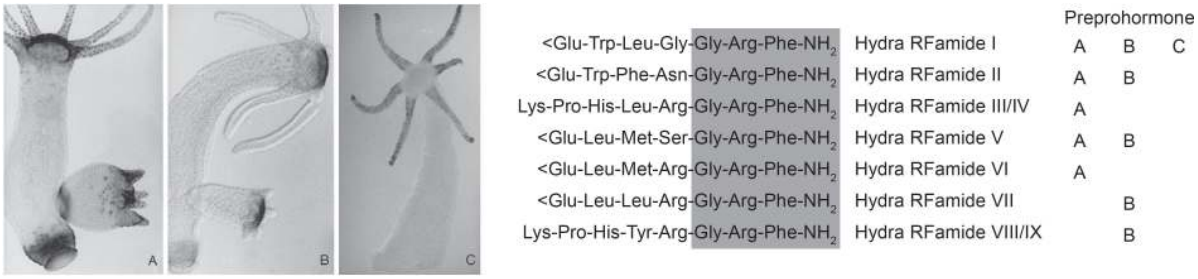

Figure 1.11.: **Expression pattern and derivates of the preprohormones of Hydra-RFamides.** Left) Expression pattern of preprohormones A-C. Right) Hydra-RFamides I-IX derived from preprohormones A-C. From Darmer et al. 1998.

overlap with the expression pattern of HyNaC2 - HyNaC5. In addition to the expression of HyNaCs and Hydra-RFamides I and II in the head region, the neuropeptides are also found in the peduncle region. Since HyNaCs and Hydra-RFamides are supposed to be responsible for muscle contractions at the tentacle basis, the expression of Hydra-RFamides in the peduncle region suggests other, yet unknown RFamide receptors and different physiological processes.

FMRFamides and Hydra-RFamides that are known to activate FaNaC and HyNaC, respectively [36, 45, 78], are missing in mammals. However these neuropeptides are able to alter channel activity and channel properties in ASIC [22]. Thus neuropeptides from the phylum cnidaria and other invertebrates seem to affect the biophysical properties of ion channels of higher evolved and more complex phyla. From phylogenetic analysis, HyNaC and ASIC have been demonstrated to be part of a monophyletic group inside the DEG/ENaC family that presumably has evolved from a common ancestor. Modulation of ASICs by neuropeptides suggests a conservation of the ligand binding site and the physiological relevance of neuropeptides for ASICs. However, an evidence for regulation of ASIC activity by neuropeptides *in vivo* is still missing.

Peptide signalling seems to play a crucial role in neuronal activity in *Hydra magnipapillata* and other cnidaria. In the sea anemone, the RFamide related peptide Antho-RWamide I and II induces muscle contractions. These muscle contractions were not mediated by an increased neuronal activity but by a direct activation of muscle cells [82]. Considering findings from HyNaC, controling muscle activity might be the main physiological function of RF/RWamides in cnidaria.

1.4. Aim of the study

In previous works of our group [36, 45] four subunits of the peptide gated sodium channel (HyNaC) subfamily have been identified in *Hydra magnipapillata*, HyNaC2 - HyNaC5. The three subunits HyNaC2/3/5 form a functional heterotrimer. Interestingly, HyNaC4 does not form a functional ion channel together with the other HyNaC subunits 2, 3 and 5. Furthermore HyNaC2/3/5 is activated by the two neuropeptides *Hydra* RFamides I and II while *Hydra* RFamides III and IV have no effect on HyNaC2/3/5 activity. HyNaC2/3/5 is expressed at the head region of *Hydra magnipapillata* whereas *Hydra* RFamides I and II are found at the head as well as the foot region.

Taken together it is likely that other HyNaC subunits are expressed in *Hydra magnipapillata* that interact with HyNaC4, that are activated by other *Hydra* RFamides than I and II, or that are expressed at the peduncle region.

The aim of this study was to find novel members of the *Hydra* sodium channel subfamily in *Hydra magnipapillata* and to characterize their biophysical properties as well as their expression pattern.

2. Materials and Methods

2.1. Biological Materials

2.1.1. Heat competent *Escherichia coli*

TOP 10 heat competent *Escherichia coli* (*E. coli*) were used to transform Plasmid-DNA. The origin of TOP 10 cells was the strain DH10B^{TM}. The transformation efficiency of these cells was about 10^9 cfu/μg. Top 10 cells were prepared by the provider Invitrogen life technologies (Carlsbad, CA, USA) to accept Plasmid DNA by heat shock at 42 °C.

2.1.2. *Xenopus laevis* oocytes

All electrophysiological examinations of ion channels in this work were performed using *Xenopus laevis* oocytes in stage V and VI. These cells are precursors of the mature egg cells. The diameter of the oocytes is about 1 mm and the cells show a two-coloured pattern. The animal pole is coloured in black or dark brown, the vegetal pole is coloured in light yellow. Each pole covers one half of the oocyte (figure 2.3). Oocytes in stage V and VI express only a small amount of endogenous ion channels in the cell membrane and, when injected with cRNA, express foreign ion channels or other proteins willingly including posttranslational modifications [54, 109].

2.1.3. Materials for molecular purposes

Standard chemicals used in this work were acquired from Merck (Darmstadt, Germany), Roth (Karslruhe, Germany) or Sigma-Aldrich (St. Louis, USA). A list of ready-to-use materials, enzymes and kits for molecular biology that mostly were purchased from other manufacturers, can be seen in table 2.1.

Ready-to-use materials

1 kb DNA ladder	Thermo Scientific, Schwerte, Germany
100 bp DNA ladder	New England Biolabs, Ipswich, USA
DEPC H_2O	Roth, Karlsruhe, Germany
Red-Safe	Intron, Korea
dNTPs	Roth, Karlsruhe, Germany

Kit systems

High Pure PCR Product Purification Kit	Roche, Mannheim, Germany
High Pure PCR Cleanup Micro Kit	Roche, Mannheim, Germany
High Pure Plasmid Isolation Kit	Roche, Mannheim, Germany
DNA Clean and Concentrator	Zymo Research, Irvine, USA
RNA Clean and Concentrator	Zymo Research, Irvine, USA
mMessage Machine SP6 Kit	Invitrogen life technologies, Carlsbad, USA
Quantitect Reverse Transcription Kit	Qiagen, Venlo, Netherlands
SMARTer RACE cDNA amplification Kit	Clontech, Saint-Germain-en-Laye, France
InFusion HD Cloning Kit	Clontech, Saint-Germain-en-Laye, France
TOPO TA Cloning Kit	Invitrogen life technologies, Carlsbad, USA

Enzymes

T4 DNA ligase	New England Biolabs, Ipswich, USA
Taq DNA polyemerase	New England Biolabs, Ipswich, USA
KAPA HiFi DNA polymerase	Clontech, Saint-Germain-en-Laye, France
Restriction endonucleases	New England Biolabs, Ipswich, USA
Calf intestinal alkaline phosphatase	New England Biolabs, Ipswich, USA

Table 2.1.: **Ready-to-use materials, enzymes and kit systems for molecular biology**

DNA-Oligonucleotides

All DNA-Olignucleotides, also called PCR primers, were purchased from MWG-Eurofins, Ebersberg, Germany. The primers were unmodified, purified via HPLC and delivered as dry powder. Dissolving and delution was done with ultrapure water. The working concentration of primers was 10 ng/μl.

DNA Vectors / Plasmids

The DNA vector that was used for protein expression in *Xenopus* oocytes, also called pRSSP6009, was a derivate of pUC18 and contained an ampicilline resistance, a 5'

untranslated region of *Xenopus laevis* β-globin and a polyA-tail at the 3'end of the multiple cloning site. This modification was an optimization for an expression of proteins in *Xenopus laevis* oocytes. The multiple cloning site (MCS) was flanked by an SP6 and a psp3 promoter sequence that was used for cRNA Synthesis (see chapter 2.5.2).

2.2. PCR methods and DNA purification

2.2.1. Agarose gel electrophoresis and DNA purification

The agarose gel electrophoresis is a standard procedure to detect DNA or RNA. Depending on the size of the DNA or RNA fragment, an agarose gel concentration between 0.8 % (up to 10000 nucleotides) and 1.5 % (100 nucleotides) was chosen to isolate different DNA/RNA fragments from each other. The agarose was dissolved in 1x TAE Buffer (50x: 242 g Tris-Base, 57.1 ml glacial acid (100%), 100 ml 0.5 M EDTA, add H_2O to 1 litre) by heating up the solution to its boiling point in a microwave. After the agarose was completely dissolved, 0,5 μl/10 ml Red-Safe staining dye was added. The still liquid agarose solution was put on a chill mold and wells were formed using plastic combs. When the agarose gel was cooled down and strain-hardened, the Gel was put in a horizontal running chamber (Bio-Rad, Munich, Germany). This chamber was filled with 1x TAE buffer. Before loading on the agarose gel, the DNA and RNA samples were mixed with 6x gel-loading buffer. The 6x gel-loading buffer consisted of: Bromphenol-blue 0.25 %, xylene cyanol FF 0.25 %, glycerin 30-40 %, Tris-HCl 10 mM, EDTA 50 mM, pH 7.5. RNA first had to be denaturated 10 minutes at 65 °C to avoid secondary structures that influence the running properties of RNA. When the wells were loaded, the chambers were connected to a power supply (Power Pac 3000; Bio-Rad, Munich, Germany). The gel electrophoresis was performed at 80 - 120 V for about 30 minutes. The agarose gel then was analyzed with a UV-transilluminator (Gel Doc XR; Bio-Rad, Munich, Germany) connected to a personal computer running the software Quantity One (BioRad, Munich, Germany).

When the desired DNA or RNA fragment was detected on the agarose gel, the DNA band on the gel could be excised with a scalpel and cleaned up with the High Pure PCR Product Purification Kit (Roche, Mannheim, Germany).

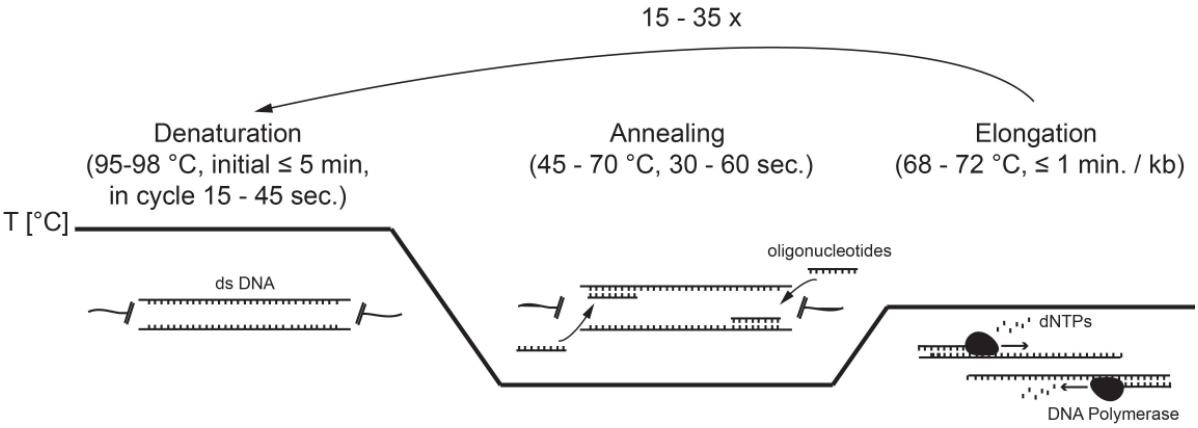

Figure 2.1.: **Principle of the polymerase chain reaction.** A PCR can be divided into three parts: denaturation, annealing and elongation. Before amplification of a target DNA sequence, the double stranded DNA has to be denaturated so that PCR primers can bind to the separated DNA strands. After denaturation the PCR mixture is cooled down and the PCR primers bind to the DNA strands. The PCR mixture is heated up again to the temperature optimum of the DNA polymerase. After amplification the PCR cycle starts again.

2.2.2. Variations of the polymerase chain reaction (PCR)

The PCR method, invented by Saiki et al., 1985 [99], was used in this work to create different kinds of DNA mutations, to clone new HyNaC subunits from *Hydra magnipapillata* cDNA and also to detect positive clones of heat-competent *E. coli*. The principle of the PCR method is illustrated in figure 2.1. A standard protocol for a PCR reaction using the Taq DNA polymerase is shown in table 2.2. For different purposes there are different PCR types that are further described below. The thermocycler T3000 from Biometra (Göttingen, Germany) was used to perform the PCR reaction.

Site directed mutagenesis by Quickchange PCR

The Quickchange PCR is a method originally invented by the company Stratagene (Santa Clara, USA). With this method it is possible to exchange, insert or delete one or more nucleotides in the DNA sequence *in vitro* and to change the amino acid sequence of the coded peptide. All pointmutations in this work were done with this method.

For Quickchange PCR two complementary primers with the pointmutation in the

Pipette scheme		**PCR program**			
50 - 100 ng	DNA	intitial denaturation	95 °C	3 - 5 min.	
1 μl	dNTP	cyclic denaturation	95 °C	30 sec.	
1.5 μl	Primer A	primer annealing	45 - 65 °C	30 sec.	35x
1.5 μl	Primer B	DNA elongation	68 °C	30 sec./kb	
5 μl	Taq 10x Buffer	final elongation	68 °C	3 - 5 min	
1 μl	Taq DNA polymerase	cool down	4 °C	pause	
to 50 μl	H_2O				

Table 2.2.: **Standard protocol of the PCR reaction with Taq DNA polymerase.**

center of the priming sequence were created to mutate the sequence. A mispriming nucleotide strongly reduces priming efficiency of DNA olignucleotides. Therefore the pointmutation was flanked with 10 to 15 nucleotides to improve priming efficiency. The melting temperature (TM) had to be at about 70 °C or higher to avoid unspecific priming. Therefore the PCR primers had a size of at least 30 nucleotides, depending on the GC-content of the DNA sequence. During PCR the whole plasmid was amplified, so that a new plasmid containing the point mutation was generated. Since only a small amount of DNA was necessary for transformation of heat competent *E. coli*, only a few PCR cycles (10-15) were required. To ensure that only the desired and not an unspecific mutation was created, a polymerase with proofreading activity (3'-5' exonuclease activity) was chosen. In this work the DNA polymerase KAPA HiFi from Peqlab (Erlangen, Germany) was used.

When the PCR was completed, the original DNA plasmid (template) had to be eliminated. The original plasmid was extracted from bacteria and so was methylated, whereas the newly synthesized DNA was not. Therefore DpnI, a restriction enzyme that digests DNA at methylated guanosines, was used to eliminate the original DNA. After two hours of incubation with DpnI the enzyme was inactivated by heat at 80 °C for 20 minutes. The DpnI treated DNA then was directly transformed into competent bacteria.

InFusion PCR method

The InFusion PCR is a method based on the InFusion cloning kit from the company Clontech (Saint-Germain-en-Laye, France). In this PCR reaction special primers were used that consisted of two parts. One part isomerized with the DNA template, the other part consisted of the flanking sequences (approximately 15 nucleotides) of the cloning site

of the target DNA vector. Hence PCR products from InFusion primers had overhangs at the 5' and the 3' end that overlapped with the target DNA vector. The target vector or the target cloning site respectively had to be digested / linearized before starting the InFusion cloning reaction.

The PCR product as well as the linearized target vector were cleaned by agarose gel extraction and then set up in the InFusion reaction. During this reaction the overlapping sequence of the PCR product isomerized with the target sequence and the InFusion Enzyme then ligated the DNA fragments.

Recombinant PCR for creating chimeras between different HyNaC subunits

The recombinant PCR was used to create chimeras between two different HyNaC proteins. Therefore two PCRs were performed successively. In the first PCR each part of the target sequences that were planned to be linked to each other, was amplified. For this first PCR long primers with two different parts were needed, comparable to the InFusion PCR primers. One part isomerized with the DNA sequence of the template DNA to amplifiy it in the first PCR. The other part of this PCR primer had a size of about 15 nucleotides overlapping with the corresponding DNA sequence. In the second PCR both amplicons from the first PCR together with flanking primers that bind to the 5' and the 3' end of the full length DNA sequence were set up. During the second PCR both amplicons from the first PCR isomerized and were amplified as a full length DNA sequence. To clone this new full length coding sequence into a DNA cloning vector, restriction sites were put at the 5' and 3' end of the final amplicon. For PCR protocol see table A.4 in appendix. For a scheme showing the mechanism of recombinant PCR see figure 2.2.

2.3. Cloning of new HyNaC subunits

2.3.1. Sequence identification and primer design

To find new HyNaC sequences, a BLAST search in the NCBI database for sequences showing homology to HyNaC2 - HyNaC5 was performed. Three fully annotated sequences were found: HyNaC6, HyNaC9 and HyNaC10. PCR primers binding at the 5' and the 3' end of these sequences were created to amplify the complete sequences from *Hydra* cDNA. Sequences that showed partial homology to already known HyNaC subunits were amplified using 5' or 3' RACE PCR from *Hydra* cDNA. Primers for RACE

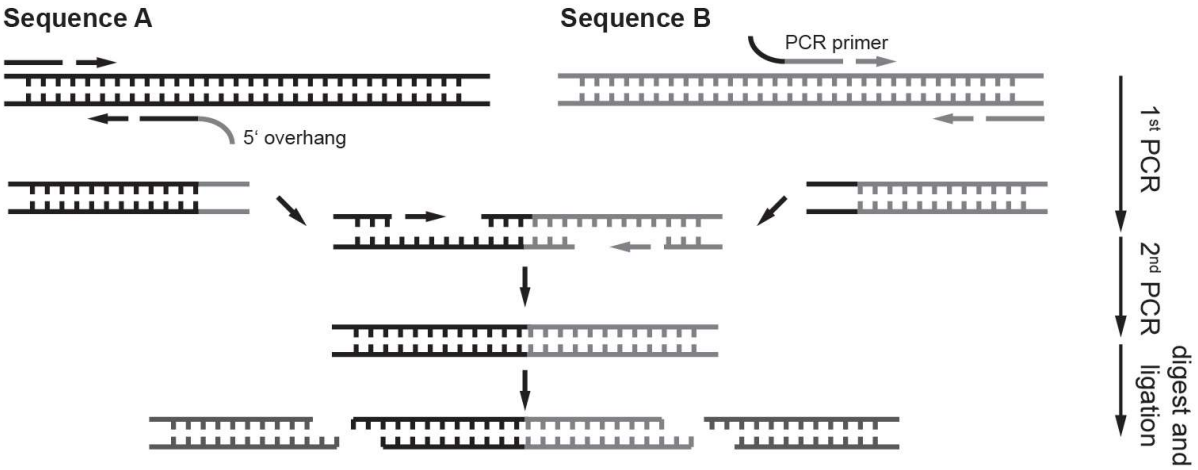

Figure 2.2.: **Mechanism of the recombinant PCR.** In a first PCR reaction the desired DNA sequences are amplified that are planned to be linked to each other. PCR primers for the first PCR reaction produce PCR products with homologous overlapping sequences. In a second PCR the overlapping sequences isomerize and together with flanking primers the full length chimeric DNA sequence is amplified. The 5' and 3' ends of the full length DNA sequence are digested by restriction endonucleases. The digested PCR product than is ligated into a DNA cloning vector linearized with the corresponding restriction enzymes.

PCR were created to amplify in 5' or 3' direction starting within a homologous area thus producing known but also yet unknown DNA sequences. RACE PCR products with corresponding DNA sequence were combined *in silico* to a putative full length HyNaC sequence. Primers binding at the 5' or the 3' end of this artificial sequence were used to amplify the full length PCR product. To verify RACE PCR results, the reaction for each HyNaC subunit was performed at least 2 times with cDNA from two different batches. Five more HyNaC sequences could be identified by RACE PCR. Accession numbers: HyNaC6 HG422725, HyNaC7 HG422726, HyNaC8 HG422727, HyNaC9 HG422728, HyNaC10 HG422729, HyNaC11 HG422730 and HyNaC12 HG422731.

cDNA synthesis and preparation for cDNA

To perform RACE PCR, it was necessary to transcribe RNA into cDNA. Total RNA was isolated form one day starved adult *Hydra magnipapillata* strain 105. The isolated total RNA was a kind gift of Anne Kuhn, COS, Heidelberg. The cDNA synthesis

was performed by using the SMARTer RACE cDNA amplification kit from Clontech (Saint-Germain-en-Laye, France). Using this kit it was possible to create either 3' or 5' RACE ready cDNA. The transcription of RNA into cDNA was performed with the SMARTscribe reverse transcriptase. As a special feature of this kit, the cDNA synthesis created cDNAs that carried a specific binding site at the 3' or 5' end. This binding site was used later in RACE PCR as the template for the corresponding RACE primer provided by Clontech.

RACE PCR and cloning of PCR products

RACE PCR is a difficult method because high background cDNA and low amounts of target cDNA exacerbate the efficiency of the polymerase chain reaction. To increase the PCR efficiency the touchdown PCR method was used. During touchdown PCR the annealing temperature was reduced stepwise. In this work the first two steps contained each five PCR cycles, the first one at about 70 °C and the second one at a five degrees celsius lower primer annealing temperature. At this high temperature conditions only specific priming should take place leading to an amplification of the target sequence above background cDNA. During the third step of the touchdown PCR the temperature was reduced to 45-50 °C. At a low annealing temperature PCR primers bind more often but also more unspecifically. But since during the first ten PCR cycles the target DNA sequence has been amplified several times, unspecific priming and amplification of DNA might no longer interfere with the amplification of the target sequence.

Since the SMARTer RACE cDNA amplification kit was used to generate cDNA, the RACE PCR primer provided by this kit was used. This primer, so-called Universal primer A, was needed as the corresponding primer. Together with the sequence specific primers that were directed either to the 5' end (5'RACE) or to the 3' end (3'RACE) of the cDNA, the target sequence was amplified. For PCR protocol see table A.5 in appendix. The Taq DNA Polymerase (New England Biolabs, Ipswich, USA) was used to amplify the DNA during PCR because it creates 3' adenine overhangs that can be used for the TOPO TA Cloning Kit (Invitrogen life technologies, Carlsbad, USA).

2.4. DNA cloning methods and analyses

2.4.1. Restrictive digestion of PCR-products and plasmid-vectors

Enzymatic and site directed digestion of DNA fragments was performed by using restriction endonucleases, so-called restriction enzymes (New England Biolabs, Ipswich, USA). Restriction digest was used to subclone DNA fragments into plasmid-vectors, to linearize DNA for RNA synthesis or to test successful cloning. Restriction endonucleases recognize defined palindromic DNA sequences where they cut the DNA strand specifically. At the restriction site a specific overhang is left that can be used for ligation of DNA fragments. The restriction digests were done as the manufacturer of the enzymes recommended, regarding temperature, duration and buffer type. Restriction enzymes were purchased from New England Biolabs (Ipswich, USA). For the digestion of 1 μg DNA 10 Units of enzyme were used. Agarose gel electrophoresis was used to test the DNA for complete digestion and to clean up excised DNA fragments.

2.4.2. Cloning and transformation of ligated DNA fragments

T4 ligation

The T4 DNA ligase is an enzyme from the bacteriophage T4. It is able to ligate DNA fragments with one another at their 5' and 3' ends by catalyzing the phosphorylation of the 3' -OH and the 5'-Phosphate at the ribose backbone of doublestranded DNA to a phosphodiester bond. For the ligation of DNA fragments the T4 ligase requires ATP and does not discriminate between sticky or blunt ends. At room temperature sticky end ligations took about 15 minutes, whereas blunt end ligations needed about two hours. Reducing the reaction temperature improved ligation results and efficiency but extended the reaction time. For ligation of PCR products into a cloning vector, usually a three times higher concentration of the insert than of the cloning vector was taken. The concentration of the DNA ligation components was determined with a NanoDrop spectrophotometer (NanoDrop 2000c, Thermo Scientific, Waltham, USA).

TOPO TA cloning

TOPO TA Cloning is a licensed cloning method from Invitrogen life technologies (Carlsbad, USA). With this method PCR products created by Taq DNA polymerase can be subcloned easily. As a special feature of Taq DNA polymerase it generates a short adenosine tail at the 3' end of PCR products. The TOPO TA cloning vector has already

been linearized by the provider at a cloning site, which is flanked by thymidins. Thus the PCR product can bind the vector by AT binding. The binding is supported by a Topoisomerase I near the cloning site, an enzyme that ligates DNA fragments.

Preparation and transformation of heat-competent *E. coli*

As described above, the used strain of *E. coli* was TOP10 provided by Invitrogen life technologies (Carlsbad, USA). To transform DNA constructs into *E. coli*, 1 - 5 μl of the ligation reaction was added to 50 μl of deep frozen bacteria (-80 °C), while they were being thawd on ice. After 30 minutes of incubation on ice the bacteria were heat shocked at 42 °C for 60 seconds. Then they were put back on ice to be chilled for 2 minutes. 300 μl of LB medium was added followed by a 60 minutes incubation at 37 °C to let the bacteria grow and produce resistance to antibiotics. This resistance was coded on the transformed DNA cloning vector. 50 - 100 μl of the bacterial suspension then was put on an agarose plate, which was charged with the antibiotic ampicillin or kanamycin, depending on the resistance coded on the cloning vector.

Preparation of plasmid DNA from transformed *E. coli*

Transformed bacteria were grown on agarose plates where they formed colonies over night. Single colonies then were picked up with a pipette tip or a sterile toothpick and put in 3 ml LB medium containing the same antibiotic as on the agarose plate. The bacteria were incubated for another 16 to 20 hours at 37 °C. The cultured bacteria were mixed gently by continously shaking at about 200 rpm. After this incubation time the cultured bacteria were centrifuged and the DNA was extracted by using the "High pure plasmid isolation kit" provided by Roche Applied Science (Mannheim, Germany).

DNA sequencing

DNA sequencing was performed by MWG Eurofins (Ebersberg, Germany). Therefore 1 μg DNA per sequencing was put in one Eppendorf tube and filled with water up to a volume of 15 μl. If the sequencing primer was not listed to be in stock at MWG Eurofins, 15 μl of 10 pmol/μl primer for the first and 5 μl of 10 pmol/μl for each further sequencing was sent to MWG Eurofins. Sequenced DNA could be downloaded as sequence data files and were analyzed by using Lasergene 10 from DNASTAR, Inc.

2.4.3. Cloning of *in situ* probes for HyNaC subunits and whole mount *in situ* hybridization

In situ probes were used to identify the expression pattern of HyNaC proteins. Therefore parts of the coding sequence of the corresponding HyNaC protein were subcloned into pBluescript KS, a cloning vector that contained a T3 and T7 promoter flanking the multiple cloning site. The size of the *in situ* probe was between 600 and 1400 bp, depending on which *in situ* probe showed the best and most accurate result. The following whole mount *in situ* hybridization was done by Anne Kuhn, Center for organismal studies, Heidelberg, Germany. Therefore the DNA sequence of the *in situ* probes was transcribed into an RNA *in situ* probe that carried an antibody conjugated to an alkaline phosphatase that hydrolysed BMP purple as its substrate [53]. When hydrolysed, BMP purple turned into a blue dye.

2.5. Electrophysiology

2.5.1. Preparation of *Xenopus laevis* oocytes

Adult female animals were anaesthesized with tricaine methanesulfonate from Sigma-Aldrich (St. Louis, USA) (2 g/400 ml) for about 15 minutes. When anaesthesized completely the animals were put on ice and the abdomen was cut open carefully on the lower right or the lower left region 1 - 2 cm above the hip. The ovarial lobes then were pulled out with forceps, cut lose and put into oocyte Ringer's solution 2 (OR-2). While pulling out the oocytes the *Corpus luteum* had to remain in the peritoneum. The abdomen was stitched up, the animal was cleaned with water to free it from the narcotics and then put into a dark basin to recover. The oocytes were still in ovarial lobes and had to be decollated first. Therefore the oocytes were transferred into OR-2 containing 30 mg/ml collagenase from *Clostridium histolyticum* (∼300 U/mg, Worthington, Lakewood, USA) and the ovarial lobes were opened mechanically with forceps. After two hours at room temperature and under constant mixing with a vertical shaker (VIBRAMAX 100, Heidolph, Schwabach, Germany) the oocytes were washed several times with OR-2 to clean the oocytes from the collagenase and cell particles. Using a microscope (Stemi2000C, Carl Zeiss Microscopy GmbH, Jena, Germany), only healthy and two coloured oocytes with a clean separation between animal and vegetale pole in stage V and VI were isolated for injection of cRNA (figure 2.3).

oocyte Ringer's solution 2		**standard bath solution**	
Component	Concentration	Component	Concentration
NaCl	82.5 mM	NaCl	140 mM
KCl	2.5 mM		
Na_2HPO_4	1.0 mM		
$MgCl_2$	1.0 mM	$MgCl_2$	1.0 mM
$CaCl_2$	1.0 mM	$CaCl_2$	1.8 mM
HEPES	5.0 mM	HEPES	10 mM
PVP	0.5 g/l		
Penicilline	1,000 Units/l		
Streptomycine	10 mg/l		
pH adjusted to 7.3 with NaOH		pH adjusted to 7.4 with NaOH	

Table 2.3.: **Components and concentrations of oocyte Ringer's solution 2 (OR-2) and standard bath solution (SB).**

Figure 2.3.: ***Xenopus laevis* as a model organism.** A) Adult female *Xenopus laevis* was the donor animal of B) oocytes that were used for heterologous expression of ion channels and electrophysiological studies.

2.5.2. RNA synthesis and injection

DNA coding for all HyNaC subunits, wild type as well as mutant DNA, was cloned into the oocyte expression vector pRSSP6009, a DNA vector optimized for protein expression in *Xenopus laevis* oocytes. This vector contained the 5' end of β-globin located upstream of the multiple cloning site. The two promoters SP6 and psp3 flanked the multiple cloning site and allowed transcription of the cDNA sequence into cRNA. The transcription was performed by using the kit mMESSAGE MACHINE SP6 or psp3 from Invitrogen life technologies (Carlsbad, USA). Before the cDNA could be transcribed into cRNA, the cloning vector had to be linearized first by restriction digest. Linearization of pRSSP6009 containing sequences of all HyNaC subunits except HyNaC6 was done with the restriction enzyme MluI (New England Biolabs, Ipswich, USA). HyNaC6 had an intrinsic recognition sequence for MluI, thus EcoRI (New England Biolabs, Ipswich, USA) was used for linearization. After an incubation time of two hours at 37 °C the linearized DNA vector was cleaned up with the kit DNA Clean and Concentrator from Zymo Research (Irvine, USA). The HyNaC coding sequence within the cleaned and linearized DNA vector was then transcribed to RNA by the mMessage Machine SP6 kit (Invitrogen life technologies, Carlsbad, USA) for 2 hours at 37 °C. When the transcription was finished the RNA was cleaned up with the kit RNA Clean and Concentrator

from Zymo Research (Irvine USA). Using a NanoDrop (NanoDrop2000c, Thermo Scientific, Waltham, USA) the RNA concentration was determined and adjusted to 400 ng/μl with RNAse free H_2O (Roth, Karlsuhe, Germany). Depending on the expression level of the different HyNaC compositions in *Xenopus laevis* oocytes the RNA was diluted with RNAse free H_2O. 41.6 nl of RNA then was injected into *Xenopus laevis* oocytes using a microinjector (Nanoliter 2000, World precision Instruments, Sarasota, USA). A plexiglass capillary was put on the microinjector to inject the RNA into the oocyte. The Capillary had been pulled out beforehand by a vertical puller (Flaming/Brown Micropipette Puller Model P-97, Sutter Instrument, Novato, USA) with a diameter between 10 - 20 μm. Since the diameter of the tip of the pulled out capillary was too small to guarantee the injection of consistent volumes it was broke manually with forceps and then filled with paraffin oil. Freed from air bubbles this capillary was put on the microinjector and then the RNA was sucked up into the capillary via the microinjector.

2.5.3. Two electrode voltage clamp technique

The Two electrode voltage clamp technique (TEVC) is a method invented by Marmont and Cole (1949) to study the electrical properties of a cell membrane and the ion channels located in it. This method was used for the electrophysiological characterization of ion transport processes across the cell membrane of *Xenopus laevis* oocytes. Therefore two electrodes, potential and current electrode, were put into the *Xenopus laevis* oocyte. Since cell membranes are impermeable for most ions, oocytes are good capacitors that can store negative as well as positive charges. Each electrode had a reference electrode located outside the cell, so that the electrochemical gradient across the cell membrane could be detected, the so-called cellmembrane potential. The current electrode was used to apply a current across the oocyte membrane to generate an artificial membrane potential, the so-called clamping potential. The current needed to clamp the membrane potential to the artificial clamping potential was defined as the net ion flux across the membrane (figure 2.4). In this work oocytes were usually clamped at -70 mV.

Recently, HyNaC2/3/5 has been shown to be permeable for Ca^{2+} by Dürrnagel et al., 2012 [35]. Therefore, all electrophysiological measurements were performed at least 30 minutes after the injection of 50 nl 20 mM EGTA (20 mM EGTA and 10 mM HEPES in H_2O, pH 7.4). An influx of Ca^{2+} induces an activation of calcium activated chloride channels (CaCCs), ion channels endogenously expressed in *Xenopus laevis* oocytes. The injection of EGTA captured the influxing Ca^{2+} and prevented the activation of CaCCs. So just the HyNaC induced currents were detected.

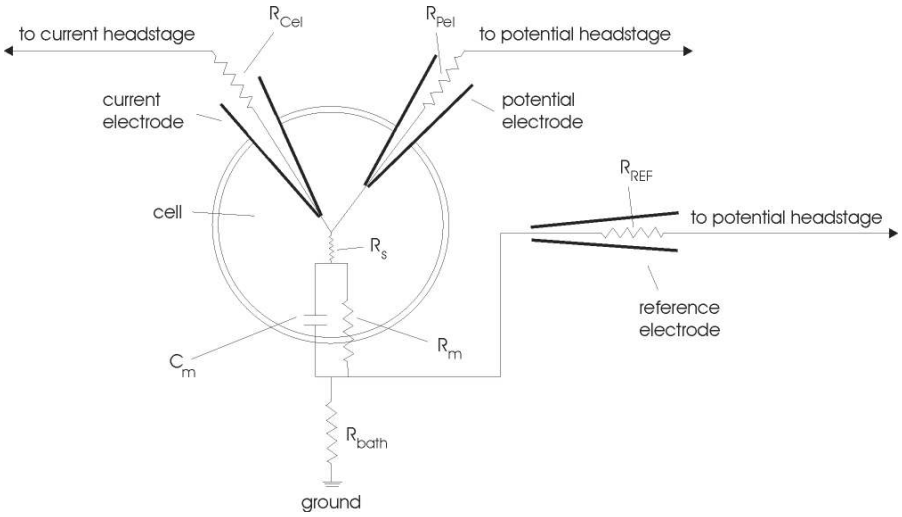

Figure 2.4.: **The two electrode voltage clamp technique.** The two electrode voltage clamp technique (TEVC) relies on two electrodes put into a cell that allow on the one hand to measure membrane potential and on the other hand to apply a defined current across the membrane to generate an artificial clamping membrane potential. The current needed to generate this clamping potential is defined as the net ion flux across the membrane. Illustration adapted from npi manual for TurboTec03X with kind permission of npi-electronics. C_m = membrane capacity, R_m = membrane resistance, R_{CEL} = current electrode resistance, R_{PEL} = potential electrode resistance, R_{REF} = reference electrode resistance, R_S = series resistance.

TEVC set-up

The *Xenopus laevis* oocyte was fixed to a glass pipette by negative pressure and moved into an apparature called oocyte cross. This oocyte cross contained two brackets to fix the two electrodes (current and voltage) and to move them forward and backward and into the oocyte. The reference electrodes for both electrodes were also located in the bath medium within the oocyte cross. A pump was connected to the cross above the oocyte and was used to pump solutions from a petridish into the apparature. This petridish was placed on a turntable totally carrying 20 petri-dishes. This turntable as well as the pump were controlled with the OTC-20 (npi Electronics, Tamm, Germany) [81]. Furthermore the OTC-20 was controlled by a computer running the software Cell-Works 6.2.2 (npi Electronics, Tamm, Germany). The electrodes were connected to the two electrode amplifier TurboTec03X (npi Electronics, Tamm, Germany) that was also

connected to the computer. To visualize the detected signals from the electrodes, the amplifier additionally was connected to the oscilloscope HM507 (Hameg Instruments, Mainhausen, Germany).

Capillaries and electrodes for TEVC technique

To measure the ion current across the membrane of the *Xenopus laevis* oocyte, electrodes had to be put into the cell. Therefore plexiglass capillaries were pulled out with a vertical puller (Flaming/Brown Micropipette Puller Model P-97, Sutter Instrument, Novato, USA) with a diameter resulting in an electrical resistance of 0.1 to 1 MΩ. The tip was filled with 1 mM KCl solution and then a thin silver wire of 15 micrometer diameter, as part of the electrode, was put into the KCl filled capillary. This wire previously had been coated with Cl^- ions by electroplating.

Solutions for electrophysiological measurements

The standard solution for superfusion of *Xenopus* oocytes during electrophysiological measurements was "Standard bath solution" (SB) (table 2.3). All substances used in this work during electrophysiological measurements, like Hydra-RFamides, diminazene and amiloride, were solved in SB. For low and high Ca^{2+} measurements as well as Na^+ free measurements, alterations of SB were used (Tab.2.4).

sodium free SB 1 mM Ca^{2+}		**sodium free SB 10 mM Ca^{2+}**	
Component	Concentration	Component	Concentration
NMDG-Cl	140 mM	NMDG-Cl	126.5 mM
$CaCl_2$	1.0 mM	$CaCl_2$	10.0 mM
HEPES	10.0 mM	HEPES	10 mM
pH adjusted to 7.4 with HCl		pH adjusted to 7.4 with HCl	

Table 2.4.: **Sodium free SB solutions for detecting calcium permeability of HyNaCs.**

2.6. Recording and statistical analysis

2.6.1. Recording of TEVC detected currents

Recording of the TEVC detected currents was performed with the software Cellworks 6.2.2 (npi Electronics, Tamm, Germany). The sampling frequency was 0.1 to 1 kHz with a filtering rate of 20 Hz. Recorded data was saved on a hard drive and analyzed with the softwares Cellworks and Igor Pro 6.02A (WaveMetrics). The standard condition for electrophysiological measurements was at a clamping potential of -70 mV at room temperature.

2.6.2. Statistical analysis and figures

Statistical analysis was done with Microsoft Excel for Mac 2008. Significance of data points was determined by the student's paired or unpaired t-test. Level of significance in this work is shown as follows: $p > 0.05$ = not significant (n.s.), $p < 0.05$ (*), $p < 0.01$ (**), $p < 0.001$ (***). The presented data in this work are mean values ± standard error of the mean (SEM). SEM is calculated as standard deviation divided by the square root of the number of data points n. Every measurement was performed at least five times in *Xenopus laevis* oocytes from at least two different batches. All figures shown in this work and created from the collected data were edited with Adobe Illustrator CS6.

Concentration dependent activation (EC_{50}) or inhibition (IC_{50})

The affinity of the different HyNaCs for different activators (EC_{50}) and inhibitors (IC_{50}) were calculated by using the Hill Equation (Hill, 1910; equation 2.1). Therefore the activator/inhibitor was applied in an increasing concentration from almost no effect to a saturated effect. The currents were normalized to the highest detected current. The Hill fit for these measurements was performed with Igor Pro 6.02A (WaveMetrics).

$$I = a + \frac{(I_{max} - a)}{[1 + (\frac{EC_{50}}{[c]})^n]} \tag{2.1}$$

I_{max} = highest detected current
a = residual current
[c] = ligand concentration
EC_{50} = ligand concentration that leads to a half maximal activation of ion channels
n = Hill coefficient

Calculation of HyNaC reversal potentials and calcium permeabilites

Important for the calculation of reversal potentials is to detect background currents generated by endogenous ion channels in *Xenopus laevis* oocytes or damages in the oocyte membrane caused by the electrodes. HyNaCs are closed at rest, so the background current was detected by performing the experiment under absence of the activating ligand. This current then was subtracted from the current detected at Hydra-RFamide I activated HyNaCs.

Reversal potentials were detected by clamping the membrane potential to -100 mV and then changing the potential continuously to +30 mV over two seconds. The first detected positive current data point was defined as the reversal potenial (E_{Rev}). The effect of membrane potential (V) to the transmembrane current (I) is called I-V relationship.

HyNaCs are permeable for calcium [35]. Therefore the oocytes were injected with 20 mM EGTA before performing measurements to abolish the effect of endogenously expressed calcium activated chloride channels (CaCCs).

Since HyNaC2/3/5 is permeable for calcium, it was of interest to find out if the newly cloned HyNaCs in this work were also permeable for calcium. Based on the Goldman-Hodgkin-Katz equation the permeability for Ca^{2+} was calculated from the shift in reversal potential (E_{Rev}) when Na^+ is exchanged by Ca^{2+} as the main permeant cation [9, 76] (equation 2.2).

$$\frac{P_{Ca^{2+}}}{P_{Na^+}} = \frac{[Na^+]_o(1 + e^{\frac{E_{Ca}*F}{R*T}})}{4[Ca^{2+}]_o e(\frac{\Delta E_{Rev}*F}{R*T})} \tag{2.2}$$

$\Delta E_{Rev} = E_{Na^+}\text{-}E_{Ca^{2+}}$
R = gas constant
F = Faraday constant
T = temperature in Kelvin

For the determination of E_{Rev} for Na^+ as the main permeant cation, the voltage ramp was performed with SB solution containing 140 mM Na^+. E_{Rev} for Ca^{2+} was determined with Na^+ free SB solution containing 10 mM Ca^{2+}.

Since ions behave differently in solutions, the ionic activity was used for calculations instead of the concentration [c]. The ionic activity allows a higher accuracy of the calculations. To calculate the ionic strength, a modification of the Davies equation was used [9, 30](equation 2.3).

$$\log_{10} f_i = -0.509 z^2 \left(\frac{\sqrt{I}}{1+\sqrt{I}} - 0.2 \right) \tag{2.3}$$

f_i= activity coefficient of single ions i
I = ionic strength
z = valence

thereby the ionic strength I is defined as follows [9]

$$I = 0.5 \sum c_i z_i^2 \tag{2.4}$$

2.7. Phylogenetic Analysis of DEG/ENaC family members

In this work four new cDNAs with homology to HyNaC2 - HyNaC5 were cloned from *Hydra magnipapillata* total RNA. The proteins coded by these cDNAs were called HyNaC9 - HyNaC12. Three further subunits, HyNaC6 - HyNaC8, already had been cloned by Dr. Stefan Dürrnagel and were characterized in this work. These new cDNAs were submitted to the GenBank^{TM}/EBI database. Accession numbers see table A.1 in appendix. To analyze and compare the sequence homology between the new HyNaCs and other DEG/ENaC ion channel family members, sequences of other DEG/ENaC proteins were downloaded from the NCBI data base (Table A.1 in appendix). The protein sequences of HyNaC subunits and other DEG/ENaC ion channel family members were aligned using the program ClustalX [73]. Highly divergent regions that were not conserved between the different proteins were deleted. The revised sequences were then aligned again using ClustalX (figure A.1 in appendix) and then used for creating phylogenetic trees (figure 3.3). Phylogenetic trees were created with the program TREE PUZZLE [102] by maximum likelihood analysis (ML). The phylogenetic trees created with TREE PUZZLE were illustrated with the bioinformatic software Unipro UGENE [87] or Dendroscope 3 [61].

To align only HyNaC members and to compare the full length sequences (figure 3.1) the program MegAlign v. 10 provided by DNA Star Inc. was used.

3. Results

3.1. Cloning and phylogenetic analysis of new members of the *Hydra* sodium channel (HyNaC) subfamily

3.1.1. HyNaC subunits share conserved structures of the DEG/ENaC ion channel superfamily

So far, four HyNaC subunits were known from *Hydra magnipapillata* [36, 45]. In order to identify additional putative HyNaC subunits, a BLAST analysis was performed. A subsequent homology cloning from *Hydra magnipapillata* cDNA revealed seven novel HyNaC subunits. They were named HyNaC6 - HyNaC12 (Accession numbers see table 1 from appendix). HyNaC6 - HyNaC8 had already been cloned by Dr. Stefan Dürrnagel and were characterized in this work.

Similar to the already known HyNaC subunits 2 - 5, all newly cloned HyNaC subunits had a length between 454 and 507 amino acids and a predicted molecular weight between 52.9 and 58.4 kDa. The overall sequence identity between HyNaC2 - HyNaC11 varied from 29% to 70%. HyNaC6 and HyNaC7 showed a higher identity of 75%, the highest identity of 85% was found between HyNaC3 and HyNaC11. HyNaC12 showed the lowest sequence identity of 14% to 19% to the other HyNaCs. Compared to two other representatives of the DEG/ENaC ion channel family, rASIC1a and rBASIC, the sequence identity varied between 10 and 30% (table 3.1). Thus, six out of the seven newly cloned HyNaC subunits showed a high degree of sequence identity to the already known subunits HyNaC2 - HyNaC5.

Considering the high degree of sequence identity between HyNaC2 - HyNaC11, in the next step it was of interest if conserved structures typical for the DEG/ENaC ion channel family were present in the newly cloned HyNaC proteins. Figure 3.1 shows a ClustalW alignment of all HyNaC subunits and, for comparison, rBASIC and rASIC1a.

Like other DEG/ENaC channels, HyNaC6 - HyNaC12 have short intracellular N- and C-termini, two transmembrane domains (TMDs) and a large extracellular domain

	HyNaC2	HyNaC3	HyNaC4	HyNaC5	HyNaC6	HyNaC7	HyNaC8	HyNaC9	HyNaC10	HyNaC11	HyNaC12	rAsic1a	rBASIC
HyNaC2		29.9	30.3	42.1	44.7	41.7	30.1	29.3	30.0	31.2	15.8	28.0	23.0
HyNaC3	29.9		65.5	29.7	28.9	29.8	51.6	64.7	68.8	84.7	18.3	28.5	26.3
HyNaC4	30.3	65.5		28.4	27.5	29.1	50.0	59.7	62.1	62.3	15.6	28.4	25.6
HyNaC5	42.1	29.7	28.4		52.5	51.7	28.6	30.6	29.3	28.8	16.5	28.1	20.5
HyNaC6	44.7	28.9	27.5	52.5		74.7	29.1	30.8	27.6	29.5	13.7	25.4	20.4
HyNaC7	41.7	29.8	29.1	51.7	74.7		29.3	29.4	28.3	29.2	16.1	24.0	20.2
HyNaC8	30.1	51.6	50.0	28.6	29.1	29.3		48.9	49.4	51.8	17.4	29.2	26.7
HyNaC9	29.3	64.7	59.7	30.6	30.8	29.4	48.9		64.9	63.2	16.3	28.3	27.8
HyNaC10	30.0	68.8	62.1	29.3	27.6	28.3	49.4	64.9		64.8	17.8	27.6	26.1
HyNaC11	31.2	84.7	62.3	28.8	29.5	29.2	51.8	63.2	64.8		18.4	28.7	26.0
HyNaC12	15.8	18.3	15.6	16.5	13.7	16.1	17.4	16.3	17.8	18.4		17.4	16.6
rAsic1a	28.0	28.5	28.4	28.1	25.4	24.0	29.2	28.3	27.6	28.7	17.4		29.4
rBASIC	23.0	26.3	25.6	20.5	20.4	20.2	26.7	27.8	26.1	26.0	16.6	29.4	

Percent identity

Table 3.1.: **Sequence identity of HyNaC subunits.** Sequence identities of HyNaCs, rASIC1a and rBASIC in percent, calculated from ClustalW analysis (MegAlign 10, DNA Star). HyNaC subunits showing very low or very high sequence identity are highlighted. Accession numbers see table A.1 in appendix.

(ECD).

The **histidin-glycine (HG) motif** is located at the intracellular N-terminal domain about 15 amino acids before TMD1 and is found in all members of the DEG/ENaC ion channel family. This protein motif was also present in all new HyNaC proteins. Shortly before TMD1 a conserved **di-arginine motif** (RR) is found in most DEG/ENaC ion channel family members. For HyNaC2 - HyNaC9 and HyNaC11 this RR motif was completely conserved. In the protein sequence of HyNaC10 the first arginine was exchanged to a cysteine, whereas for HyNaC12 the RR motif was missing. A highly conserved **tryptophane (W)** located at the N-terminal end of TMD1 is conserved in most DEG/ENaC channels including all newly cloned HyNaC proteins. At the proximal end of the ECD a conserved **FPAxTxCN** sequence is found. In general, this sequence was conserved in all HyNaC subunits, but in different HyNaC subunits single amino acids of this motif were changed. The x, which represents a variable amino acid, was occupied by hydrophobic, non polar amino acids like valine (V) or phenylalanine (F) in all HyNaC subunits.

DEG/ENaCs share **conserved cysteines** in the ECD, so-called cysteine rich domains, that are crucial for the tertiary structure of the protein. Twelve cysteines conserved in all HyNaC subunits were found in their extracellular domains.

The so-called **DEG position**, named by its first description in a mutant degenerin

channel in *C. elegans* [12], is located immediately N-terminal to TMD2. In all HyNaC proteins it was occupied by a glycine.

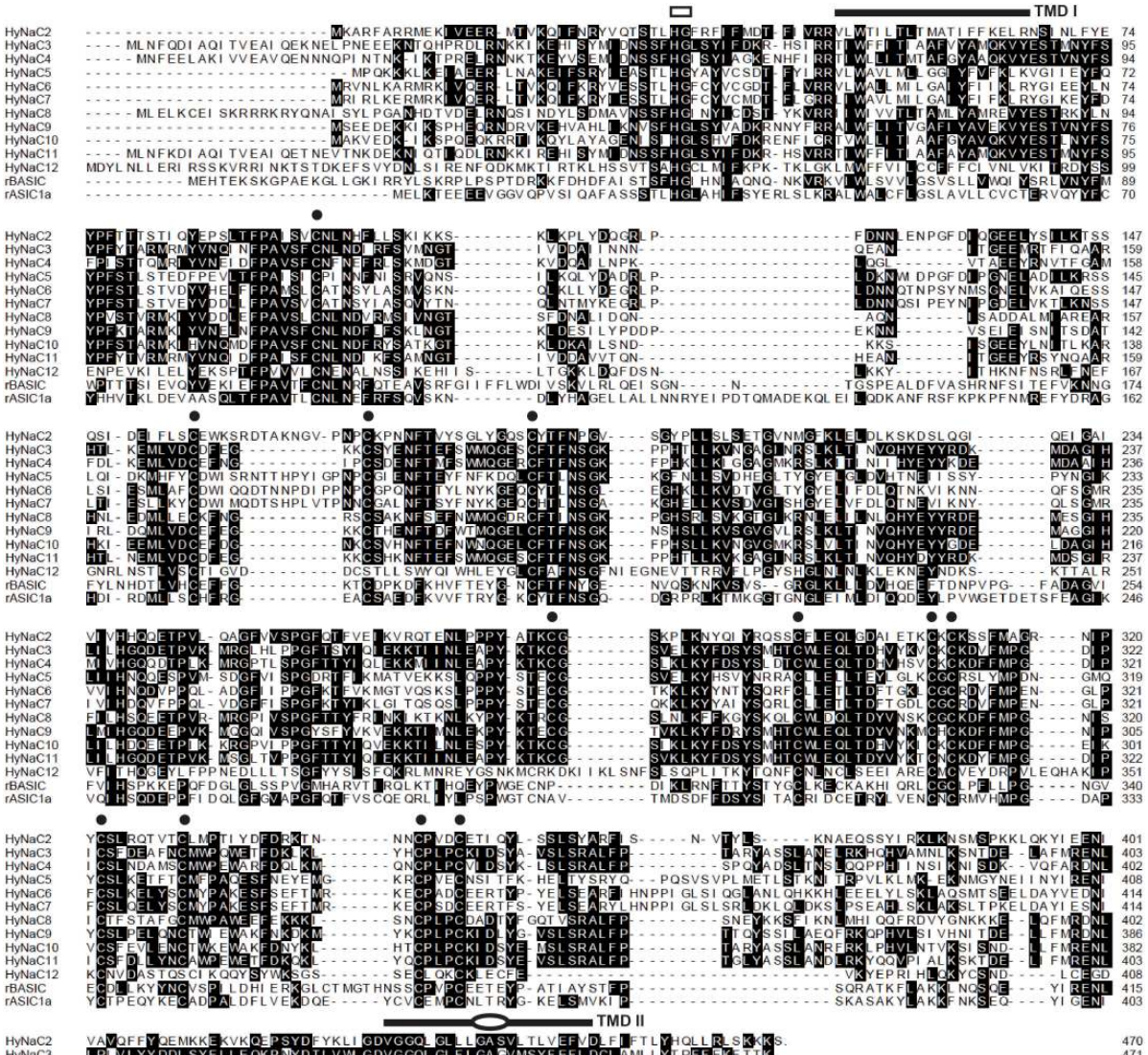

Figure 3.1.: **All HyNaC subunits share conserved DEG/ENaC motifs.** ClustalW Protein alignment of HyNaC proteins. Conserved amino acids are highlighted in black. 23 C-terminal amino acids of rASIC1a have been truncated. Black bars = TMDI and TMDII, black dots = highly conserved cysteins, black ellipse = selectivity filter, open bar = HG motif. Accession number table A.1 in appendix.

The selectivity filter in the center of TMD2 is formed by a **glycine/serine-x-serine (G/S-x-S) motif** [35, 67, 68, 69, 103, 106, 120]. All newly cloned HyNaC subunits contained this G/S-x-S motif, in most cases formed by a GAS (glycine-alanine-serine) or a GAG (glycine-alanine-glycine) sequence. Interestingly, the amino acid sequence of HyNaC12 contained a GFS motif that is found only in few invertebrate DEG/ENaC channels from *D. melanogaster* and *C. elegans*, suggesting that HyNaC12 might show a different ion selectivity than the other HyNaCs.

3.1.2. Phylogenetic analysis of HyNaCs and other DEG/ENaC ion channel family members

To illustrate the phylogenetic distance between all HyNaC subunits, their protein sequences were aligned with the software ClustalX. Based on this alignment a maximum likelihood (ML) tree was created using TREEPUZZLE. In this analysis, HyNaC subunits were compared to rASIC1a and rBASIC.

The ML tree drawn by Dendroscope in figure 3.2 revealed clustering of HyNaC subunits into two subclusters. One cluster was formed by HyNaC3, HyNaC4 and HyNaC8 – HyNaC11, another cluster was formed by HyNaC2 and HyNaC5 – HyNaC7. HyNaC2 - HyNaC11 were located on a common branch separated from the branch of rBASIC and rASIC1a. HyNaC12 was not part of these clusters and was isolated from HyNaC2 - HyNaC11, rBASIC and rASIC1a.

To further study the phylogenetic distance of the HyNaC subfamily to other members of the DEG/ENaC ion channel family, a second ML analysis was performed using TREEPUZZLE. The phylogenetic tree containing 75 members of the DEG/ENaC ion channel family (figure 3.3) revealed a formation of different subclusters. One branch of this phylogenetic tree was formed by the HyNaC, BASIC and ASIC subfamilies, which all formed subclusters on this branch (figure 3.3). Three other branches were formed by ENaC, FaNaC and seven degenerins from *C. elegans*, respectively. Interestingly, both peptide gated ion channel subfamilies within the DEG/ENaC channel family, HyNaC and FaNaC, were located on different branches of the phylogenetic tree, indicating that they are no direct orthologues. PPK channels from *Drosophila spp.* formed two branches with 4 and 5 subfamily members, respectively (figure 3.3). All remaining DEG/ENaC ion channel family members were isolated or formed small branches containing two proteins. Interstingly, HyNaC12 was neither located on the branch of HyNaCs, ASICs and BASICs nor on branches with other members of the DEG/ENaC ion channel family.

Similar to previous findings for **HyNaC2/3/5** [45], HyNaC6 - HyNaC11 are closely related to ASICs and BASICs while they are distantly related to FaNaC. The large phylogenetic distance between HyNaC12 and other HyNaC proteins suggests an evolution from different ancestor proteins, different gating mechanisms and functions.

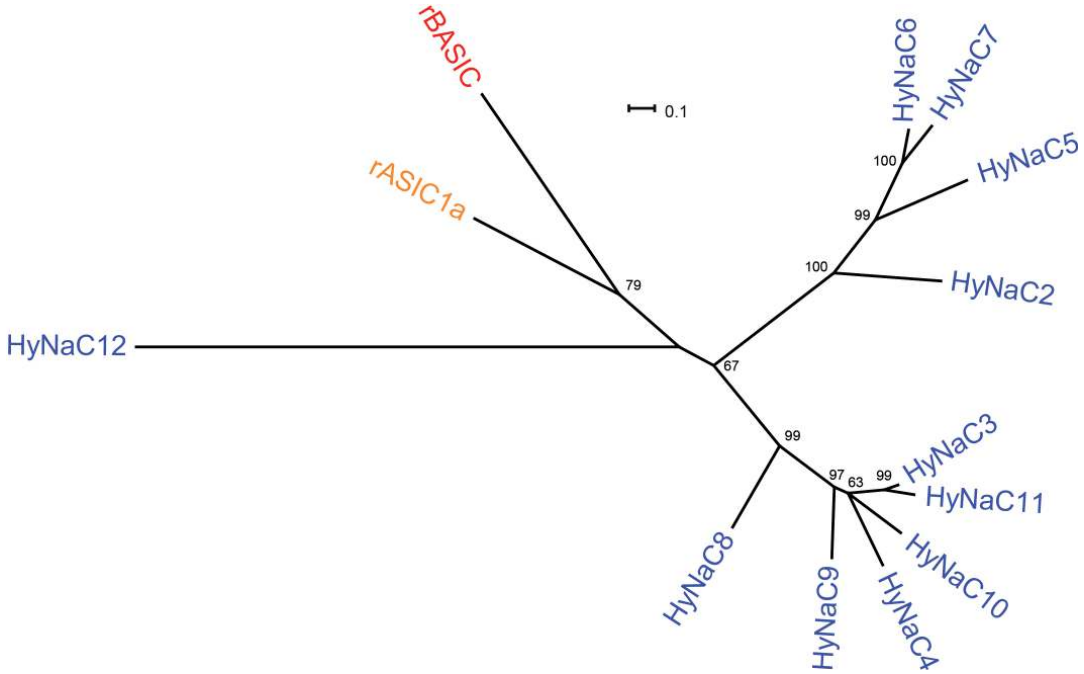

Figure 3.2.: **Phylogenetic tree demonstrating the genetic relation between HyNaC subunits.** ML tree of HyNaCs, unrooted phylogram drawn by Dendroscope 3 [61]. HyNaC proteins were compared to rBASIC and rASIC1a. Numbers at branches show fidelity of the branch in %. Scale bar indicates amino acid exchanges per site. Accession numbers see table A.1 in appendix.

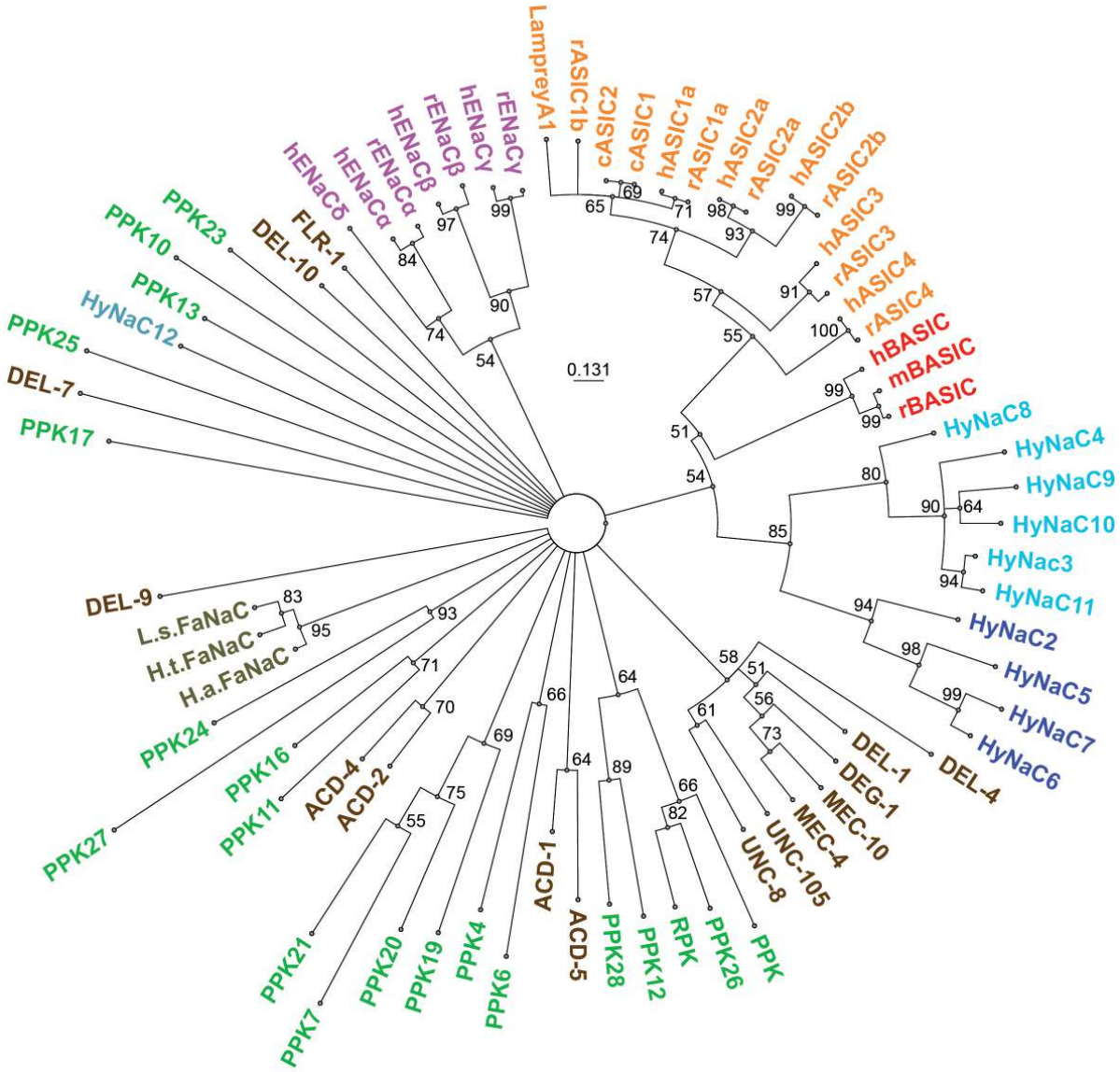

Figure 3.3.: **Phylogenetic tree of the DEG/ENaC ion channel family.** Phylogenetic tree from ML analysis performed with TREEPUZZLE and 75 members of the DEG/ENaC ion channel family. Illustration done with UGENE [87], showing an unrooted circularized phylogram. For ClustalX alignment that underlies the phylogenetic tree, see figure A.1 and for accession numbers see table A.1 in appendix.

3.1.3. Expression pattern of the members of the HyNaC subfamily

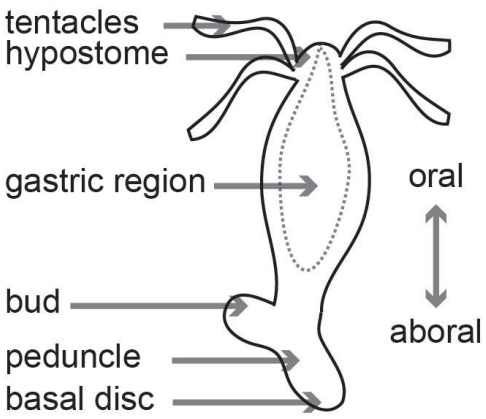

Figure 3.4.: **Scheme showing the anatomy of *H. magnipapillata*.**

In situ hybridization (ISH) was used to study the expression pattern of the newly cloned HyNaC subunits. Whole mount ISH of HyNaC subunits were performed by Anne Kuhn in the Centre for Organismal Studies (COS), Heidelberg. It has previously been shown that *hynac2* – *hynac5* are expressed at the tentacle basis of *Hydra magnipapillata* [36, 45]. For anatomical overview of *Hydra magnipapillata* see figure 3.4.

ISH revealed the expression of all new HyNaC mRNAs except *hynac12* in adult *Hydra magnipapillata*. Similar to *hynac2/ 3/5*, *hynac6* and *hynac11* were expressed at the tentacle basis. *hynac6* was expressed at the aboral side, whereas *hynac11* was expressed at the oral and aboral side of the tentacle basis. Surprisingly, *hynac7*, *hynac9* and *hynac10* were expressed at the peduncle of *Hydra magnipapillata*, right above the basal disc. In addition, an expression of *hynac10* mRNA was detected at the hypostome and a low expression level of *hynac9* was detected along the complete body axis. The expression pattern of *hynac8* was equally distributed over the whole body column of the adult animal. In contrast, ISH did not show any expression of *hynac12* in *Hydra magnipapillata* (figure 3.5).

Reviewing previous findings of the expression pattern of *hynac2* - *hynac5* demonstrated that *hynac2* and *hynac3* were expressed in the tentacle basis as well as in the whole body column. The expression level in the whole body column was lower than at the tentacle basis. *hynac4* and *hynac5* were found exclusively at the tentacle basis (figure 3.5).

The finding that *hynac* RNA was not exclusively expressed at the tentacle basis suggests new physiological roles of HyNaCs *in vivo* apart from tentacle contractions. **HyNaC2/3/5** is activated by Hydra-RFamides I and II [36], which both derive from preprohormone A. Since preprohormone A is expressed at the tentacle basis as well as the peduncle [28], HyNaC proteins expressed at the peduncle region could be activated by Hydra-RFamides *in vivo*.

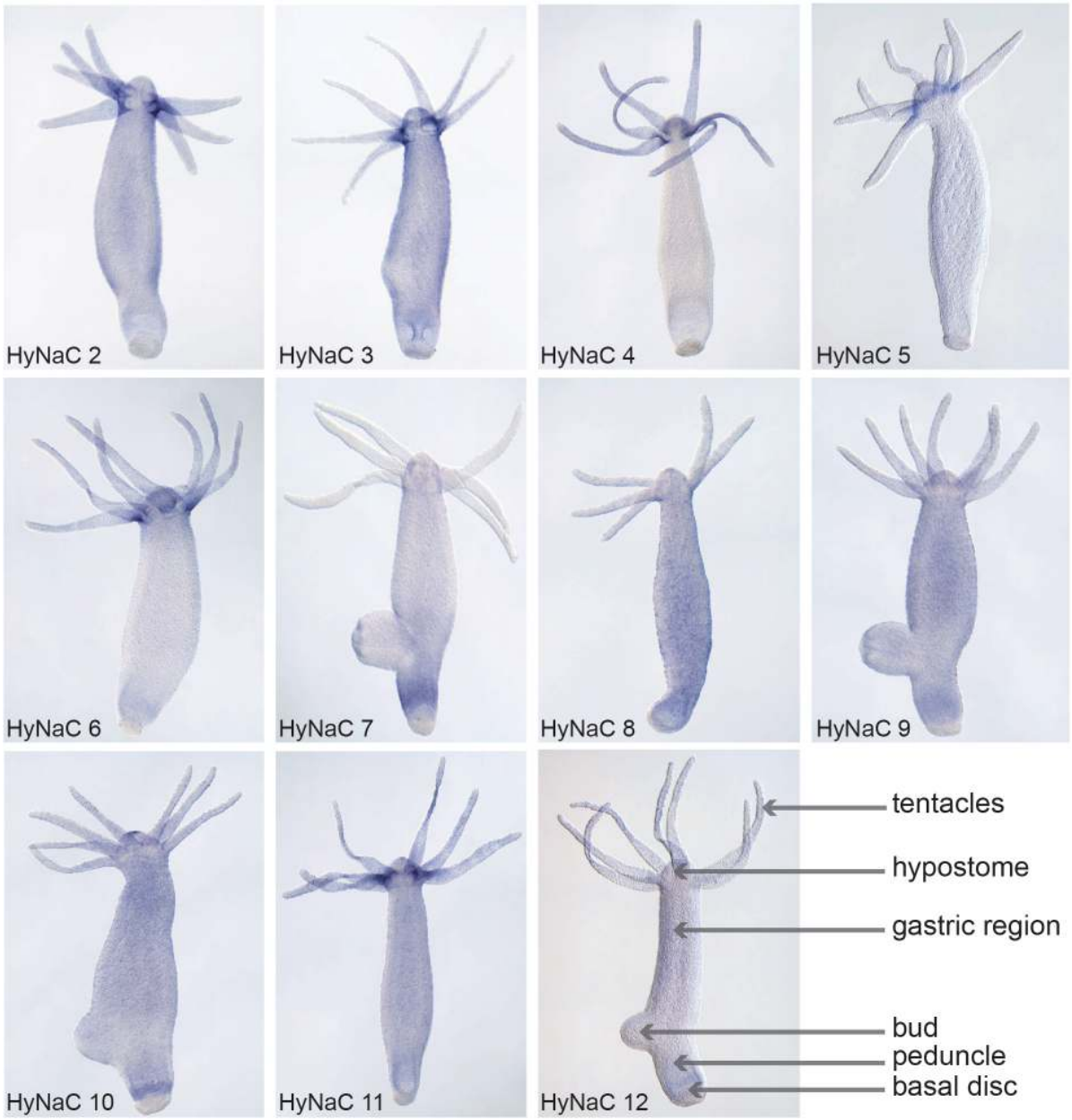

Figure 3.5.: **Whole mount *in situ* hybridization of HyNaC subunits in *Hydra magnipapillata*.** Whole mount *in situ* hybridization was performed by Anne Kuhn, COS, Heidelberg. *In situ* probes were detected by an antibody conjugated to an alkaline phosphatase; positive *in situ* hybridization highlighted in dark blue.

3.2. Rules of subunit assembly and apparent ligand affinity of HyNaCs

3.2.1. New HyNaC subunits form heterotrimeric ion channels

To test the newly cloned HyNaC proteins for subunit assembly and formation of functional ion channels, cRNA was injected initially in pools of four different HyNaC subunits into *Xenopus laevis* oocytes. When the injection of a cRNA pool resulted in functional ion channel formation, one, two or three cRNAs of this pool were injected simultaneously. Electrophysiological examinations were performed using TEVC.

A natural ligand for **HyNaC2/3/5** is Hydra-RFamide I. Furthermore **HyNaC2/3/5** is blocked by extracellular calcium, and lowering the concentration of extracellular Ca^{2+} to 10 nM activates the channel independently from any ligand [36]. Thus the new HyNaC combinations were tested for functional subunit assembly by reducing the extracellular Ca^{2+} concentration and by application of 5 μM Hydra-RFamide I (figure 3.6).

When injected alone, no HyNaC subunit was able to form an active ion channel. The injection of a pool of 4 subunits from the two subclusters of HyNaC proteins never elicited any current when HyNaC2 was missing. Simultaneous expression of HyNaC2 and a second HyNaC subunit led to the assembly of an active ion channel only in the case of HyNaC2/3. This channel had already been described previously [45].

However, heterologous expression of three proteins resulted in the formation of several functional ion channels that were closed at rest and activated by neuropeptides (figure 3.6, table 3.2), demonstrating that the new HyNaC subunits form heteromultimeric ion channels. HyNaC2 was identified as a necessary subunit for every functional ion channel. When HyNaC2 was missing, no subunit combation resulted in a functional channel. Corresponding to the subunit clustering in the phylogenetic analysis, the two other subunits that were required in addition to HyNaC2 could be divided into two subgroups. The first subgroup consisted of HyNaC3, HyNaC4 and HyNaC8 – HyNaC11 and the second subgroup of HyNaC2 and HyNaC5 – HyNaC7. To form a functional channel one representative of each subgroup was required in addition to HyNaC2.

Not every heterotrimeric subunit combination containing HyNaC2 resulted in a functional ion channel. HyNaC2 and HyNaC5 formed a functional heterotrimeric channel with HyNaC3, HyNaC9 and HyNaC11. HyNaC2 and HyNaC7 formed ion channels with every subunit of the first subgroup except HyNaC8. Furthermore HyNaC2 and

HyNaC6 formed heterotrimeric ion channels together with all subunits from the first subgroup (table 3.2). All functional channels were activated by lowering the extracellular Ca^{2+} concentration. Hydra-RFamide I activated every functional channel except **HyNaC2/9/5**, suggesting a different natural ligand for **HyNaC2/9/5** (table 3.2). When activated by neuropeptides, all new HyNaCs showed a biphasic current in *Xenopus* oocytes (figure 3.6), as it has been reported previously for **HyNaC2/3/5** [36, 35], suggesting that all newly cloned HyNaCs are permeable for Ca^{2+}.

In contrast to all other HyNaC subunits, HyNaC12 could neither be activated by Hydra-RFamide I nor by lowering the extracellular Ca^{2+} concentration when coexpressed with pools of other HyNaC subunits. The pools of HyNaC subunits always contained HyNaC2 and HyNaC12 and one member of each subgroup with the exception of HyNaC3. Also the introduction of an amino acid exchange at the so-called DEG position (G436T), which is known to generate consitutively active ion channels in degenerins from *C. elegans* [12], did not activate HyNaC12.

The results from ISH (figure 3.5) demonstrate that only some HyNaC subunits show

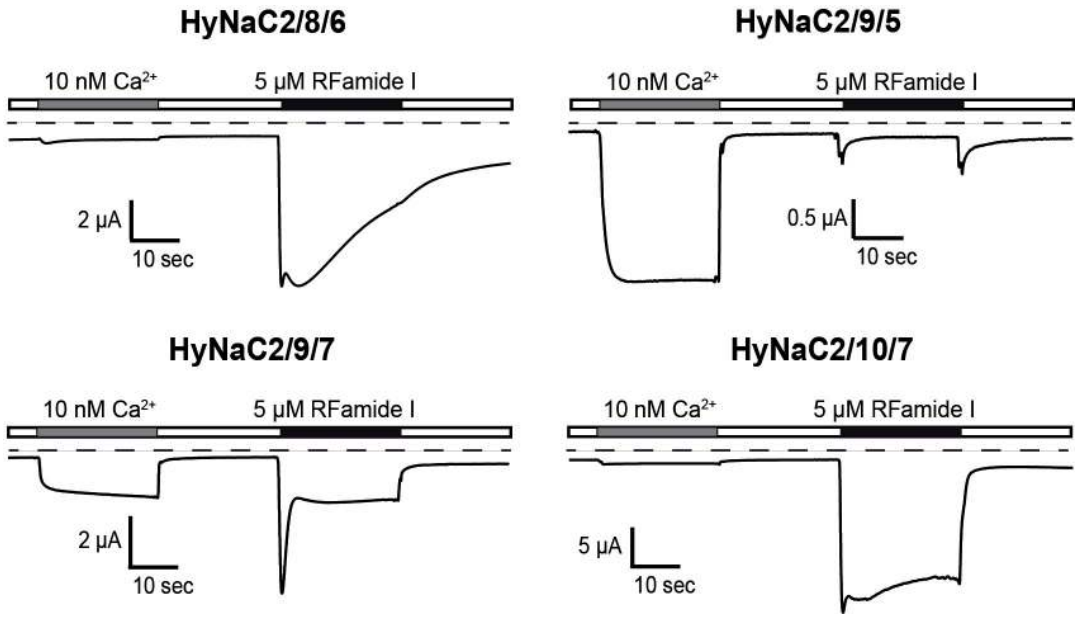

Figure 3.6.: **Representative current traces of new HyNaC heterotrimers.** Representative TEVC current traces of *Xenopus laevis* oocytes expressing HyNaC heterotrimers. New HyNaC combinations were tested for activation by application of 5 μM Hydra-RFamide I (black bars) and by reducing the extracellular Ca^{2+} concentration (grey bars). Oocytes were **not** injected with EGTA before measurement.

an overlapping expression pattern. To curtail the large number of possible HyNaC heterotrimers, only those combinations were analyzed in detail that had overlapping expression in ISH (table 3.2, highlighted in grey).

2	3	4	8	9	10	11
5	+	-	-	(+)	-	+
6	+	+	+	+	+	+
7	+	+	-	+	+	+

Table 3.2.: **Two subgroups of HyNaC subunits form functional heterotrimeric ion channels.** Possible trimeric combinations of all different HyNaCs. A functional channel is represented by "+", a non-functional channel by "-". **HyNaC2/9/5**, which was not activated by Hydra-RFamide I but by lowering the extracellular Ca^{2+} concentration is shown by "(+)". Based on the results from the *in situ* hybridization (figure 3.5), putative physiological HyNaC combinations are highlighted in grey.

Nine Hydra-RFamides (I - IX) are presumably generated from three preprohormones found in *Hydra magnipapillata*. Four Hydra-RFamides, RFamide I to RFamide IV, previously have been tested on **HyNaC2/3/5**. Only Hydra-RFamides I and II activate **HyNaC2/3/5** with high affinity [28, 36]. Since the new HyNaC subunits increased the number of putative physiological HyNaC channels from one to six, it was of interest to find out if these ion channels are activated by Hydra-RFamides III-IV. Additionaly, another, yet untested, Hydra-RFamide, RFamide V, was applied to the new HyNaC channels.

Interestingly, no HyNaCs were activated by Hydra-RF-amides III, IV and V (5 μM each), as it is demonstrated in figure 3.7 for **HyNaC2/11/5**. HyNaC12 was also not activated by Hydra-RFamide III-V when coexpressed with a pool of four different HyNaC subunits.

In summary, similar to **HyNaC2/3/5**, HyNaC6 - HyNaC11 are subunits of heterotrimeric ion channels, which are activated by Hydra-RFamide I. By cloning of HyNaC6 the interaction partner of HyNaC4 was identified, since in presence of HyNaC2 both subunit assemble to the functional heterotrimer **HyNaC2/4 /6**. Since no HyNaC combination was activated by Hydra-RFamides III to V, Hydra-RFamide I and II remain

as the only known natural ligands for HyNaCs.

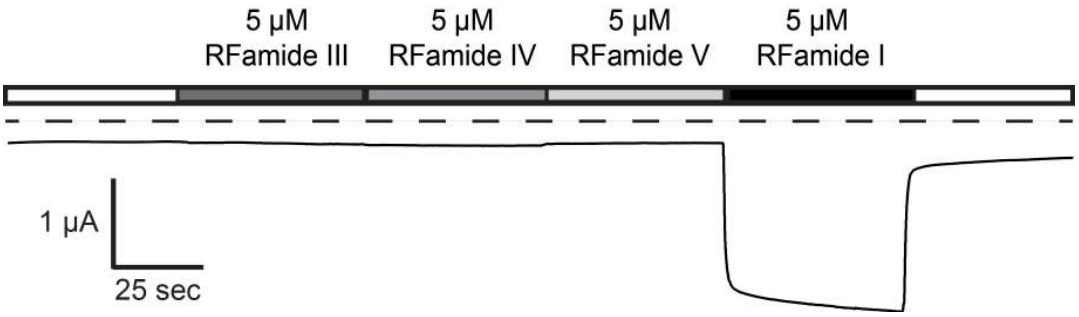

Figure 3.7.: **Hydra RFamides III - V do not activate HyNaCs.** *Xenopus* oocyte expressing **HyNaC2/11/5**. TEVC recording demonstrating the effect of Hydra-RFamides I and III - IV (5 μM each) on HyNaC activity.

3.2.2. Hydra-RFamides I and II are high affinity ligands of HyNaCs

In a recent study **HyNaC2/3/5** has been shown to be permeable for Ca^{2+}, which leads to the activation of an endogenous intracellular calcium activated chloride channel (CACC) in *Xenopus laevis* oocytes [35]. The activation of the CACC channels causes a biphasic current of HyNaC2/3/5. After injection of EGTA, a Ca^{2+}-chelator that binds free calcium ions (chapter 2.5.3), the activation of **HyNaC2/3/5** by Hydra-RFamide follows a simple on/off characteristic. Since all new HyNaCs showed a biphasic current when activated by Hydra-RFamide I, suggesting a high calcium permeability, all further studies were performed after injection of EGTA into the oocytes.

To study the apparent ligand affinity of the new HyNaC heterotrimers, Hydra-RFamide I was applied in increasing concentrations. For a detailed overview of apparent ligand affinities (EC_{50}) for Hydra-RFamide I see table A.2 in appendix. When oocytes were not previously injected with EGTA, **HyNaC2/3/5** was activated by Hydra-RFamide I with an EC_{50} of 4.8 $\pm$ 2 μM, as it was published in 2010 by Dürrnagel et al. After injection of EGTA the apparent ligand affinity for Hydra-RFamide I of **HyNaC2/3/5** was in the same range with an EC_{50} of 3.5 $\pm$ 0.6 μM (figure 3.8, table A.2). Exchanging HyNaC3 by HyNaC11, resulting in **HyNaC2/11/5**, reduced the apparent ligand affinity for Hydra-RFamide I to 13.8 $\pm$ 1.9 μM ($p < 0.001$, figure 3.8, table A.2).

Interestingly, heterotrimers containing HyNaC6 instead of HyNaC5 showed a five to ten times higher apparent affinity for Hydra-RFamide I than **HyNaC2/3/5** ($p \leq 0.001$). The apparent affinity of HyNaC6 containing heterotrimers varied between 0.29 $\pm$ 0.06

μM for **HyNaC2/3/6** and 0.70 ± 0.08 μM for **HyNaC2/4/6** (figure 3.8, table A.2).

Two heterotrimers containing HyNaC7, **HyNaC2/3/7** and **HyNaC2/9/7**, even showed an up to 100 times higher apparent ligand affinity than **HyNaC2/3/5** ($p \leq 0.001$). The highest apparent ligand affinity of all HyNaCs for Hydra-RFamide I was found for the heterotrimer **HyNaC2/9/7** with an EC_{50} of 0.04 ± 0.01 μM (figure 3.8, table A.2).

In contrast, **HyNaC2/10/7** showed a much lower affinity for Hydra-RFamide I than **HyNaC2/3/5**. Since an application of 100 μM Hydra-RFamide I did not induce maximum activation, the EC_{50} could not be calculated via the Hill equation and the apparent EC_{50} value for **HyNaC2/10/7** for Hydra-RFamide I was estimated to be ≥ 30 μM.

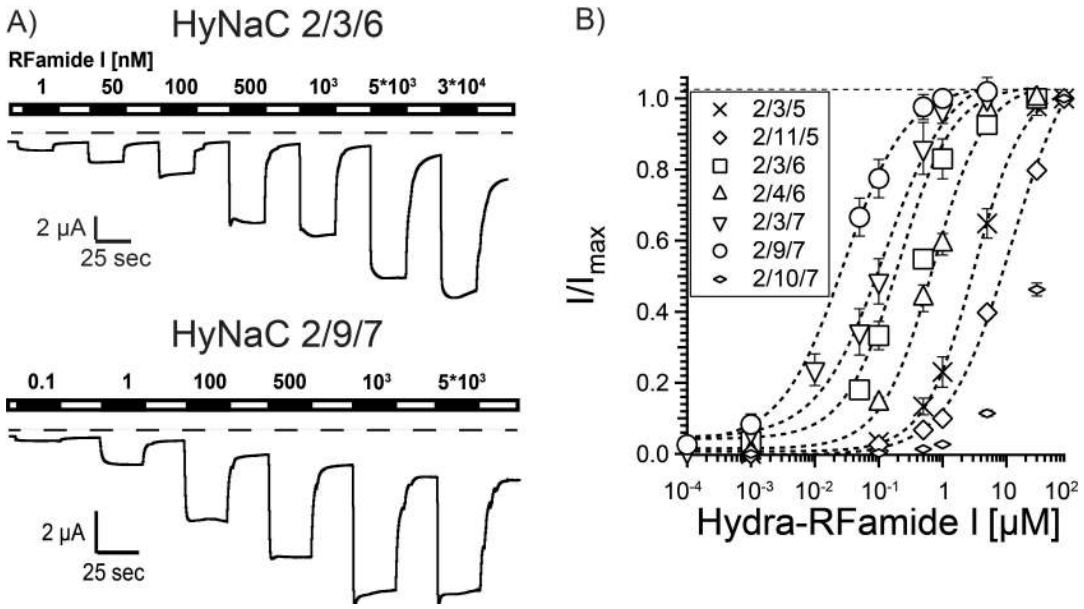

Figure 3.8.: **HyNaCs are activated with high affinity by Hydra-RFamide I.** A) *Xenopus* oocytes expressing HyNaCs were tested for concentration dependent activation by Hydra-RFamide I using TEVC. B) Concentration-response curves based on statistical analysis of measurements from A). The Hill equation was used to calculate the EC_{50} value. Data points = mean values ± SEM, $n \geq 9$.

The neuropeptide Hydra-RFamide II is another ligand for **HyNaC2/3/5**. The apparent affinity of **HyNaC2/3/5** for Hydra-RFamide II is about ten times higher than for Hydra-RFamide I in the range of 300 nM [36]. After an injection of the calcium chelator EGTA into *Xenopus* oocytes the apparent affinity of **HyNaC2/3/5** for Hydra-RFamide II was 1.6 ± 0.3 μM (figure 3.9, table A.2).

Similar to **HyNaC2/3/5**, all HyNaCs that were activated by Hydra-RFamide I were

also activated by Hydra-RFamide II. Consistently, most HyNaC combinations containig subunits HyNaC6 or HyNaC7 showed an increased apparent affinity for Hydra-RFamide II compared with **HyNaC2/3/5**. The apparent ligand affinities of most of the new HyNaCs for Hydra-RFamide II were in the same range as for Hydra-RFamide I (figure 3.9, table A.2). Similar to Hydra-RFamide I, the apparent affinity of **HyNaC2/10/7** for Hydra-RFamide II was ≥ 30 μM. The low affinity of **HyNaC2/10/7** for both tested neuropeptides suggests another ligand to be the main activator of this channel.

Surprisingly, the apparent affinity of **HyNaC2/11/5** for Hydra-RFamide II was about fourteen times higher than for Hydra-RFamide I with 0.95 ± 0.16 μM ($p < 0.001$, figure 3.9, table A.2).

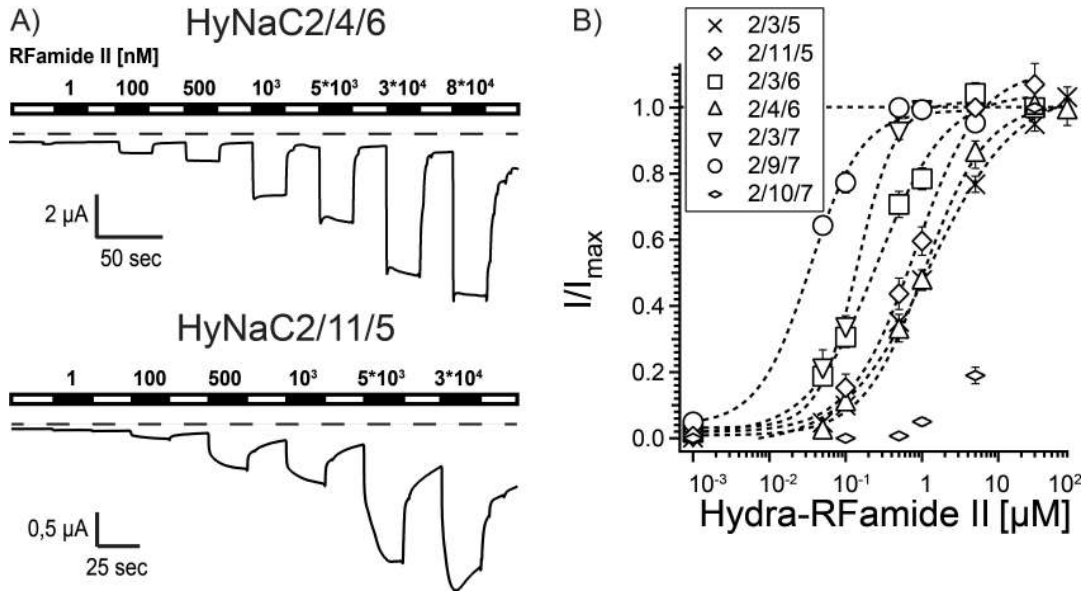

Figure 3.9.: **Hydra RFamide II activates HyNaCs.** A) TEVC recordings of the concentration dependent activation of HyNaCs by Hydra-RFamide II in *Xenopus* oocytes. B) Concentration-response curves showing HyNaC activation by Hydra-RFamide II. Data points = mean values ± SEM, n ≥ 7.

3.2.3. Apparent ligand affinity of HyNaCs is determined by TMD2 and adjacent amino acids

The apparent affinity for Hydra-RFamide I of **HyNaC2/3/7** is about 20-fold higher than for **HyNaC2/3/5**. Since two HyNaC subunits of both heterotrimers are the same, the difference in the apparent ligand affinity has to be determined by the third one. To identify the amino acids of HyNaC7 that cause the higher apparent affinity of **HyNaC2/3/7**, a chimeric approach with HyNaC5 and HyNaC7 was used.

Cottrell et al. could show that 120 amino acids at the proximal end of the ECD are responsible for the apparent ligand affinity of the peptide gated DEG/ENaC channel FaNaC from *Helisoma trivolvis* and *Helix aspersa* [27]. So in the first steps chimeras were created between HyNaC5 and HyNaC7 starting from the N-terminus stepwise to the distal end of the ECD.

The N-terminus together with TMD1 of HyNaC5, when exchanged by the corresponding part of HyNaC7 (figure 3.10, CH5_7b), did not increase apparent ligand affinity of **HyNaC2/3/5**. In addition, exchanging the first half of the ECD of HyNaC5 by HyNaC7 (figure 3.10, CH5_7c) did also not increase the apparent ligand affinity of **HyNaC2/3/5**. This finding is in contrast to previous findings with FaNaC. Both chimeras remained at an EC_{50} of 3.5 μM or lower (figure 3.10, CH5_7b and CH5_7c). A significant four-fold increase in apparent ligand affinity of **HyNaC2/3/5** was found when the N-terminal domain together with TMD1 and the complete ECD of HyNaC5 was exchanged by HyNaC7 (figure 3.10, CH5_7d).

Since exchanging the initial two thirds of HyNaC5 by HyNaC7 only slightly increased the apparent ligand affinity, it is unlikely that the area responsible for the apparent ligand affinity of HyNaCs is the same as of FaNaCs. Therefore, in the next step chimeras were created between HyNaC5 and HyNaC7 starting from the C-terminus.

HyNaC7 has a C-terminus that is 25 amino acids longer than HyNaC5. An isolated exchange of the C-terminal domain between HyNaC5 and HyNaC7 did not alter the apparent ligand affinity of **HyNaC2/3/5** (figure 3.10, CH5_7e). Also a truncation of the C-terminus of HyNaC7 to the length of the C-terminus of HyNaC5 did not alter the apparent ligand affinity of **HyNaC2/3/7** (figure 3.10, Hy7c-trunk), demonstrating that the C-terminus has no direct effect on the apparent ligand affinity of HyNaCs. When TMD2 was exchanged between HyNaC5 and HyNaC7, the apparent affinity slightly but significantly increased to 1.73 $\pm$ 0.25 μM (figure 3.10, CH5_7TM). In contrast, exchanging the complete ECD of HyNaC5 by HyNaC7 had no effect on the apparent

affinity of **HyNaC2/3/5** (figure 3.10, CH5_7m).

In contrast to single exchanges, swapping the C-terminal domain together with TMD2 of HyNaC5 by HyNaC7 significantly increased the apparent ligand affinity of **HyNaC2/3/5** about ten-fold to 0.44 ± 0.08 μM (figure 3.10 and figure 3.11, CH5_7i). When 80 amino acids of the distal ECD of HyNaC5 were additionally swapped by HyNaC7, the apparent ligand affinity was further increased to 0.04 ± 0.01 μM. This Chimera (CH5_7j, figure 3.10 and figure 3.11) showed the same apparent ligand affinity as **HyNaC2/3/7**. Swapping larger parts of the ECD of HyNaC5 by HyNaC7 did not change the high affinity of CH5_7j (figure 3.10, CH5_7k and CH5_7l). Figure 3.11 shows representative current traces of **HyNaC2/3/5** and **HyNaC2/3/7** as well as chimeras between HyNaC5 and HyNaC7 that have the strongest effect on apparent ligand affinity (CH5_7i and CH5_7j).

Taken together TMD2 and adjacent amino acids of HyNaC7 are responsible for the high apparent ligand affinity of **HyNaC2/3/7**.

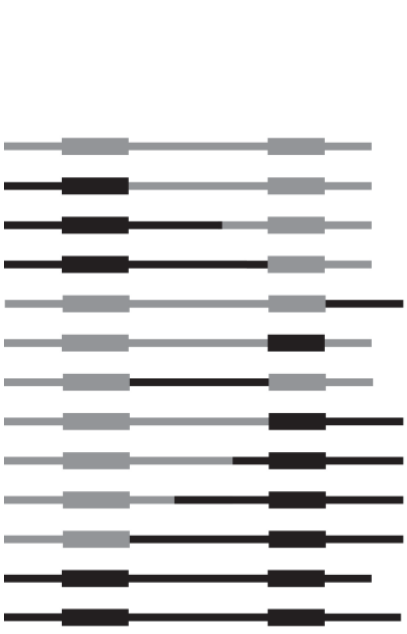

	EC_{50} ± SEM [µM]	Hill Coeff. ± SEM	n	ttest to HyNaC7	ttest to HyNaC5
HyNaC 5	3.48 ± 0.55	1.20 ± 0.1	9	***	n.s.
CH5_7b	3.80 ± 0.48	0.82 ± 0.1	7	***	n.s.
CH5_7c	> 30 µM	0.63 ±0.1	7	***	**
CH5_7d	0.93 ± 0.14	0.92 ± 0.1	10	***	**
CH5_7e	2.63 ± 0.50	1.11 ± 0.1	7	***	n.s.
CH5_7 TM	1.73 ± 0.25	0.93 ± 0.1	11	***	**
CH5_7m	4.49 ± 1.30	0.65 ± 0.1	6	***	n.s.
CH5_7i	0.44 ± 0.08	2.36 ± 1.2	12	**	***
CH5_7j	0.04 ± 0.01	0.96 ± 0.1	9	n.s.	***
CH5_7k	0.22 ± 0.05	0.96 ± 0.1	10	n.s.	***
CH5_7l	0.17 ± 0.02	1.78 ± 0.4	9	n.s.	***
Hy7c-trunk	0.09 ± 0.01	1.40 ± 0.1	7	n.s.	***
HyNaC 7	0.14 ± 0.04	1.60 ± 0.4	16	n.s.	***

Figure 3.10.: **TMD2 and adjacent amino acids are associated with high ligand affinity of HyNaC7.** Left) Scheme of chimeras between HyNaC5 (grey) and HyNaC7 (black). Right) Statistical analysis of apparent ligand affinities (EC_{50}) for Hydra-RFamide I of HyNaC chimeras coexpressing HyNaC2/3. Chimeras showing a significantly increased affinity compared to HyNaC5 are highlighted by a black frame. Significance tested by student's t test.

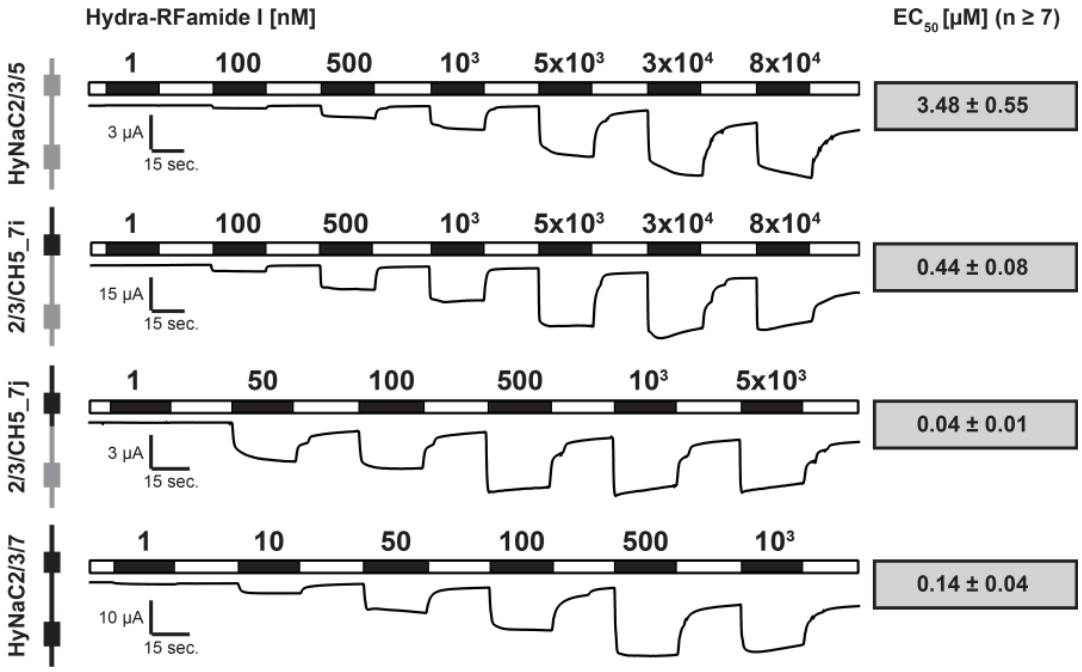

Figure 3.11.: **Representative current traces of chimeras between HyNaC5 and HyNaC7.** TEVC recordings of *Xenopus* oocytes expressing wildypte HyNaC5, HyNaC7 and chimeras CH5_7i and j together with corresponding subunits HyNaC2/3 showing concentration dependent activation by Hydra-RFamide I. Structure of HyNaC5_7 chimeras (grey HyNaC5, black HyNaC7) and EC_{50} ± SEM are indicated.

3.3. Ion selectivity and permeability of HyNaCs

3.3.1. HyNaCs are unselective cation channels

In a previous study, **HyNaC2/3/5** has been shown to be an unselective cation channel, which is permeable for Na^+ and at a lower extent also for K^+ and Li^+ [36]. The E_{Rev} of HyNaCs in this work was studied via TEVC. I/V (current/voltage) relationship was tested by continously increasing the oocyte membrane potential from -100 to +30 mV over 2 seconds. The channels were activated with Hydra-RFamide I at the EC_{50} of each HyNaC. Background currents were determined by voltage ramps in abscence of the ligand and were subtracted from currents in the presence of the ligand. Standard bath solution containg 140 mM Na^+ as the main permeant ion was used to superfuse the oocytes.

At a negative membrane potential of -100 mV Hydra-RFamid I evoked a strong inward current for all tested HyNaCs. Increasing the membrane potential to positive values

reduced the amplitude of inward current. Similar to **HyNaC2/3/5**, E_{Rev} was in the range of +10 mV for all tested HyNaCs (figure 3.12 A, table 3.3), suggesting all HyNaCs to be unselective cation channels.

3.3.2. Calcium permeability is a universal feature of peptide gated HyNaCs

In addition to conducting monovalent cations, **HyNaC2/3/5** is also highly permeable for the divalent cation Ca^{2+} [35]. Dürrnagel et al. could demonstrate that **HyNaC2/3/5** has small inward currents when Ca^{2+} is the main permeant ion [35]. When these authors increased the extracellular concentration of Ca^{2+} from 1 to 10 mM, E_{Rev} of **HyNaC2/3/5** shifted from -43 mV to - 17 mV. Since the equilibrium potential of Ca^{2+} is highly positive, this positive shift indicated a relative calcium permeability of **HyNaC2/3/5** [35]. As shown in section 3.3.1, E_{Rev} is in the range of +10 mV when Na^+ is the main permeant ion. Here, E_{Rev} of HyNaCs was determined when Ca^{2+} was the main permeant ion in a concentration of 1 mM or 10 mM. Based on the shift of E_{Rev}, when the extracellular cation was changed from 140 mM Na^+ to 10 mM Ca^{2+}, the permeability ratio $P_{Ca^{2+}}/P_{Na^+}$ was calculated (more detailed description shown in "Materials and methods" chapter 2.6.2). For **HyNaC2/3/5**, it has been shown recently to be in the range of 3 [35]. To study the effect of the extracellular Ca^{2+} concentration, NaCl was replaced by the impermeable NMDG-Cl (N-methyl-D-glucamine).

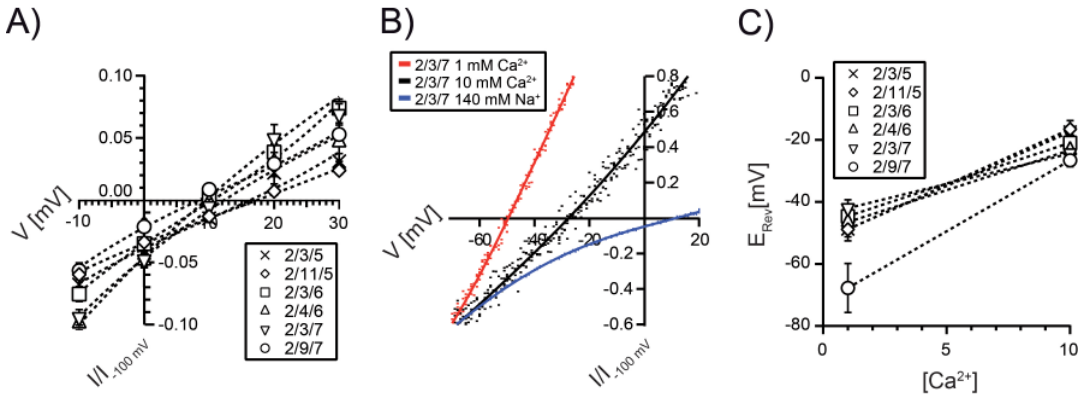

Figure 3.12.: **HyNaCs are unselective cation channels.** A) E_{Rev} of HyNaCs in the active state (Hydra-RFamide I). B) E_{Rev} of HyNaC2/3/7 with 140 mM NaCl or low (1 mM) and high (10 mM) Ca^{2+} as the main permeant ions. C) Diagram of E_{Rev} of HyNaCs with 1 and 10 mM Ca^{2+} as the main permeant ion.

Interestingly, increasing the extracellular Ca^{2+} concentration from 1 to 10 mM caused a positive shift of reversal potential in all tested HyNaCs, suggesting Ca^{2+} permeability of all HyNaCs (figure 3.12 B and C).

Similar to **HyNaC2/3/5**, all HyNaCs had a ratio $P_{Ca^{2+}}/P_{Na^{+}}$ in the range of 3, showing that all HyNaCs are highly permeable for Ca^{2+} (table 3.3). Taken together, HyNaCs are unselective cation channels that are highly permeable for Ca^{2+}.

HyNaC	$E_{Rev140mMNa^{+}}$ [mV]	$E_{Rev10mMCa^{2+}}$ [mV]	$P_{Ca^{2+}}/P_{Na^{+}}$	n
2/3/5	15.8 ± 1.5	-17.5 ± 3.4	3.4	9
2/11/5	17.3 ± 1.1	-16.5 ± 2.7	3.3	13
2/3/6	8.5 ± 1.9	-21.0 ± 2.2	3.7	10
2/4/6	11.6 ± 1.4	-23.3 ± 2.0	2.7	8
2/3/7	13.9 ± 2.7	-24.4 ± 2.5	2.8	13
2/9/7	7.4 ± 0.5	-26.6 ± 2.1	2.9	11

Table 3.3.: **Shift of E_{Rev} at Na^{+} or Ca^{2+} as the main permeant ions allows calculation of Ca^{2+} permeability.** From the shift of E_{Rev} with Na^{+} or Ca^{2+} as the main permeant ion, the calcium permeability ratio $P_{Ca^{2+}}/P_{Na^{+}}$ was calculated (chapter 2.6.2). Mean values ± SEM, n = number of experiments.

3.3.3. An arginine at the DEG-position induces weak constitutive activity of HyNaCs

HyNaC2/3/5 has been demonstrated previously to be closed at rest and to be activated by its ligands Hydra-RFamide I and II [36]. Golubovic showed that exchanging the glycine at the so-called DEG position, closely distal to TMD2, by a threonine induces weak constitutive activity in HyNaC2, HyNaC3 and HyNaC4 [44]. In contrast, Mogil et al. described a dominant negative point-mutation of ASIC3 [84]. Exchanging the glycine at the DEG-position of ASIC3 by an arginine generates an ASIC3 mutant subunit that inhibits ASIC currents when co-expressed together with native ASICs. In this work, the glycine at the DEG position of HyNaC2, HyNaC3 and HyNaC5 was exchanged by an arginine (DEGR) to test whether this subunit inhibits channel activity as well. Mutated HyNaC subunits were coexpressed with wild type (wt) HyNaC subunits. cRNAs of heterotrimeric HyNaC combinations that included one or more mutated HyNaC subunits were injected into *Xenopus laevis* oocytes at a concentration of 400 ng/μl, whereas wt **HyNaC2/3/5** was injected in a 1:20 dilution. To study properties of DEGR mutant

HyNaC subunits, HyNaC heterotrimers were activated with 1 μM Hydra-RFamide I to test for activation and blocked with 1 mM amiloride to test for constitutive activity.

In a first approach HyNaC heterotrimers were tested that contained only one mutated HyNaC subunit. Surprisingly, instead of inactivating HyNaCs, an arginine at the DEG-position of HyNaC2 induced weak constitutive activity of 0.6 $\pm$ 0.2 μA (figure 3.13 A - C, **HyNaC2-DEGR/3/5**). A similar exchange at the DEG-position of HyNaC3 also induced constitutive currents but of smaller amplitude (0.1 $\pm$ 0.1 μA, figure 3.13 B and C, **HyNaC2/3-DEGR/5**). In contrast, an arginine at the DEG-position of HyNaC5 did not induce constitutive activity (figure 3.13 B and C, **HyNaC2/3/5-DEGR**).

HyNaC2-DEGR/3/5 as well as **HyNaC2/3-DEGR/5** still were activated by Hydra-RFamide I, but the current amplitude was significantly reduced compared to wild type **HyNaC2/3/5** (figure 3.13 C). In addition, the arginine substitution changed current kinetics. When **HyNaC2-DEGR/3/5** and **HyNaC2/3-DEGR/5** were activated by Hydra-RFamide I, the application of the peptide induced an immediate transient inward current. The transient current was followed by an almost complete inhibition of HyNaC currents by Hydra-RFamide I (figure 3.13 A). Since an inhibition of HyNaCs by Hydra-RFamide I has never been reported before, neither in this work nor in previous works [36, 45], an arginine at the DEG position is likely to alter channel gating properties. HyNaC heterotrimers containing the HyNaC5-DEGR mutation only showed an extremely weak activation by 1 μM Hydra-RFamide I, suggesting that HyNaC5-DEGR is a dominant negative point-mutation.

Interestingly, coexpression of two or more HyNaC-DEGR mutants led to an almost complete reduction of ion channel activity except for **HyNaC2-DEGR/3wt/5-DEGR** (figure 3.13 C). **HyNaC2-DEGR/3wt/5-DEGR** showed a larger constitutive activity than **HyNaC2-DEGR/3/5** but 1 μM Hydra-RFamide I induced currents of the same amplitude (figure 3.13 C).

Taken together, in contrast to ASIC3, an arginine at the DEG-position of HyNaC2 and HyNaC3 induced constitutive activity of HyNaCs. Interestingly, when HyNaC5-DEGR was coexpressed together with HyNaC2-DEGR the constitutive activity of HyNaCs was further increased. In contrast, other HyNaC heterotrimers containing two or more DEGR mutant HyNaC subunits showed very low or no activation by peptide and no constitutive activity.

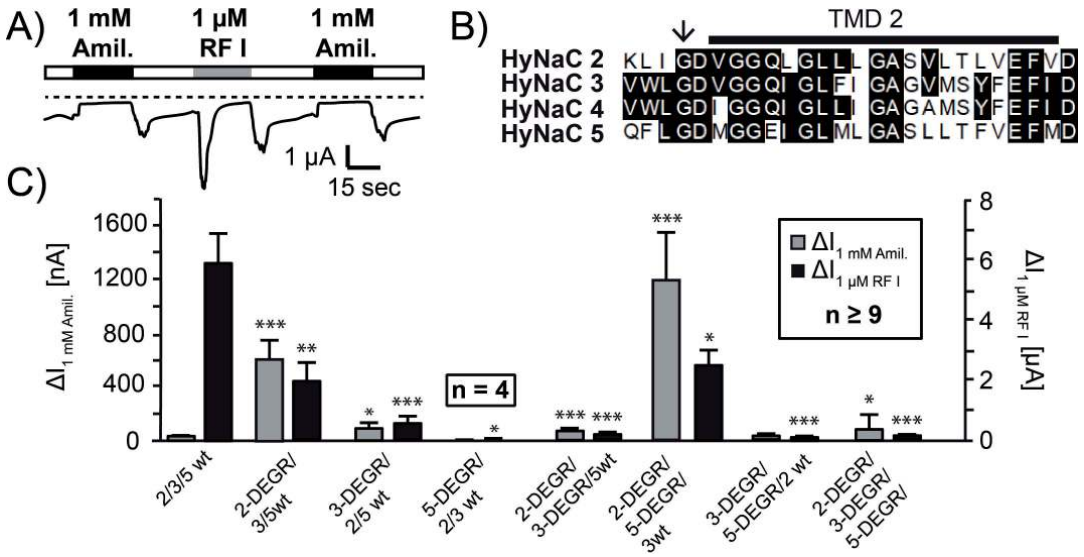

Figure 3.13.: **An arginine at the DEG position of HyNaC2 and HyNaC3 induces constitutive activity.** A) **HyNaC2-DEGR/3/5** is blocked by 1 mM amiloride and activated by 1 μM Hydra-RFamide I. B) ClustalW alignment between HyNaC2 – HyNaC5, the DEG-position is indicated (black arrow). C) Statistical analysis of constitutive amiloride-sensitive currents (grey) and current amplitude induced by 1 μM Hydra-RFamide I (black). Asterisks show significant differences to wildtype **HyNaC2/3/5**.

3.4. Diminazene is a potent inhibitor of HyNaCs and alters feeding reaction in *Hydra magnipapillata*

Currents elicited by **HyNaC2/3/5** are blocked with low affinity by amiloride with an IC_{50} of approximately 120 μM. Due to the low affinity for amiloride, previous *in vivo* studies concerning the physiological role of HyNaCs required a high concentration of 100 μM to delay the feeding reaction in *Hydra magnipapillata* significantly [36]. Therefore a more potent inhibitor would be useful to study the role of HyNaCs in the living animal. Diarylamidines, including diminazene, block ASICs in the nanomolar range and BASIC in the micromolar range [21, 118]. To study the effect of diminazene on HyNaCs, channels were activated with a constant concentration of peptide and increasing concentrations of diminazene. The IC_{50}, the concentration of inihibitor leading to a half maximal inhibition of channel activity, was then determined.

The application of diminazene to all putative physiological HyNaC heterotrimers led to a concentration dependent inhibition of HyNaC currents (figure 3.14 A). An overview of IC_{50} values of HyNaCs for diminazene is shown in table A.3 in appendix. Compared to

amiloride, diminazene inhibited most HyNaC currents with a much higher apparent affinity in the high nanomolar range. Most HyNaCs showed a nearly complete block of ion channel activity at a concentration of 10 μM diminazene, whereas a concentration of 100 μM amiloride caused an inhibition of HyNaCs of approximately 70 %. While most HyNaCs were blocked in the high nanomolar range, **HyNaC2/11/5** and **HyNaC2/10/7** showed an apparent affinity for diminazene lower than 5 μM (figure 3.14 B, table A.3). Similar to the low diminazene affinity of **HyNaC2/11/5** and **HyNaC2/10/7**, these two HyNaCs also showed a lower amiloride affinity than other HyNaCs (table A.3). However, diminazene was a more potent inhibitor for HyNaC activity than amiloride.

To study the effect of the inhibition of HyNaC activity by diminazene on animal behaviour, Anne Kuhn at the Centre for Organismal Studies (COS), Heidelberg, treated adult *Hydra magnipapillata* with diminazene during feeding reaction. The feeding reaction, characterized by tentacle curling, was triggered by an application of 10 μM glutathione (GSH) into the bath medium of the animals. During the experiment, the animals were held in bath medium containing different concentrations of diminazene.

Anne Kuhn could show that an application of 10 μM GSH in the abscence of diminazene resulted in approximately 50 % of animals moving their tentacles 30 seconds after GSH application. 1:30 minutes later all animals were moving their tentacles. As

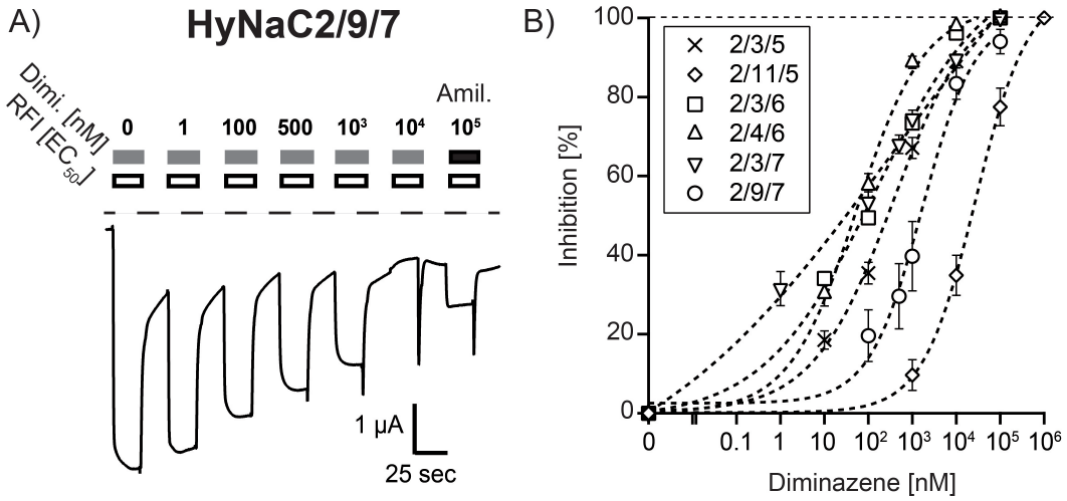

Figure 3.14.: **Diminazene is a potent inhibitor of HyNaCs.** A) HyNaCs were activated with Hydra-RFamide I at EC_{50} and treated with increasing concentrations of diminazene. 100 μM amiloride was applied finally to demonstrate affinity for amiloride. B) Concentration-response curve showing apparent ligand affinity of HyNaCs for diminazene. Indicated are mean values ± standard error of the mean (SEM).

a negative control, an application of 300 μM diminazene in abscence of GSH did not induce tentacle curling.

A concentration of 100 μM diminazene in the bath medium had a weak inhibitory effect on the feeding reaction induced by GSH. Increasing the concentration of diminazene to 200 μM resulted in a significant delay of animals showing feeding reaction. The fraction of animals moving their tentacles reached a level of 100 % about 3:30 minutes after the application of GSH. An application of 300 μM diminazene reduced the number of animals displaying feeding reaction by approximately 70 % during the complete measurement of 4:30 minutes (figure 3.15, n=50).

Even though diminazene inhibited HyNaC currents in *Xenopus* oocytes with a much higher potency, it did not inhibit the feeding reaction more efficiently than amiloride. In contrast, 100 μM amiloride had a stronger inhibitory effect on the feeding reaction [36] than 100 μM diminazene. However, diminazene inhibited the feeding reaction supporting previous findings of the physiological role of HyNaCs *in vivo* [36].

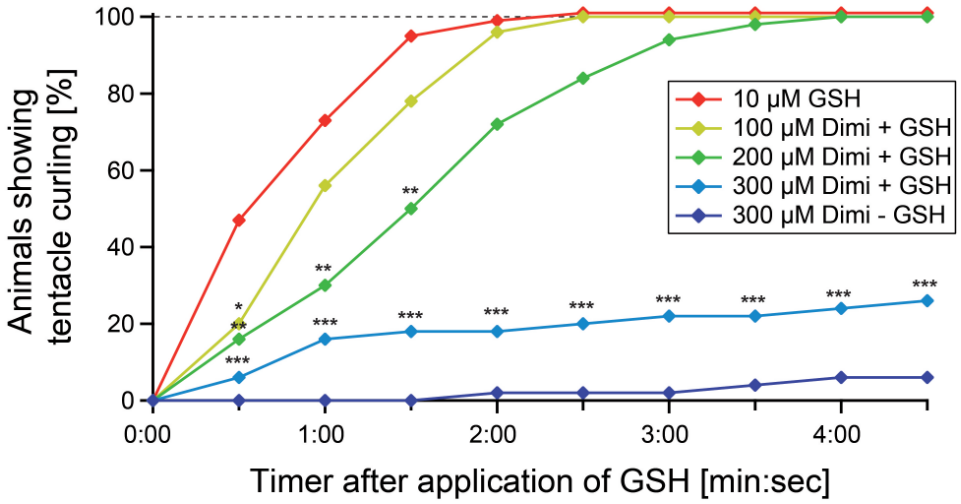

Figure 3.15.: **Diminazene blocks feeding reaction in *Hydra magnipapillata*.** Feeding reaction studies and statistics were performed by Anne Kuhn, COS, Heidelberg. Animals were held in medium containing different concentrations of diminazene. 10 μM GSH was applied to induce feeding reaction. Test for significance to control conditions by student's t test.

4. Discussion

4.1. The *Hydra* sodium channel subfamily, a group of DEG/ENaC ion channel family members

In this work seven novel members of the *Hydra* sodium channel subfamily were cloned. With the exception of HyNaC12, the novel members of the HyNaC subfamily show a high degree of sequence homology to the already known HyNaC subunits. No further proteins with homology to DEG/ENaCs could be found by BLAST analysis and homology cloning in *Hydra*. Therefore, most likely, HyNaC2 - HyNaC12 comprise the complete HyNaC subfamily in *H. magnipapillata*. The *Hydra* species shows a high transposase activity. Transposase is an enzyme that excises and in some cases also duplicates special DNA sequences, so-called transposons, and religates them at another position into the genome. The transposase activity causes a large genome in *H. magnipapillata* consisting of about 60 % of transposable elements, including a huge amount of retrotransposons [20]. The transposase activity might have led to the variety of different HyNaC subunits by duplicating HyNaC genes.

The phylogenetic tree in figure 3.3 demonstrates that HyNaC2 - HyNaC11 are closely related to ASICs and BASICs. Within the DEG/ENaC family HyNaCs, ASICs and BASICs form a cluster. This supports recent findings from Golubovic et al. that showed comparable clustering of HyNaCs, ASICs and BASICs [45]. In contrast to the phylogenetic tree from Golubovic et al., in figure 3.3 ENaCs, FaNaCs and degenerins do not cluster on one common branch. A previous phylogenetic analysis published by Kellenberger et al. showed the same clustering of ENaCs, FaNaCs and degenerins as reported by Golubovic et al. [70]. Supporting my data, a phylogenetic tree from Waldmann et al. demonstrated that ENaCs, FaNaCs and the degenerins show a relatively large genetic distance and do not cluster on a common branch[114]. It is hard to conclude whether ENaCs, FaNaCs and degenerins are closely related to each other or not. The composition and number of proteins in phylogenetic analyses change the apparent phylogenetic relationship between proteins. But HyNaCs, ASICs and BASICs consistently

form a cluster, suggesting these three subfamilies to form a monophyletic group within the DEG/ENaC family as it had already been hypothesized by Golubovic et al. [45].

Interestingly, HyNaC2 and HyNaC5 - HyNaC7 as well as HyNaC3, HyNaC4 and HyNaC8 - HyNaC11 form two subclusters within the HyNaC branch. So there are two populations of HyNaC subunits that might have separated from each other from a common ancestor.

HyNaC12, as the sequence identity already suggested (table 3.1), is located far away from the ASIC/BASIC/HyNaC branch (figure 3.1). Furthermore it does not form a branch with any other subfamily of the DEG/ENaC ion channel superfamily. Some PPK channels, like PPK10 and PPK13, are also isolated from other PPK branches. The same applies for the degenerins in *C. elegans*. It is known that the genetic divergence in invertebrates is much higher than in vertebrates. Genetic divergence describes the separation of subspecies over time by mutation of the coding sequence. Due to the high divergence in invertebrates, their genome and proteome change faster than in vertebrates causing loss of proteins or fast mutational changes in the amino acid sequences [3, 31, 44]. The distance of HyNaC12 to other HyNaCs might therefore be a result or a relict caused by the fast evolution in *Hydra magnipapillata*.

As far as it is known, the DEG/ENaC ion channel family is found only in multicellular metazoans [70]. The genus *Hydra magnipapillata* is about 500 million years old and belongs to the phylum Cnidaria. So *Hydra* is supposed to be one of the oldest known genera that expresses DEG/ENaC ion channels. Since Cnidaria and Bilateria seperated from each other many millions of years ago, both orders have evolved indepently for a very long time. DEG/ENaC characeristics that are shared between HyNaC and DEG/ENaC channels from Bilaterian organisms are supposed to be ancient features of the DEG/ENaC family. BASIC and ASICs exclusively are found in vertebrates, whereas HyNaC is limited to the genus *Hydra*. Orthologues of HyNaCs might also be found in other Cnidarian organisms. The close phylogenetic relation between the subfamilies HyNaC, BASIC and ASIC suggests a common ancestor that has evolved before the branching point of Bilateria and Cnidaria [83]. In insects, molluscs and worms, this monophyletic group is missing. As already discussed by Golubovic et al., due to the high divergence in invertebrate animals, it is possible that this monophyletic group got lost over time in Bilaterian invertebrates [45].

The phylum Cnidaria was one of the first organisms evolving a nervous system [39]. Since HyNaC is supposed to be expressed at the post-synaptic membrane of the neuromuscular junction of *Hydra magnipapillata* [44, 36], the physiological role of ancient

DEG/ENaC ion channel family members might have contributed to efferent neuronal signalling and inducing muscle contractions. Supporting this hypothesis, AnthoRWamide, an RFamide related peptide from *Anthozoa*, induces muscle contractions in the sea anemone [82]. Sea anemones and *Hydra* belong to the phylum Cnidaria [83] and muscle contraction might underly the same mechanism in both genera. However, an evidence for the expression of a HyNaC related member of the DEG/ENaC superfamily in *Anthozoa* is missing.

4.2. HyNaCs are heterotrimeric peptide gated ion channels

As shown previously, the HyNaC subunits 2, 3 and 5 form the functional heterotrimer HyNaC2/3/5 [36]. This ion channel is activated by Hydra-RFamides I and II. Also a HyNaC2/3 heteromer has been shown to form a functional cation channel [45]. This phenomenon is also known from the epithelial sodium channel ENaC, where the α and the β or the γ subunits form a functional channel $\alpha\beta$ or $\alpha\gamma$ ENaC [16]. The heterotrimer $\alpha\beta\gamma$ ENaC produces larger currents than a channel containing two subunits and so was supposed to be the functional trimeric channel [16]. Similarly, HyNaC2/3/5 showed larger currents than HyNaC2/3 and in addition showed an increased apparent affinity for its ligand Hydra-RFamide. Therefore Dürrnagel et al. proposed that HyNaC2/3/5 is the physiological subunit combination [36].

Like HyNaC2/3/5, the newly cloned HyNaC subunits form heterotrimeric cation channels (table 3.2). Due to the large number of subunits, a variety of different functional ion channels is formed. These ion channels are activated by Hydra-RFamides I and II, and in addition are also activated by lowering the extracellular Ca^{2+} concentration. HyNaC2 has been found to be the "master subunit" that is necessary for every heterotrimeric subunit combination. ENaC and HyNaC show a relatively large phylogenetic distance, but the role of HyNaC2 can be compared to the role of αENaC. When αENaC is missing no functional epithelial sodium channel is formed [16].

Interestingly, in contrast to ASICs and BASIC, no homotrimeric HyNaC channel has been found. Homomeric ion channels are not exclusive to the ASIC and BASIC subfamilies but are also found in the FaNaC [25, 63] and the PPK [2] subfamilies. Likewise heteromeric ion channels are not exclusive to the HyNaC subfamily since it is also found in the ASIC [70] and ENaC [16] subfamilies. Considering a common ancestor of the DEG/ENaC ion channel superfamily one can only speculate whether the ancestral

channel was homo- or heterotrimeric. However, formation of functional heterotrimeric ion channels by three different subunits is a shared feature of the HyNaC subfamily, with the possible exception of HyNaC12.

The phylogenetic trees shown in figure 3.2 and figure 3.3 reveal that HyNaC subunits can be divided into two subgroups. HyNaC3, HyNaC4 and HyNaC8 - HyNaC11 form the first subgroup and HyNaC2 and HyNaC5 - HyNaC7 form the second subgroup. One member of each subgroup, in addition to HyNaC2, is required to form a functional heterotrimeric ion channel. The variety of HyNaCs might be the result of an adaptation of HyNaCs to different physiological functions.

HyNaC12 was the only HyNaC subunit that was inactive. Expression of HyNaC12 with a pool of different other HyNaC subunits and the application of Hydra-RFamides I and II or reducing the extracellular Ca^{2+} concentration did not elicit any current in *Xenopus* oocytes. Even the so called DEG-mutation (HyNaC12 G436T) that causes channel hyperactivity in degenerins and other DEG/ENaC ion channels [33] did not activate the channel. Although this was not tested, it is possible that HyNaC12 is not transported to the cell surface. As mentioned before, it is rather unlikely that there are yet unknown HyNaC subunits left in *H. magnipapillata* that interact with HyNaC12. Considering its isolated position in the phylogenetic tree (figure 3.3), HyNaC12 might form a homotrimeric ion channel that is not activated by Hydra-RFamides. For example HyNaC12 could form a mechanosensitive ion channel. When MEC-4 and MEC-10, two mechanosensitive DEG/ENaC ion channels from *C. elegans*, were cloned, the wildtype channels did also not elicit any current in *Xenopus* oocytes [40]. MEC-4 and MEC-10 are supposed to be connected to a mechanotransducing complex [47] and in oocytes this complex is missing. Not before MEC-4 or MEC-10 were coexpressed in *Xenopus* oocytes together with MEC-2, a stomatin related protein, the channels were activated by mechanical stimuli [46]. If HyNaC12 were mechanosensitive, it would also not be expected to be active in *Xenopus* oocytes. However, the questions about the physiological role and the biophysical properties of HyNaC12 remain open.

Interestingly, the new HyNaC combinations mostly had a much higher affinity for Hydra-RFamides I and II than HyNaC2/3/5. HyNaC2/9/7 showed an EC_{50} of 40 nM for Hydra-RFamide I (figure 3.8), which is approximately 100-times higher than of HyNaC2/3/5. Furthermore, HyNaC2/11/5 showed different affinities for Hydra-RFamides I and II. While HyNaC2/9/7 showed the same apparent affinities for both peptides, the apparent affinity of HyNaC2/11/5 for RFamide II was 14-times higher than for RFamide I. These differences in ligand affinity might allow to differentially ac-

tivate different HyNaC heterotrimers in the same tissue. Finally, lack of activation of HyNaC2/9/5 by Hydra-RFamides I - V suggests yet another and still unknown ligand of HyNaCs.

4.3. The expression pattern of new subunits indicates an additional physiological role of HyNaCs

From previous studies it is known that HyNaC2 - HyNaC5 are expressed at the tentacle basis of the adult animal. It has been proposed that HyNaC2/3/5 is expressed in neuromuscular cells where it is involved in tentacle movement during feeding reaction [36, 45]. This has been confirmed by animal behavioural studies at which an application of the DEG/ENaC blocker amiloride inhibited the tentacle movement during feeding reaction [36], presumably by inhibiting HyNaC activity. ISH for the subunits *hynac*6 and *hynac*11 showed that both subunits are also expressed at the tentacle basis (figure 3.5). Like *hynac*4, *hynac*6 is also expressed at the aboral end of the tentacle basis. Since HyNaC4 did not form a functional ion channel together with HyNaC2, HyNaC3 or HyNaC5, it was hypothesized that this subunit interacts with a not yet described partner [36, 45]. Interestingly, together with HyNaC2 and HyNaC6, HyNaC4 formed a heterotrimeric ion channel, HyNaC2/4/6. Hence HyNaC6 might be the postulated binding partner of HyNaC4. Since HyNaC2/3/5 is located at the oral end and HyNaC2/4/6 at the aboral end of the tentacle basis, one can speculate that those two HyNaC heterotrimers act as antagonists in the movement of the tentacles. An activation of HyNaC2/3/5 at the oral side of the tentacle basis could induce curling of the tentacles, whereas an activation of HyNaC2/4/6 at the aboral side could induce elongation of the tentacles.

*hynac*7 and *hynac*10 instead were found in the peduncle region, which is located right above the basal disc. This is the first description of HyNaC subunits expressed in this region. HyNaC heterotrimers in the peduncle also require HyNaC2 to be functional. *hynac*2 has previously been described to be expressed only at the tentacle basis [36, 45]. Since HyNaC2 is the "master subunit" for every HyNaC heterotrimer, the expression pattern of *hynac*2 - *hynac*5 was reviewed. In this work it has been shown that, in addition to the tentacle basis, *hynac*2 and *hynac*3 show a weak expression level in the whole body colum. So it is likely that functional heterotrimers are also formed in the peduncle region.

The physiological role of HyNaCs in the peduncle might differ from the role of HyNaCs at the tentacle basis. The peduncle region has been proposed to represent an ancient

type of a heart [105]. *Hydra* is missing a blood circulation system, but since this animal is smaller than 1 cm and the body wall is only formed by two cell layers, diffusion of nutrition is sufficient [105]. In the peduncle region most of the fluid of the gastric cave is stored. The animals show spontanous contraction of the body column [88] that results in an equal distribution of substances in the gastric cave. When elongated again most of the volume from the gastric cave is transported back into the peduncle [105]. Since this is a neurogenic event mediated by contraction and relaxation of ectodermal muscle cells [105, 110], HyNaCs in this area might contribute to this mechanism. Indeed the application of Hydra-RFamide III increased the contraction rate of the peduncle in *H. magnipapillata* [105]. However, Hydra-RFamides I and II had no effect on the number and time course of body contractions [105]. Also no HyNaCs so far were sensitive for Hydra-RFamide III. However, this does not exclude a role of HyNaCs expressed at the peduncle for the body colum contraction. Thus HyNaCs might contribute to the feeding reaction as well as to the distribution of nutrition across the gastric cave.

*hynac*8 and *hynac*9 are expressed in a similar pattern and are distributed over the whole animal (figure 3.5). In addition, *hynac*9 shows a slightly increased expression level in the foot region. Even though the putative physiological role of HyNaC8 and HyNaC9 remains unclear, these subunits form heterotrimeric channels that might also contribute to neuronal signalling in *Hydra magnipapillata*.

*hynac*12 so far could neither be detected in adult nor in developing animals. It is possible that the expression level of *hynac*12 is below the detection threshold of the whole mount *in situ* hybridization. Two different *in situ* probes were used with different lengths of 700 bp and 1.5 kb. In both cases the *in situ* hybridization did not reveal any expression of *hynac*12 above background staining of the whole animal.

4.4. TMD2 and adjacent amino acids are important for the apparent ligand affinity of HyNaCs

HyNaC2/3/7 is about 20 times more sensitive for Hydra-RFamide I than HyNaC2/3/5 (figure 3.8). Since both heterotrimers only differ in one subunit, the increased affinity had to be determined by HyNaC7. By systematically swapping parts of HyNaC5 and HyNaC7, TMD2 and adjacent amino acids were identified to be reponsible for the higher affinity of HyNaC7.

The C-terminal domain of HyNaC7 is 25 amino acids longer than of HyNaC5. The C-terminal domain is a target for a variety of intracellular modifications in ASICs and

ENaCs, for example for phosphorylation and ubiquitination [1, 34, 56, 58, 59, 64, 107, 122]. But since the C-terminal domain had no effect on the apparent ligand affinity of HynaC5 and HyNaC7, it is unlikely that intracellular modifications are important for the increased apparent affinity of HyNaC7.

An isolated exchange of TMD2 that differs only in three amino acids between HyNaC5 and HyNaC7 only slightly increased the apparent ligand affinity of HyNaC5. TMD2 and the C-terminal domain had to be exchanged simultanously from HyNaC5 to HyNaC7 to increase the apparent ligand affinity of HyNaC5 by a factor of ten (figure 3.10, CH5_7i). In addition, an exchange of 80 amino acids proximal of TMD2 led to the same apparent ligand affinity as HyNaC7 (figure 3.10, CH5_7j). The ligand binding in ASICs is supposed to take place in the extracellular domain, presumably at the acidic pocket. One model posits that in this acidic pocket a Ca^{2+} ion is bound. A protonation of the acidic amino acids in this pocket would cause a release of the Ca^{2+} ion, leading to conformational changes in the ECD. These conformational changes are supposed to be transmitted across the thumb domain over the wrist to TMD2 causing pore opening [7, 21, 62, 89]. Mutational analyses of the acidic pocket altered apparent ligand affinities of ASICs, indicating changes in the gating properties of the mutated ion channels [89]. Even though HyNaCs are not gated by protons and an evidence for an acidic pocket in HyNaCs is missing, the close phylogenetic distance between ASICs and HyNaCs suggests a conservation of gating and ligand binding mechanisms between these two DEG/ENaC subfamilies. It is likely that ligand binding also induces conformational changes in the ECD of HyNaCs that are transmitted to TMD2 causing channel opening. As figure 4.1 A demonstrates, amino acids forming the acidic pocket in rASIC1a barely overlap with the high affinity chimera CH5_7j. Thus, considering a conservation of ligand binding and gating mechanism between ASIC and HyNaC, the ligand binding domain might not be causing the high affinity of HyNaC7 (figure 3.10). The higher apparent ligand affinity of HyNaC7 might rather be caused by a facilitation of the gating of HyNaC7 compared to HyNaC5 than by a facilitation of ligand binding efficiency of HyNaC7 (figure 4.1).

FaNaC from *Helix aspersa* shows an about 35-times higher apparent ligand affinity for FMRFamide than FaNaC from *Helisoma trivolvis* [63, 78]. Cottrell et al. demonstrated that a region of about 120 amino acids proximal to TMD1 caused the increased affinity of *H.a.* FaNaC [27]. Interestingly, exchanging the homologous region of *H.a.* FaNaC and *H.t.* FaNaC in HyNaC5 and HyNaC7 did not increase apparent ligand affinity of HyNaC5. In contrast, an exchange of this region strongly decreased the apparent ligand affinity, presumably by an impairment of the protein structure of this chimera

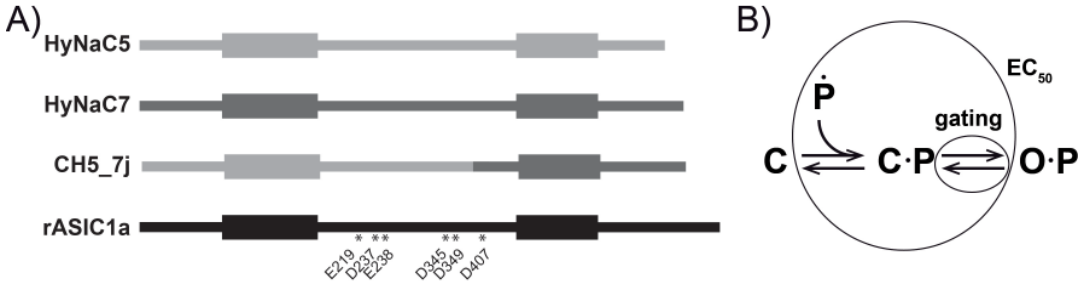

Figure 4.1.: **Putative position of acidic pocket in HyNaCs.** A) Scheme of HyNaC5, HyNaC7, CH5_7j and rASIC1a and the position of amino acids forming the acidic pocket in rASIC1a. B) Scheme of putative activity states in HyNaCs. C = closed; P = peptide; CP = closed, peptide bound; OP = open, peptide bound.

(CH5_7c, figure 3.10). However, TMD2 and the C-terminal domain of *H.a.* FaNaC did not increase the apparent ligand affinity of *H.t.* FaNaC. Even though FaNaCs and HyNaCs do not seem to be direct orthologues (figure 3.3), both channels are gated by RFamide neuropeptides and belong to the DEG/ENaC family, suggesting comparable ligand binding mechanisms. It is possible that Cottrell et al. identified the ligand binding site of FaNaCs. In contrast, in this work it is likely that by using a chimeric approach between HyNaC5 and HyNaC7, the efficacy of HyNaCs, the efficiency of channel gating (figure 4.1 B), has been identified.

4.5. Calcium permeability is a characteristic feature of the HyNaC subfamily

Sodium selectivity is a common feature of DEG/ENaC ion channels. $\alpha\beta\gamma$ ENaC as well as $\delta\beta\gamma$ ENaC show a 50 times higher selectivity for Na^+ over K^+ [16, 19]. Compared to ENaC, the selectivity of HyNaC, ASIC and BASIC for Na^+ over K^+ is low [9, 35, 36, 74, 113, 119, 120]. In addition, recently published data from Dürrnagel et al. demonstrated, that HyNaC2/3/5 is an unselective cation channel, which is highly permeable for Ca^{2+} [35, 36]. So far, high Ca^{2+} permeability of HyNaC2/3/5 has been reported to be a unique feature within the DEG/ENaC family [35].

The conserved DEG/ENaC selectivity filter, the G/S-X-S motif, located in TMD2 is part of the molecular sieve and mainly responsible for the sodium selectivity of DEG/ENaC family members [67]. It is found at the narrowest part of the ion pore and is crucial for ion permeation [68, 106]. In HyNaC subunits 2 to 11 this motif is formed

by a G-A-S, a G-A-G or a G-S-S motif that fits well to other vertebrate DEG/ENaC family members like ASICs and BASICs. HyNaC12 instead shows a G-F-S motif. The alanine or serine, respectively, in the center of the selectivity filter of HyNaC2 - HyNaC11 are much smaller than the phenylalanine of HyNaC12. The selectivity filter is facing the ion pore and since HyNaC12 is inactive, one could speculate that the larger side chain of the G-F-S motif of HyNaC12 somehow blocks the permeation pathway within the ion pore. But the side chain of the amino acid in the center of the G/S-X-S motif has been proposed to be directed away from the ion permeation pathway [77, 103]. Supporting this, the G-F-S motif is also found in some other invertebrate DEG/ENaC family members, like RPK and PPK12 from *Drosophila melanogaster* or DEG-1 from *Caenorhabditis elegans* (figure A.1). RPK is a constitutively active sodium channel [2], whereas DEG-1 is a mechanosensitive sodium channel [18]. These two channels show two completely different activation mechanisms but still show sodium selectivity. Even though an evidence for HyNaC12 to be a functional ion channel is missing, considering the structure of its selectivity filter, HyNaC12 is likely to be selective for sodium.

Like HyNaC2/3/5, in this work all new functional HyNaCs have been demonstrated to be cation channels. In agreement with previous findings all new HyNaC combinations have also been shown to be highly permeable for calcium with a ratio $P_{Ca^{2+}}/P_{Na^{+}}$ in the range of 3. Thus, high calcium permeability is a common feature within the complete HyNaC subfamily, with the possible exception of HyNaC12. Beyond the DEG/ENaC superfamily, channels from the vertebrate nervous system like the NMDA receptor have been reported to be highly permeable for calcium, too. The NMDA receptor is a ligand gated ion channel that is activated by glutamate and that is permeable to sodium, potassium and calcium. This ion channel is found in the postsynaptic membrane of neurons and contributes to the depolarization of the postsynaptic neuronal cell. The calcium influx through NMDA receptors in the postsynaptic cell induces intracellular signaling cascades that are associated with synaptic plasticity, long term potentiation and memory [65, 75]. *Hydra* is missing a central nervous system and hence lacks higher neuronal processes like learning. Since HyNaC2/3/5 has been proposed to induce tentacle movement by depolarization of neuromuscular cells [36], HyNaC might have comparable physiological functions as NMDA receptors and ASICs like depolarizing the postsynaptic membrane. An influx of calcium is known to activate several intracellular mechanisms including intracellular modification of proteins and the regulation of gene expression.

Hydra magnipapillata is a freshwater organism. The sodium concentration in freshwater is about 0.2 mM/l, whereas the calcium concentration is about 0.8 mM/l [92]. In

contrast, the sodium concentration in saline water and blood is much higher in the range of 6.5 mM/l. *Hydra magnipapillata* is a small animal with a body wall consisting only of two cell layers [111]. It is likely that the sodium and calcium concentration within the body of *Hydra* is the same as of its environment. Hence high calcium permeability of HyNaCs might be an adaptation to the low sodium concentration in freshwater. If HyNaC was highly selective for sodium and impermeable for calcium, the sodium concentration in freshwater might not be sufficient to depolarize the posystynaptic muscle cell membrane.

The calcium permeability of HyNaCs is partly due to an aspartate located at the entrance of the ion pore of HyNaC2, HyNaC3 and HyNaC5. An exchange of this aspartate by a cystein in all three subunits strongly decreases the calcium permeability of HyNaC2/3/5 to a ratio $P_{Ca^{2+}}/P_{Na^{+}} = 0.44$ [35]. This aspartate is a highly conserved amino acid that has been identified to be mainly responsible for the Ca^{2+} block of ASICs [90]. HyNaC6 and HyNaC7, which are the closest relatives of HyNaC5 and supposed to fulfill the same function in the HyNaC heterotrimer, in contrast contain an asparagine at this position. The hypothesis of Dürrnagel et al suggested that the conserved aspartate in ASICs and HyNaC2/3/5 attracts calcium and thus stimulates the permeation of calcium through the ion pore [35]. Despite HyNaC6 and HyNaC7 containing an asparagine at this conserved position, their calcium permeability is not reduced. All other HyNaC subunits except HyNaC12 contain this conserved aspartate. Since HyNaCs form heterotrimers, it is likely that two aspartates are sufficient to attract Ca^{2+} and for a high Ca^{2+} permeability.

4.6. Diminazene, a potent blocker of HyNaC currents

The block by amiloride is a hallmark of the DEG/ENaC ion channel superfamily. However the apparent affinity for amiloride of HyNaC2/3/5 is low compared to other DEG/ENaC channels with an IC_{50} of approximately 120 μM [16, 36]. Amiloride is able to inhibit the feeding reaction in *Hydra magnipapillata*, presumably by inhibiting HyNaC activity. Due to the low affinity, it was necessary to use a high concentration of 100 μM in *in vivo* experiments [36]. Recently it has been shown for BASICs and ASICs that diminazene is a more potent inhibitor of DEG/ENaC channel activity. BASICs are blocked by diminazene in the low micromolar range [74, 118], whereas ASICs are inhibited in the nanomolar range [23]. ENaC instead was not inhibited by diminazene [23] illustrating a selectivity of diminazene for ASIC and BASIC. Diminazene is an anti-

protozoal compound and is used in veterinary medicine for the treatment of infestation with *Trypanosoma* and *Babesia spp.* [93].

In this work it has been shown that diminazene also blocks HyNaC currents efficiently. For all tested HyNaCs the apparent affinity for diminazene was much higher than for amiloride. The highest apparent affinity for diminazene was found with HyNaC2/4/6 with an IC_{50} of about 50 nM, about 200 fold higher than the apparent affinity for amiloride of HyNaC2/3/5. *In vivo* experiments with diminazene showed that the higher affinity of HyNaCs for diminazene does not increase the efficiency of inhibiting the feeding reaction compared to amiloride. In contrast, in this work 200 μM of diminazene were needed to get the same result as for the treatment with 100 μM amiloride [36]. Increasing the concentration, a treatment with 300 μM diminazene almost completely inhibited the feeding reaction. It is difficult to explain why diminazene has a weaker effect on the feeding reaction compared to amiloride. Diminazene is known to be membrane permeable [72, 93, 115]. This higher permeability should lead to a faster up-take of diminazene *in vivo* and thus to a stronger effect. It might be possible that somehow the up-take of diminazene *in vivo* is reduced. However diminazene inhibits the feeding reaction in *Hydra magnipapillata* supporting previous findings from Dürrnagel et al., 2010.

4.7. Outlook: Transgenic animals could reveal the physiological role of HyNaCs *in vivo*

The reason for the variety of HyNaCs, which all are activated by the same ligands and which all share comparable biophysical characteristics can not be explained yet. The different expression patterns of HyNaCs and the different ligand affinities reveal a spatial as well as a functional differentiation between HyNaCs. But the physiological importance of this mechanism remains unclear. Transgenic animals could elucidate the role of the different HyNaC subunits and HyNaC heterotrimers *in vivo*. The generation of transgenic *Hydra magnipapillata* could help to identify the subcellular localization of the HyNaC subunits on the one hand, and to study their physiological role in the living animal on the other hand. Different modified proteins could be expressed under the control of different HyNaC promoters. A previous work by Nakamura et al. demonstrated transgenic approaches to be feasible in *Hydra magnipapillata* [86].

The *in situ* hybridizations done by Anne Kuhn in this work and in previous works [36, 45] demonstrate HyNaC expression at the tentacle basis, presumably in neuromus-

cular cells. With transgenic animals expressing GFP-labelled HyNaC subunits a precise subcellular localization should be possible.

The physiological role of HyNaCs still is unclear. A neurotoxic mutation of the degenerin MEC-4(d) in *C. elegans* has been shown to induce cell swelling and cell death by a constant influx of sodium into the expressing neuronal cells [18, 33]. These animals showed an altered touch sensitivity and locomotion. In this work it has been shown that an arginine at the DEG-position of HyNaC2 and HyNaC3 induces weak constitutive activity causing a constant influx of sodium and most likely also calcium into *Xenopus* oocytes. Similar to MEC-4(d) expressing *C. elegans*, transgenic animals expressing these mutant HyNaC subunits should also suffer from cell swelling and cell death. An altered animal behaviour than would allow the conclusion of the physiological role of cells that endogenously express HyNaCs.

All putative physiological HyNaC heterotrimers show a high calcium permeability. To study the physiological role of HyNaCs *in vivo*, transgenic animals could be generated expressing a Ca^{2+} permeable channelrhodopsin-2 (CatChR2) under the control of different HyNaC promoters. CatChR2 is activated by light [71]. When expressed under the control of different HyNaC promoters, this calcium channel could be activated by light simulating the physiological role of HyNaCs in the corresponding tissue.

Preparations for the generation of transgenic animals have been started already. So in ongoing experiments the generation of transgenic animals should be the next step to study the physiological role of HyNaCs *in vivo* and to identify the exact subcellular expression pattern of the HyNaC heterotrimers.

Bibliography

[1] H. Abriel, J. Loffing, J. F. Rebhun, J. H. Pratt, L. Schild, J.-D. Horisberger, D. Rotin, and O. Staub. Defective regulation of the epithelial Na^+ channel by Nedd4 in Liddle's syndrome. *Journal of Clinical Investigation*, 103(5):667–673, Mar. 1999.

[2] C. M. Adams, M. G. Anderson, D. G. Motto, M. P. Price, W. A. Johnson, and M. J. Welsh. Ripped pocket and pickpocket, novel Drosophila DEG/ENaC subunits expressed in early development and in mechanosensory neurons. *The Journal of cell biology*, 140(1):143–152, Jan. 1998.

[3] A. M. Aguinaldo, J. M. Turbeville, L. S. Linford, M. C. Rivera, J. R. Garey, R. A. Raff, and J. A. Lake. Evidence for a clade of nematodes, arthropods and other moulting animals. *Nature*, 387(6632):489–493, May 1997.

[4] M. Althaus, R. Bogdan, W. G. Clauss, and M. Fronius. Mechano-sensitivity of epithelial sodium channels (ENaCs): laminar shear stress increases ion channel open probability. *The FASEB Journal*, 21(10):2389–2399, Mar. 2007.

[5] M. S. Amin. Distribution of epithelial sodium channels and mineralocorticoid receptors in cardiovascular regulatory centers in rat brain. *AJP: Regulatory, Integrative and Comparative Physiology*, 289(6):R1787–R1797, July 2005.

[6] C. C. Askwith, C. Cheng, M. Ikuma, C. Benson, M. P. Price, and M. J. Welsh. Neuropeptide FF and FMRFamide potentiate acid-evoked currents from sensory neurons and proton-gated DEG/ENaC channels. *Neuron*, 26(1):133–141, Apr. 2000.

[7] E. Babini. Alternative Splicing and Interaction with Di- and Polyvalent Cations Control the Dynamic Range of Acid-sensing Ion Channel 1 (ASIC1). *Journal of Biological Chemistry*, 277(44):41597–41603, Aug. 2002.

[8] M. E. Barish. A transient calcium-dependent chloride current in the immature *Xenopus* oocyte. *The Journal of Physiology*, 342:309–325, Sept. 1983.

[9] E. L. Bassler. Molecular and Functional Characterization of Acid-sensing Ion Channel (ASIC) 1b. *Journal of Biological Chemistry*, 276(36):33782–33787, July 2001.

[10] L. Bianchi, B. Gerstbrein, C. Frøkjær-Jensen, D. C. Royal, G. Mukherjee, M. A. Royal, J. Xue, W. R. Schafer, and M. Driscoll. The neurotoxic MEC-4(d) DEG/ENaC sodium channel conducts calcium: implications for necrosis initiation. *Nature Neuroscience*, 7(12):1337–1344, Nov. 2004.

[11] L. M. Brockway, Z. H. Zhou, J. K. Bubien, B. Jovov, D. J. Benos, and K. T. Keyser. Rabbit retinal neurons and glia express a variety of ENaC/DEG subunits. *AJP: Cell Physiology*, 283(1):C126–C134, Feb. 2002.

[12] A. L. Brown, S. M. Fernandez-Illescas, Z. Liao, and M. B. Goodman. Gain-of-Function Mutations in the MEC-4 DEG/ENaC Sensory Mechanotransduction Channel Alter Gating and Drug Blockade. *The Journal of General Physiology*, 129(2):161–173, Jan. 2007.

[13] J. B. Bruns, M. D. Carattino, S. Sheng, A. B. Maarouf, O. A. Weisz, J. M. Pilewski, R. P. Hughey, and T. R. Kleyman. Epithelial Na^+ Channels Are Fully Activated by Furin- and Prostasin-dependent Release of an Inhibitory Peptide from the γ-Subunit. *Journal of Biological Chemistry*, 282(9):6153–6160, Dec. 2006.

[14] R. A. Caldwell. Serine protease activation of near-silent epithelial Na^+ channels. *AJP: Cell Physiology*, 286(1):190C–194, Sept. 2003.

[15] C. M. Canessa, J. D. Horisberger, and B. C. Rossier. Epithelial sodium channel related to proteins involved in neurodegeneration. *Nature*, 361(6411):467–470, Feb. 1993.

[16] C. M. Canessa, L. Schild, G. Buell, B. Thorens, I. Gautschi, J. D. Horisberger, and B. C. Rossier. Amiloride-sensitive epithelial Na^+ channel is made of three homologous subunits. *Nature*, 367(6462):463–467, Feb. 1994.

[17] M. D. Carattino. Epithelial Na^+ Channels Are Activated by Laminar Shear Stress. *The Journal of biological chemistry*, 279(6):4120–4126, Nov. 2003.

[18] M. Chalfie and E. Wolinsky. The identification and suppression of inherited neurodegeneration in *Caenorhabditis elegans*. *Nature*, 345(6274):410–416, May 1990.

[19] G. Champigny. Molecular Cloning and Functional Expression of a Novel Amiloride-sensitive Na^+ Channel. *Journal of Biological Chemistry*, 270(46):27411–27414, Nov. 1995.

[20] J. A. Chapman, E. F. Kirkness, O. Simakov, S. E. Hampson, T. Mitros, T. Weinmaier, T. Rattei, P. G. Balasubramanian, J. Borman, D. Busam, K. Disbennett, C. Pfannkoch, N. Sumin, G. G. Sutton, L. D. Viswanathan, B. Walenz, D. M. Goodstein, U. Hellsten, T. Kawashima, S. E. Prochnik, N. H. Putnam, S. Shu, B. Blumberg, C. E. Dana, L. Gee, D. F. Kibler, L. Law, D. Lindgens, D. E. Martinez, J. Peng, P. A. Wigge, B. Bertulat, C. Guder, Y. Nakamura, S. Ozbek, H. Watanabe, K. Khalturin, G. Hemmrich, A. Franke, R. Augustin, S. Fraune, E. Hayakawa, S. Hayakawa, M. Hirose, J. S. Hwang, K. Ikeo, C. Nishimiya-Fujisawa, A. Ogura, T. Takahashi, P. R. H. Steinmetz, X. Zhang, R. Aufschnaiter, M.-K. Eder, A.-K. Gorny, W. Salvenmoser, A. M. Heimberg, B. M. Wheeler, K. J. Peterson, A. Böttger, P. Tischler, A. Wolf, T. Gojobori, K. A. Remington, R. L. Strausberg, J. C. Venter, U. Technau, B. Hobmayer, T. C. G. Bosch, T. W. Holstein, T. Fujisawa, H. R. Bode, C. N. David, D. S. Rokhsar, and R. E. Steele. The dynamic genome of *Hydra*. *Nature*, 464(7288):592–596, Mar. 2010.

[21] X. Chen and S. Gründer. Structure, function, and pharmacology of acid-sensing ion channels (ASICs): focus on ASIC1a. *International Journal of Physiology, Pathophysiology and Pharmacology*, 2(2):73–22, 2010.

[22] X. Chen, M. Paukert, I. Kadurin, M. Pusch, and S. Gründer. Strong modulation by RFamide neuropeptides of the ASIC1b/3 heteromer in competition with extracellular calcium. *Neuropharmacology*, 50(8):964–974, June 2006.

[23] X. Chen, L. Qiu, M. Li, S. Durrnagel, B. A. Orser, Z.-G. Xiong, and J. F. MacDonald. Diarylamidines: High potency inhibitors of acid-sensing ion channels. *Neuropharmacology*, 58(7):1045–1053, June 2010.

[24] A. Chraïbi, V. Vallet, D. Firsov, S. K. Hess, and J. D. Horisberger. Protease modulation of the activity of the epithelial sodium channel expressed in *Xenopus* oocytes. *The Journal of General Physiology*, 111(1):127–138, Jan. 1998.

[25] G. A. Cottrell. The first peptide-gated ion channel. *The Journal of experimental biology*, 200(Pt 18):2377–2386, Sept. 1997.

[26] G. A. Cottrell. Domain near TM1 influences agonist and antagonist responses of peptide-gated Na^+ channels. *Pflügers Archiv European Journal of Physiology*, 450(3):168–177, Apr. 2005.

[27] G. A. Cottrell, M. C. Jeziorski, and K. A. Green. Location of a ligand recognition site of FMRFamide-gated Na^+ channels. *FEBS Letters*, 489(1):71–74, Jan. 2001.

[28] D. Darmer, F. Hauser, H. P. Nothacker, T. C. Bosch, M. Williamson, and C. J. Grimmelikhuijzen. Three different prohormones yield a variety of Hydra-RFamide (Arg-Phe-NH2) neuropeptides in *Hydra magnipapillata*. *Biochemical Journal*, 332 (Pt 2):403–412, June 1998.

[29] F. Davey, S. J. Harris, and G. A. Cottrell. Histochemical localisation of FMRFamide-gated Na^+ channels in *Helisoma trivolvis* and *Helix aspersa* neurones. *Journal of Neurocytology*, 30(11):877–884, Oct. 2001.

[30] C. W. Davies and T. Shedlovsky. Ion association. *Journal of The Electrochemical Society*, 1964.

[31] R. de Rosa, J. K. Grenier, T. Andreeva, C. E. Cook, A. Adoutte, M. Akam, S. B. Carroll, and G. Balavoine. Hox genes in brachiopods and priapulids and protostome evolution. *Nature*, 399(6738):772–776, June 1999.

[32] E. Deval, X. Gasull, J. Noël, M. Salinas, A. Baron, S. Diochot, and E. Lingueglia. Acid-sensing ion channels (ASICs): pharmacology and implication in pain. *Pharmacology & therapeutics*, 128(3):549–558, Dec. 2010.

[33] M. Driscoll and M. Chalfie. The mec-4 gene is a member of a family of *Caenorhabditis elegans* genes that can mutate to induce neuronal degeneration. *Nature*, 349(6310):588–593, Feb. 1991.

[34] A. Duggan. The PDZ Domain Protein PICK1 and the Sodium Channel BNaC1 Interact and Localize at Mechanosensory Terminals of Dorsal Root Ganglion Neurons and Dendrites of Central Neurons. *Journal of Biological Chemistry*, 277(7):5203–5208, Dec. 2001.

[35] S. Durrnagel, B. H. Falkenburger, and S. Gründer. High Ca^{2+} permeability of a peptide-gated DEG/ENaC from *Hydra*. *The Journal of General Physiology*, 140(4):391–402, Sept. 2012.

[36] S. Durrnagel, A. Kuhn, C. D. Tsiairis, M. Williamson, H. Kalbacher, C. J. P. Grimmelikhuijzen, T. W. Holstein, and S. Gründer. Three Homologous Subunits Form a High Affinity Peptide-gated Ion Channel in *Hydra*. *Journal of Biological Chemistry*, 285(16):11958–11965, Apr. 2010.

[37] D. Firsov, M. Robert-Nicoud, S. Gründer, L. Schild, and B. C. Rossier. Mutational Analysis of Cysteine-rich Domains of the Epithelium Sodium Channel (ENaC). Identificiation of cysteines essential for channel expression at the cell surface. *Journal of Biological Chemistry*, 274(5):2743–2749, Jan. 1999.

[38] Y. Furukawa, Y. Miyawaki, and G. Abe. Molecular cloning and functional characterization of the *Aplysia* FMRFamide-gated Na^{+} channel. *Pflügers Archiv European Journal of Physiology*, 451(5):646–656, Aug. 2005.

[39] B. Galliot, M. Quiquand, L. Ghila, R. de Rosa, M. Miljkovic-Licina, and S. Chera. Origins of neurogenesis, a cnidarian view. *Developmental Biology*, 332(1):2–24, Aug. 2009.

[40] J. García-Añoveros, J. A. García, J. D. Liu, and D. P. Corey. The nematode degenerin UNC-105 forms ion channels that are activated by degeneration- or hypercontraction-causing mutations. *Neuron*, 20(6):1231–1241, June 1998.

[41] M. Gautam and C. J. Benson. Acid-sensing ion channels (ASICs) in mouse skeletal muscle afferents are heteromers composed of ASIC1a, ASIC2, and ASIC3 subunits. *The FASEB Journal*, 27(2):793–802, Jan. 2013.

[42] T. Giraldez, D. Afonso-Oramas, I. Cruz-Muros, V. Garcia-Marin, P. Pagel, T. González-Hernández, and D. A. de la Rosa. Cloning and functional expression of a new epithelial sodium channel δ subunit isoform differentially expressed in neurons of the human and monkey telencephalon. *Journal of Neurochemistry*, 102(4):1304–1315, Aug. 2007.

[43] K. M. Glauber, C. E. Dana, and R. E. Steele. *Hydra*. *CURBIO*, 20(22):R964–R965, Nov. 2010.

[44] A. Golubovic. *Phylogenetic and electrophysiological characterization of new ion channel subunits from Hydra magnipapillata belonging to the DEG/ENaC gene family.* PhD thesis, Universitätsbibliothek Tübingen, Tübingen, Jan. 2007.

[45] A. Golubovic, A. Kuhn, M. Williamson, H. Kalbacher, T. W. Holstein, C. J. P. Grimmelikhuijzen, and S. Gründer. A Peptide-gated Ion Channel from the Freshwater Polyp *Hydra*. *Journal of Biological Chemistry*, 282(48):35098–35103, Sept. 2007.

[46] M. B. Goodman, G. G. Ernstrom, D. S. Chelur, R. O'Hagan, C. A. Yao, and M. Chalfie. MEC-2 regulates C. elegans DEG/ENaC channels needed for mechanosensation. *Nature*, 415(6875):1039–1042, Feb. 2002.

[47] M. B. Goodman and E. M. Schwarz. Transducing Touch in *Caenorhabditis elegans*. *Annual Review of Physiology*, 65(1):429–452, Mar. 2003.

[48] K. Green and G. Cottrell. Activity modes and modulation of the peptide-gated Na^+ channel of *Helix* neurones. *Pflügers Archiv European Journal of Physiology*, 443(5-6):813–821, Mar. 2002.

[49] C. J. Grimmelikhuijzen. Antisera to the sequence Arg-Phe-amide. *Cell and Tissue Research*, pages 1–12, July 1985.

[50] S. Gründer, D. Firsov, S. S. Chang, N. F. Jaeger, I. Gautschi, L. Schild, R. P. Lifton, and B. C. Rossier. A mutation causing pseudohypoaldosteronism type 1 identifies a conserved glycine that is involved in the gating of the epithelial sodium channel. *The EMBO Journal*, 16(5):899–907, Mar. 1997.

[51] S. Gründer, H. S. Geissler, E. L. Bassler, and J. P. Ruppersberg. A new member of acid-sensing ion channels from pituitary gland. *Neuroreport*, 11(8):1607–1611, June 2000.

[52] S. Gründer, N. F. Jaeger, I. Gautschi, L. Schild, and B. C. Rossier. Identification of a highly conserved sequence at the N-terminus of the epithelial Na^+ channel alpha subunit involved in gating. *Pflügers Archiv*, 438(5):709–715, Oct. 1999.

[53] C. Guder, I. Philipp, T. Lengfeld, H. Watanabe, B. Hobmayer, and T. W. Holstein. The Wnt code: cnidarians signal the way. *Oncogene*, 25(57):7450–7460, Dec. 2006.

[54] J. B. Gurdon, C. D. Lane, H. R. Woodland, and G. Marbaix. Use of frog eggs and oocytes for the study of messenger RNA and its translation in living cells. *Nature*, 233(5316):177–182, Sept. 1971.

[55] D. H. Hall, G. Gu, J. García-Añoveros, L. Gong, M. Chalfie, and M. Driscoll. Neuropathology of degenerative cell death in *Caenorhabditis elegans*. *The Journal of neuroscience : the official journal of the Society for Neuroscience*, 17(3):1033–1045, Feb. 1997.

[56] K. F. Harvey. The Nedd4-like Protein KIAA0439 Is a Potential Regulator of the Epithelial Sodium Channel. *Journal of Biological Chemistry*, 276(11):8597–8601, Jan. 2001.

[57] E. N. Hoagland, T. W. Sherwood, K. G. Lee, C. J. Walker, and C. C. Askwith. Identification of a Calcium Permeable Human Acid-sensing Ion Channel 1 Transcript Variant. *Journal of Biological Chemistry*, 285(53):41852–41862, Dec. 2010.

[58] A. M. Hruska-Hageman. PSD-95 and Lin-7b Interact with Acid-sensing Ion Channel-3 and Have Opposite Effects on H^+-gated Current. *Journal of Biological Chemistry*, 279(45):46962–46968, Aug. 2004.

[59] A. M. Hruska-Hageman, J. A. Wemmie, M. P. Price, and M. J. Welsh. Interaction of the synaptic protein PICK1 (protein interacting with C kinase 1) with the non-voltage gated sodium channels BNC1 (brain Na^+ channel 1) and ASIC (acid-sensing ion channel). *Biochemical Journal*, 361(Pt 3):443–450, Feb. 2002.

[60] M. Huang and M. Chalfie. Gene interactions affecting mechanosensory transduction in *Caenorhabditis elegans*. *Nature*, 367(6462):467–470, Feb. 1994.

[61] D. H. Huson and C. Scornavacca. Dendroscope 3: An Interactive Tool for Rooted Phylogenetic Trees and Networks. *Systematic Biology*, 61(6):1061–1067, Oct. 2012.

[62] J. Jasti, H. Furukawa, E. B. Gonzales, and E. Gouaux. Structure of acid-sensing ion channel 1 at 1.9 Å resolution and low pH. *Nature*, 449(7160):316–323, Sept. 2007.

[63] M. C. Jeziorski, K. A. Green, J. Sommerville, and G. A. Cottrell. Cloning and expression of a FMRFamide-gated Na^+ channel from *Helisoma trivolvis* and comparison with the native neuronal channel. *The Journal of Physiology*, 526(1):13–25, July 2000.

[64] E. Kamynina, C. Debonneville, M. Bens, A. Vandewalle, and O. Staub. A novel mouse Nedd4 protein suppresses the activity of the epithelial Na^+ channel. *FASEB journal : official publication of the Federation of American Societies for Experimental Biology*, 15(1):204–214, Jan. 2001.

[65] E. Kandel, J. Schwartz, T. Jessell, S. Siegelbaum, and A. J. Hudspeth. *Principles of Neural Science, Fifth Edition*. McGraw Hill Professional, Sept. 2012.

[66] S. Kang, J. H. Jang, M. P. Price, M. Gautam, C. J. Benson, H. Gong, M. J. Welsh, and T. J. Brennan. Simultaneous Disruption of Mouse ASIC1a, ASIC2 and ASIC3 Genes Enhances Cutaneous Mechanosensitivity. *PLoS ONE*, 7(4):e35225, Apr. 2012.

[67] S. Kellenberger, M. Auberson, I. Gautschi, E. Schneeberger, and L. Schild. Permeability properties of ENaC selectivity filter mutants. *The Journal of General Physiology*, 118(6):679–692, Dec. 2001.

[68] S. Kellenberger, I. Gautschi, and L. Schild. A single point mutation in the pore region of the epithelial Na^+ channel changes ion selectivity by modifying molecular sieving. *Proceedings of the National Academy of Sciences of the United States of America*, 96(7):4170–4175, Mar. 1999.

[69] S. Kellenberger, N. Hoffmann-Pochon, I. Gautschi, E. Schneeberger, and L. Schild. On the molecular basis of ion permeation in the epithelial Na^+ channel. *The Journal of General Physiology*, 114(1):13–30, July 1999.

[70] S. Kellenberger and L. Schild. Epithelial sodium channel/degenerin family of ion channels: a variety of functions for a shared structure. *Physiological reviews*, 82(3):735–767, July 2002.

[71] S. Kleinlogel, K. Feldbauer, R. E. Dempski, H. Fotis, P. G. Wood, C. Bamann, and E. Bamberg. Ultra light-sensitive and fast neuronal activation with the Ca^{2+}-permeable channelrhodopsin CatCh. *Nature Neuroscience*, 14(4):513–518, Mar. 2011.

[72] A. N. Lane, T. C. Jenkins, T. Brown, and S. Neidle. Interaction of berenil with the EcoRI dodecamer d(CGCGAATTCGCG)2 in solution studied by NMR. *Biochemistry*, 30(5):1372–1385, Feb. 1991.

[73] M. A. Larkin, G. Blackshields, N. P. Brown, R. Chenna, P. A. McGettigan, H. McWilliam, F. Valentin, I. M. Wallace, A. Wilm, R. Lopez, J. D. Thompson, T. J. Gibson, and D. G. Higgins. Clustal W and Clustal X version 2.0. *Bioinformatics*, 23(21):2947–2948, Nov. 2007.

[74] C. M. T. Lefèvre, A. Diakov, S. Haerteis, C. Korbmacher, S. Gründer, and D. Wiemuth. Pharmacological and electrophysiological characterization of the human bile acid-sensitive ion channel (hBASIC). *Pflügers Archiv European Journal of Physiology*, July 2013.

[75] J. P. Leonard and S. R. Kelso. Apparent desensitization of NMDA responses in *Xenopus* oocytes involves calcium-dependent chloride current. *Neuron*, 4(1):53–60, Jan. 1990.

[76] C. A. LEWIS. Ion-concentration dependence of the reversal potential and the single channel conductance of ion channels at the frog neuromuscular junction. *The Journal of Physiology*, 286:417–445, Jan. 1979.

[77] T. Li, Y. Yang, and C. M. Canessa. Outlines of the pore in open and closed conformations describe the gating mechanism of ASIC1. *Nature Communications*, 2:399–7, July 2011.

[78] E. Lingueglia, G. Champigny, M. Lazdunski, and P. Barbry. Cloning of the amiloride-sensitive FMRFamide peptide-gated sodium channel. *Nature*, 378(6558):730–733, Dec. 1995.

[79] L. Liu, W. A. Johnson, and M. J. Welsh. *Drosophila* DEG/ENaC pickpocket genes are expressed in the tracheal system, where they may be involved in liquid clearance. *Proceedings of the National Academy of Sciences of the United States of America*, 100(4):2128–2133, Feb. 2003.

[80] B. Lu, A. LaMora, Y. Sun, M. J. Welsh, and Y. Ben-Shahar. ppk23-Dependent Chemosensory Functions Contribute to Courtship Behavior in *Drosophila melanogaster*. *PLoS Genetics*, 8(3):e1002587, Mar. 2012.

[81] M. Madeja, U. Musshoff, and E. J. Speckmann. Improvement and testing of a concentration-clamp system for oocytes of Xenopus laevis. *Journal of neuroscience methods*, 63(1-2):211–213, Dec. 1995.

[82] I. D. McFarlane, P. A. Anderson, and C. J. Grimmelikhuijzen. Effects of three anthozoan neuropeptides, Antho-RWamide I, Antho-RWamide II and Antho-RFamide, on slow muscles from sea anemones. *The Journal of experimental biology*, 156:419–431, Mar. 1991.

[83] M. Medina, A. G. Collins, J. D. Silberman, and M. L. Sogin. Evaluating hypotheses of basal animal phylogeny using complete sequences of large and small subunit rRNA. *Proceedings of the National Academy of Sciences of the United States of America*, 98(17):9707–9712, Aug. 2001.

[84] J. S. Mogil. Transgenic Expression of a Dominant-Negative ASIC3 Subunit Leads to Increased Sensitivity to Mechanical and Inflammatory Stimuli. *Journal of Neuroscience*, 25(43):9893–9901, Oct. 2005.

[85] A. Moosler, K. L. Rinehart, and C. J. Grimmelikhuijzen. Isolation of four novel neuropeptides, the *hydra*-RFamides I-IV, from *Hydra magnipapillata*. *Biochemical and Biophysical Research Communications*, 229(2):596–602, Dec. 1996.

[86] Y. Nakamura, C. D. Tsiairis, S. Ozbek, and T. W. Holstein. Autoregulatory and repressive inputs localize *Hydra* Wnt3 to the head organizer. *Proceedings of the National Academy of Sciences*, 108(22):9137–9142, May 2011.

[87] K. Okonechnikov, O. Golosova, M. Fursov, and the UGENE team. Unipro UGENE: a unified bioinformatics toolkit. *Bioinformatics*, 28(8):1166–1167, Apr. 2012.

[88] L. M. Passano and C. B. McCullough. Co-ordinating Systems and Behaviour in *Hydra*. *The Journal of experimental biology*, 42:205–231, Apr. 1965.

[89] C. J. Passero, S. Okumura, and M. D. Carattino. Conformational Changes Associated with Proton-dependent Gating of ASIC1a. *Journal of Biological Chemistry*, 284(52):36473–36481, Dec. 2009.

[90] M. Paukert. Identification of the Ca^{2+} Blocking Site of Acid-sensing Ion Channel (ASIC) 1: Implications for Channel Gating. *The Journal of General Physiology*, 124(4):383–394, Sept. 2004.

[91] M. Paukert, S. Sidi, C. Russell, M. Siba, S. W. Wilson, T. Nicolson, and S. Gründer. A family of acid-sensing ion channels from the zebrafish: widespread expres-

sion in the central nervous system suggests a conserved role in neuronal communication. *The Journal of biological chemistry*, 279(18):18783–18791, Apr. 2004.

[92] R. Pawlowicz and R. Feistel. Limnological applications of the Thermodynamic Equation of Seawater 2010 (TEOS-10). *Limnology and Oceanography: Methods*, 10:853–867, 2012.

[93] A. S. Peregrine and M. Mamman. Pharmacology of diminazene: a review. *Acta tropica*, 54(3-4):185–203, Sept. 1993.

[94] S. J. Perry, V. A. Straub, M. G. Schofield, J. F. Burke, and P. R. Benjamin. Neuronal expression of an FMRFamide-gated Na^+ channel and its modulation by acid pH. *Journal of Neuroscience*, 21(15):5559–5567, Aug. 2001.

[95] P. Pierobon. Coordinated modulation of cellular signaling through ligand-gated ion channels in *Hydra vulgaris* (Cnidaria, Hydrozoa). *The International Journal of Developmental Biology*, 56(6-7-8):551–565, 2012.

[96] C. Planès and G. H. Caughey. Regulation of the epithelial Na^+ channel by peptidases. *Current topics in developmental biology*, 78:23–46, 2007.

[97] Y. J. Qadri, A. K. Rooj, and C. M. Fuller. ENaCs and ASICs as therapeutic targets. *AJP: Cell Physiology*, 302(7):C943–C965, Apr. 2012.

[98] B. C. Rossier and M. J. Stutts. Activation of the Epithelial Sodium Channel (ENaC) by Serine Proteases. *Annual Review of Physiology*, 71(1):361–379, Mar. 2009.

[99] R. K. Saiki, S. Scharf, F. Faloona, K. B. Mullis, G. T. Horn, H. A. Erlich, and N. Arnheim. Enzymatic amplification of beta-globin genomic sequences and restriction site analysis for diagnosis of sickle cell anemia. *Science*, 230(4732):1350–1354, Dec. 1985.

[100] H. Sakai, E. Lingueglia, G. Champigny, M.-G. Mattei, and M. Lazdunski. Cloning and functional expression of a novel degenerin-like Na^+ channel gene in mammals. *The Journal of Physiology*, 519(2):323–333, Sept. 1999.

[101] L. Schaefer, H. Sakai, M.-G. Mattei, M. Lazdunski, and E. Lingueglia. Molecular cloning, functional expression and chromosomal localization of an amiloride-sensitive Na^+ channel from human small intestine. *FEBS Letters*, 471(2-3):205–210, Apr. 2000.

[102] H. A. Schmidt, K. Strimmer, M. Vingron, and A. von Haeseler. TREE-PUZZLE: maximum likelihood phylogenetic analysis using quartets and parallel computing. *Bioinformatics*, 18(3):502–504, Mar. 2002.

[103] S. Sheng. Characterization of the Selectivity Filter of the Epithelial Sodium Channel. *Journal of Biological Chemistry*, 275(12):8572–8581, Mar. 2000.

[104] T. W. Sherwood, K. G. Lee, M. G. Gormley, and C. C. Askwith. Heteromeric Acid-Sensing Ion Channels (ASICs) Composed of ASIC2b and ASIC1a Display Novel Channel Properties and Contribute to Acidosis-Induced Neuronal Death. *Journal of Neuroscience*, 31(26):9723–9734, June 2011.

[105] H. Shimizu and T. Fujisawa. Peduncle of *Hydra* and the heart of higher organisms share a common ancestral origin. *Genesis (New York, N.Y. : 2000)*, 36(4):182–186, Aug. 2003.

[106] P. M. Snyder. A Pore Segment in DEG/ENaC Na^+ Channels. *Journal of Biological Chemistry*, 274(40):28484–28490, Oct. 1999.

[107] Z. Songyang. Recognition of Unique Carboxyl-Terminal Motifs by Distinct PDZ Domains. *Science*, 275(5296):73–77, Jan. 1997.

[108] E. Starostina, T. Liu, V. Vijayan, Z. Zheng, K. K. Siwicki, and C. W. Pikielny. A *Drosophila* DEG/ENaC Subunit Functions Specifically in Gustatory Neurons Required for Male Courtship Behavior. *Journal of Neuroscience*, 32(13):4665–4674, Mar. 2012.

[109] K. Sumikawa, I. Parker, T. Amano, and R. Miledi. Separate fractions of mRNA from *Torpedo* electric organ induce chloride channels and acetylcholine receptors in *Xenopus* oocytes. *The EMBO Journal*, 3(10):2291–2294, Oct. 1984.

[110] Y. Takaku, J. S. Hwang, A. Wolf, A. Böttger, H. Shimizu, C. N. David, and T. Gojobori. Innexin gap junctions in nerve cells coordinate spontaneous contractile behavior in Hydra polyps. *Scientific Reports*, 4, Jan. 2014.

[111] U. Technau and R. E. Steele. Evolutionary crossroads in developmental biology: Cnidaria. *Development*, 139(23):4491–4491, Nov. 2012.

[112] H. Toda, X. Zhao, and B. J. Dickson. The *Drosophila* Female Aphrodisiac Pheromone Activates ppk23+ Sensory Neurons to Elicit Male Courtship Behavior. *CellReports*, 1(6):599–607, June 2012.

[113] R. Waldmann, G. Champigny, F. Bassilana, C. Heurteaux, and M. Lazdunski. A proton-gated cation channel involved in acid-sensing. *Nature*, 386(6621):173–177, Mar. 1997.

[114] R. Waldmann and M. Lazdunski. H^+-gated cation channels: neuronal acid sensors in the ENaC/DEG family of ion channels. *Current opinion in neurobiology*, 8(3):418–424, June 1998.

[115] M. J. Waring. The effects of antimicrobial agents on ribonucleic acid polymerase. *Molecular Pharmacology*, 1(1):1–13, July 1965.

[116] H. Watanabe, T. Fujisawa, and T. W. Holstein. Cnidarians and the evolutionary origin of the nervous system. *Development, Growth & Differentiation*, 51(3):167–183, Mar. 2009.

[117] D. Wiemuth and S. Gründer. A Single Amino Acid Tunes Ca^{2+} Inhibition of Brain Liver Intestine Na^+ Channel (BLINaC). *Journal of Biological Chemistry*, 285(40):30404–30410, Sept. 2010.

[118] D. Wiemuth and S. Gründer. The Pharmacological Profile of Brain Liver Intestine Na^+ Channel: Inhibition by Diarylamidines and Activation by Fenamates. *Molecular Pharmacology*, 80(5):911–919, Oct. 2011.

[119] D. Wiemuth, H. Sahin, B. H. Falkenburger, C. M. T. Lefevre, H. E. Wasmuth, and S. Gründer. BASIC–a bile acid-sensitive ion channel highly expressed in bile ducts. *The FASEB Journal*, 26(10):4122–4130, Oct. 2012.

[120] O. Yermolaieva, A. S. Leonard, M. K. Schnizler, F. M. Abboud, and M. J. Welsh. Extracellular acidosis increases neuronal cell calcium by activating acid-sensing ion channel 1a. *Proceedings of the National Academy of Sciences of the United States of America*, 101(17):6752–6757, Apr. 2004.

[121] K. M. Zelle, B. Lu, S. C. Pyfrom, and Y. Ben-Shahar. The genetic architecture of degenerin/epithelial sodium channels in *Drosophila*. *G3 (Bethesda, Md.)*, 3(3):441–450, Mar. 2013.

[122] X. m. Zha. Acid-sensing ion channels: trafficking and synaptic function. *Molecular Brain*, 6(1):1, 2013.

[123] L. Zhong, R. Y. Hwang, and W. D. Tracey. Pickpocket Is a DEG/ENaC Protein Required for Mechanical Nociception in *Drosophila* Larvae. *Current Biology*, 20(5):429–434, Mar. 2010.

A. Appendix

A.1. List of abbrevations

°C	degree Celsius
amil.	amiloride
ASIC	acid sensing ion channel
BASIC	bile acid sensitive ion channel
bp	base pair(s)
c	chicken
C. elegans	*Caenorhabditis elegans*
Ca^{2+}	calcium ion
$CaCl_2$	calcium chloride
cDNA	complementary DNA
cfu	colony forming unit
Cl^-	chloride ion
CNS	central nervous system
cRNA	complementary RNA
DEG	degenerin
DEL	degenerin like protein
DEPC	diethylpyrocarbonate
dimi.	diminazene
DNA	deoxyribonucleic acid
EC_{50}	half maximal effective concentration
EGTA	ethylene glycol tetraacetic acid
ENaC	epithelial sodium channel
E_{Rev}	reversal potential
FaNaC	FMRFamide-gated sodium channel
Fig.	figure
FMRFamide	phe-met-arg-phe-NH_2
FLR	fluoride resistant mutant
g	gram
GABA	gamma-aminobutyric acid
GluR	glutamate receptor
GSH	glutathione
h	human
H. magnipapillata	*Hydra magnipapillata*

H^+	hydrogen
HCl	hydrogen chloride
HEPES	4-(2-hydroxyethyl)-1-piperazineethanesulfonic acid
HG-motif	histidin-glycine motif
HyNaC	*hydra* sodium channel
Hz	hertz
I	current
IC_{50}	half maximal inhibitory concentration
I_m	membrane current
I_{max}	maximal current
K^+	potassium
KCl	potassium chloride
kDa	kilodalton
l	litre
m	mouse
M	molar
MEC	mechanosensitive mutations
mg	milligram
Mg^{2+}	magnesium ion
$MgCl_2$	magnesium chloride
min	minute
ml	millilitre
ML	maximum likelihood
mM	millimolar
MΩ	megaohm
mRNA	messenger RNA
mV	millivolt
n	number of experiments
N	number of oocyte donors
nA	nanoampere
Na^+	sodium
NaOH	sodium hydroxide
ng	nanogram
NJ	neighbour joining
nl	nanolitre

nM	nanomolar
NMDA	N-methyl-D-aspartic acid
OR-2	oocyte ringer's solution - 2
OTC-20	oocyte testing carousel - 20
PNS	peripheral nervous system
PPK	pickpocket
r	rat
RNA	ribonucleic acid
RPK	ripped pocket
sec	second
SEM	standard error of the mean
Tab.	table
TEVC	two electrode voltage clamp
TMD	transmembrane domain
trunc.	truncated
UNC	uncoordinated locomotion mutant
V_m	membrane potential
μA	microampere
μg	microgram
μM	micromolar

A.2. Accession numbers of used protein sequences and protein alignment of the DEG/ENaC superfamily

ACD-1	NM_058894	HyNaC 2	AM393878
ACD-2	NM_058892	HyNaC 3	AM393880
ACD-4	NM_072829	HyNaC 4	AM393881
ACD-5	NM_058795	HyNaC 5	FN257513
cASIC1	AY956393	HyNaC 6	HG422725
cASIC2	NM_001040467	HyNaC 7	HG422726
hASIC1a	U78180	HyNaC 8	HG422727
hASIC2a	U50352	HyNaC 9	HG422728
hASIC2b	NM_18337	HyNaC 10	HG422729
hASIC3	AF095897	HyNaC 11	HG422730
hASIC4	AJ271643	HyNaC 12	HG422731
rASIC1a	U94403	LampreyA1	AAY28983
rASIC1b	AJ309926	MEC-4	X58982
rASIC2a	U53211	MEC-10	L25312
rASIC2b	AB049451	PPK	Y16225
rASIC3	AF013598	PPK4	NM_206137
rASIC4	AJ271642	PPK6	NM_137617
hBASIC	AJ252011	PPK7	NM_135172
mBASIC	Y19035	PPK10	NM_001038805
rBASIC	Y19034	PPK11	NM_001038798
DEG-1	NM_076910	PPK12	NM_137828
DEL-1	U76403	PPK13	NM_001014495
DEL-4	NM_059829	PPK16	NM_001038797
DEL-7	NM_068875	PPK17	NM_135965
DEL-9	NM_076221	PPK19	AY226547
DEL-10	NM-062901	PPK20	NM_143448
hENaCα	X76180	PPK21	NM_143447
hENaCβ	X87159	PPK23	NM_001014749
hENaCγ	X87160	PPK24	NM_143603
hENaCδ	U38254	PPK25	NM_206044
rENaCα	X70521	PPK26	NM_139868
rENaCβ	X77932	PPK27	NM_139569
rENaCγ	X77933	PPK28	NM_001014748
H.a.FaNaC	X92113	RPK	Y12640
H.t.FaNaC	AF254118	UNC-8	U76402
L.s.FaNaC	AF335548	UNC-105	NM_063301
FLR-1	AB012617		

Table A.1.: **Accession numbers of protein sequences used in this work.**

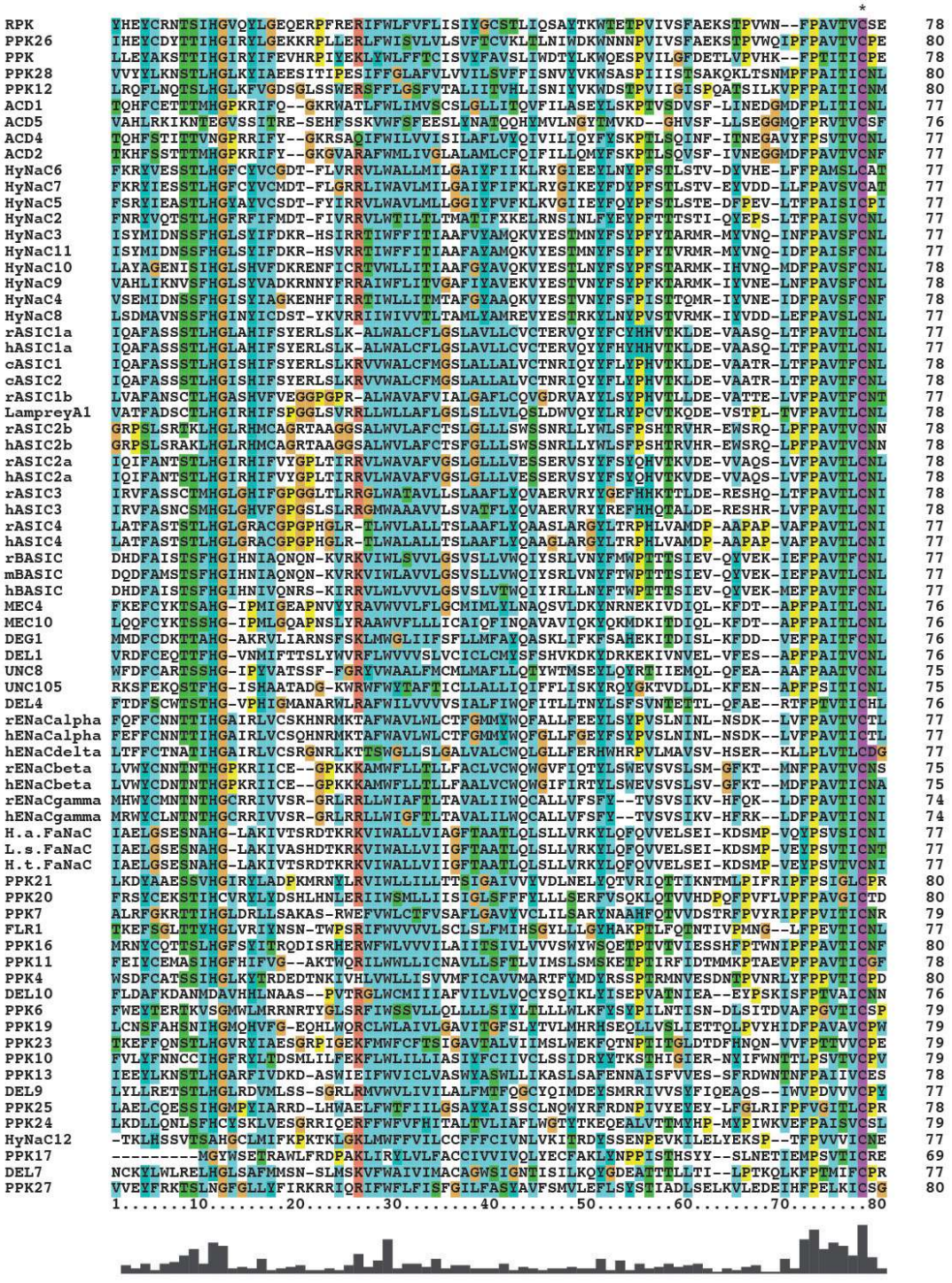

Figure A.1.: **Proteinalignment of members of the DEG/ENaC ion channel family.** Asterisks indicate fully conserved amino acids. Degree of similarity shown by histogram below the alignment. Colors indicate groups of amino acids.

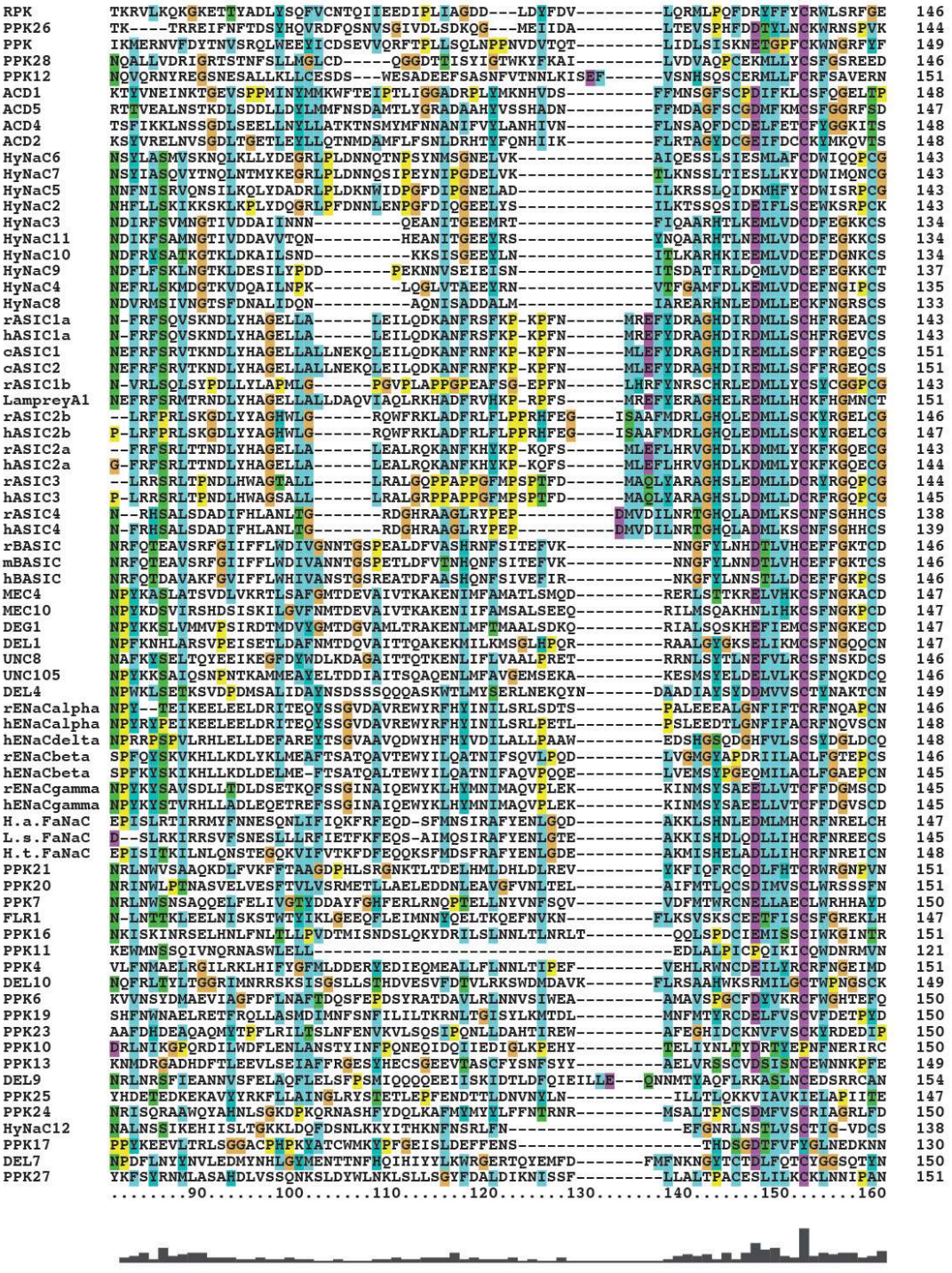

Alignment DEG/ENaC ion channel family, part 2.

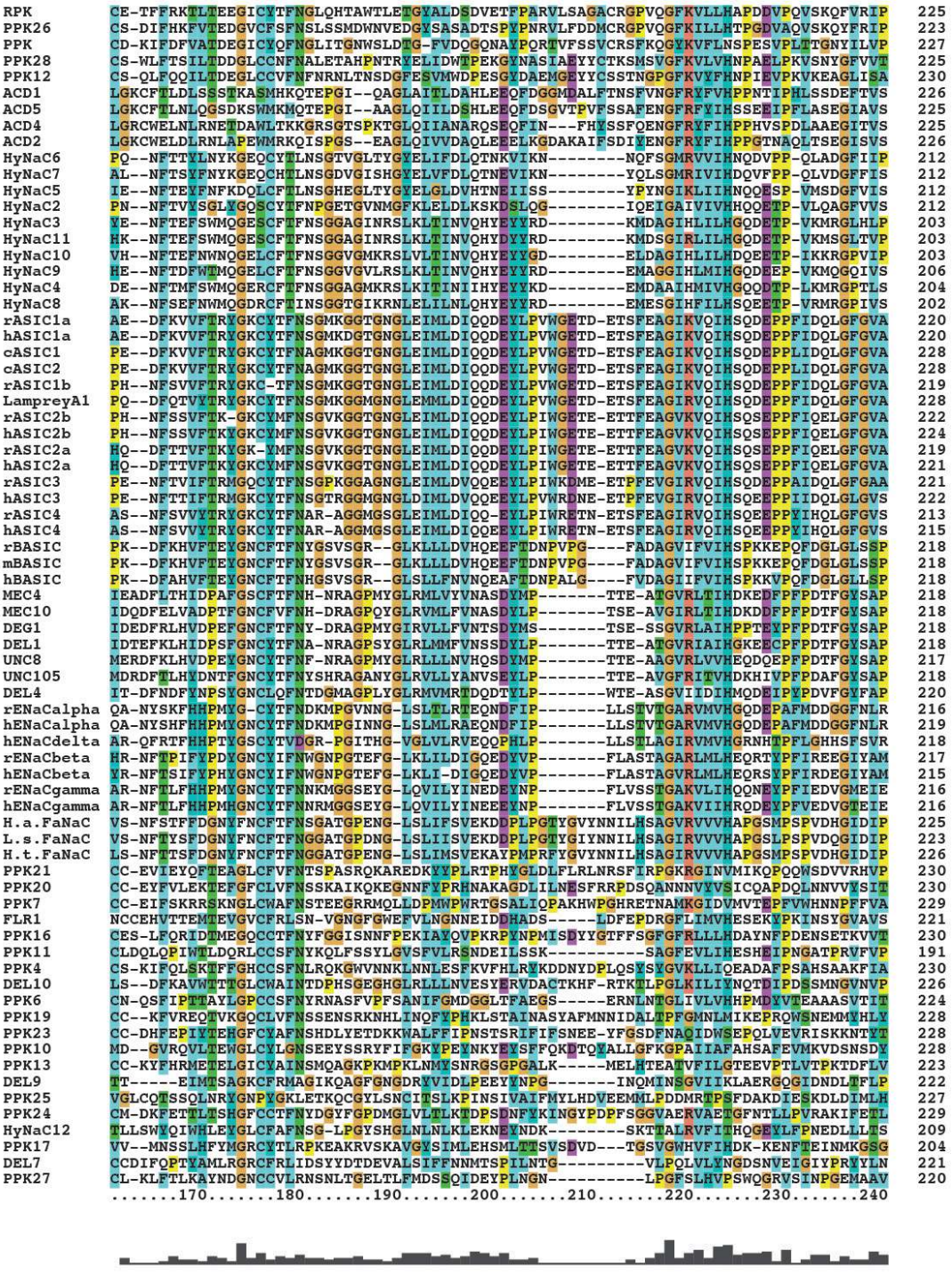

Alignment DEG/ENaC ion channel family, part 3.

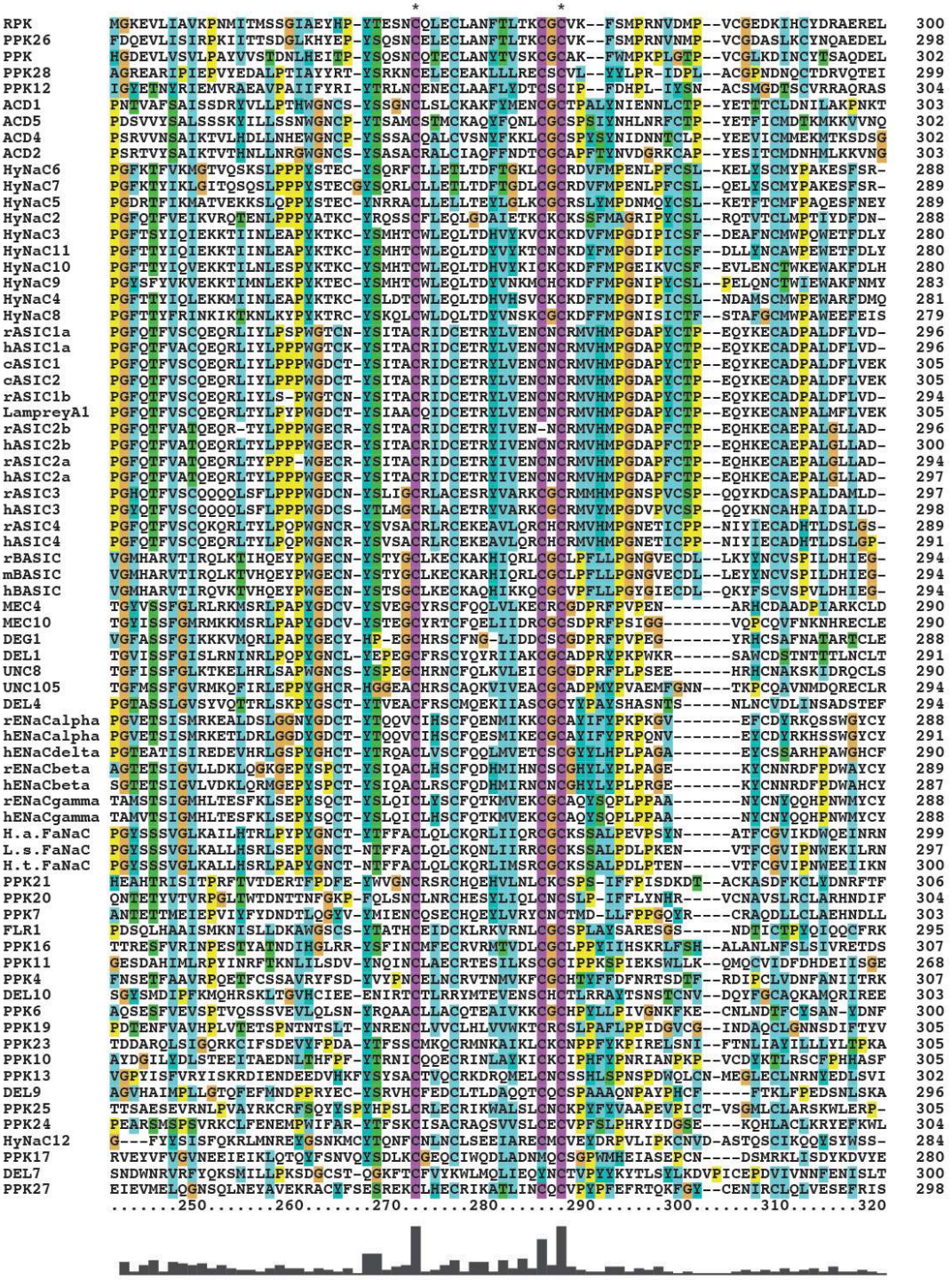

Alignment DEG/ENaC ion channel family, part 4.

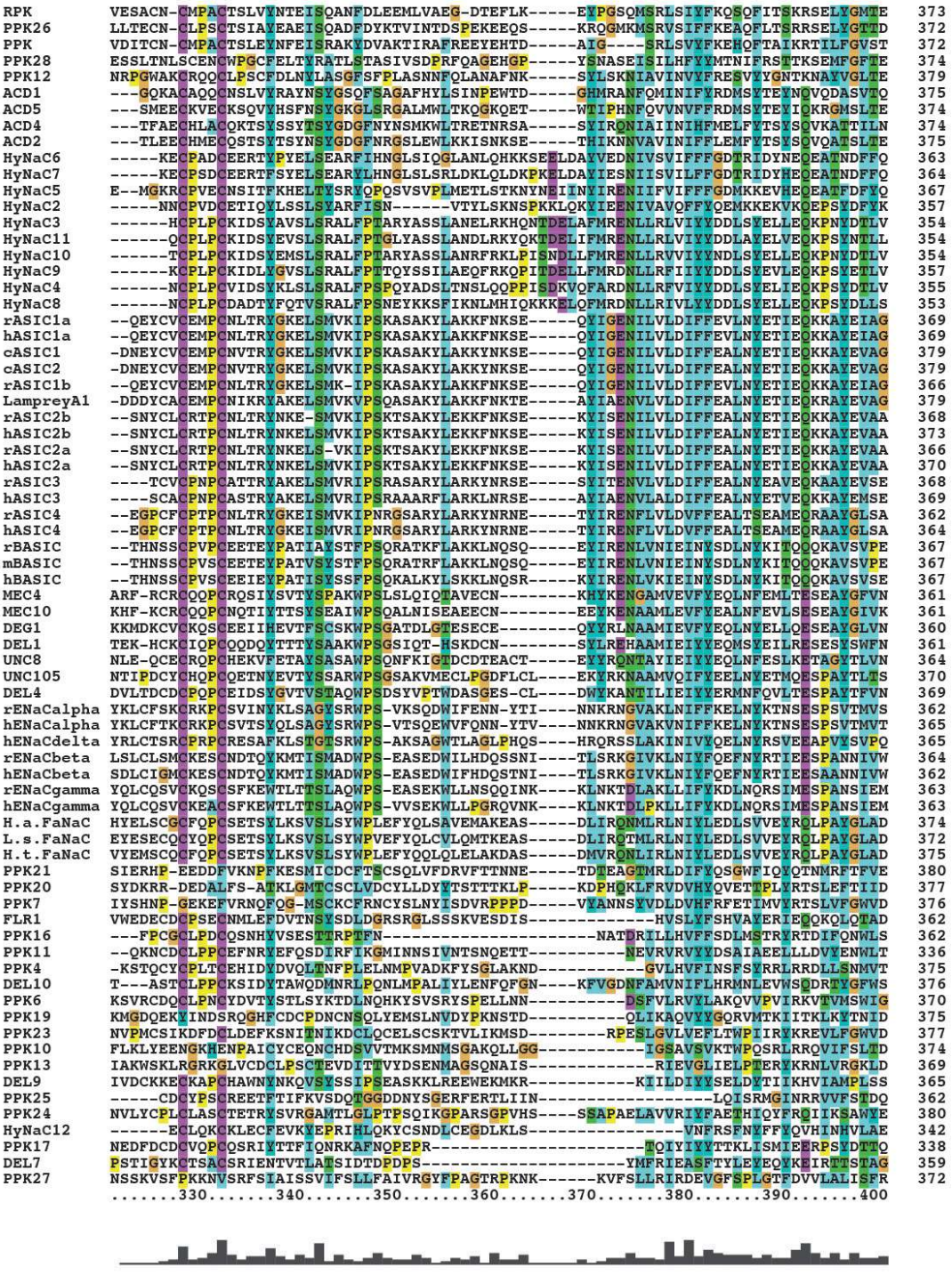

Alignment DEG/ENaC ion channel family, part 5.

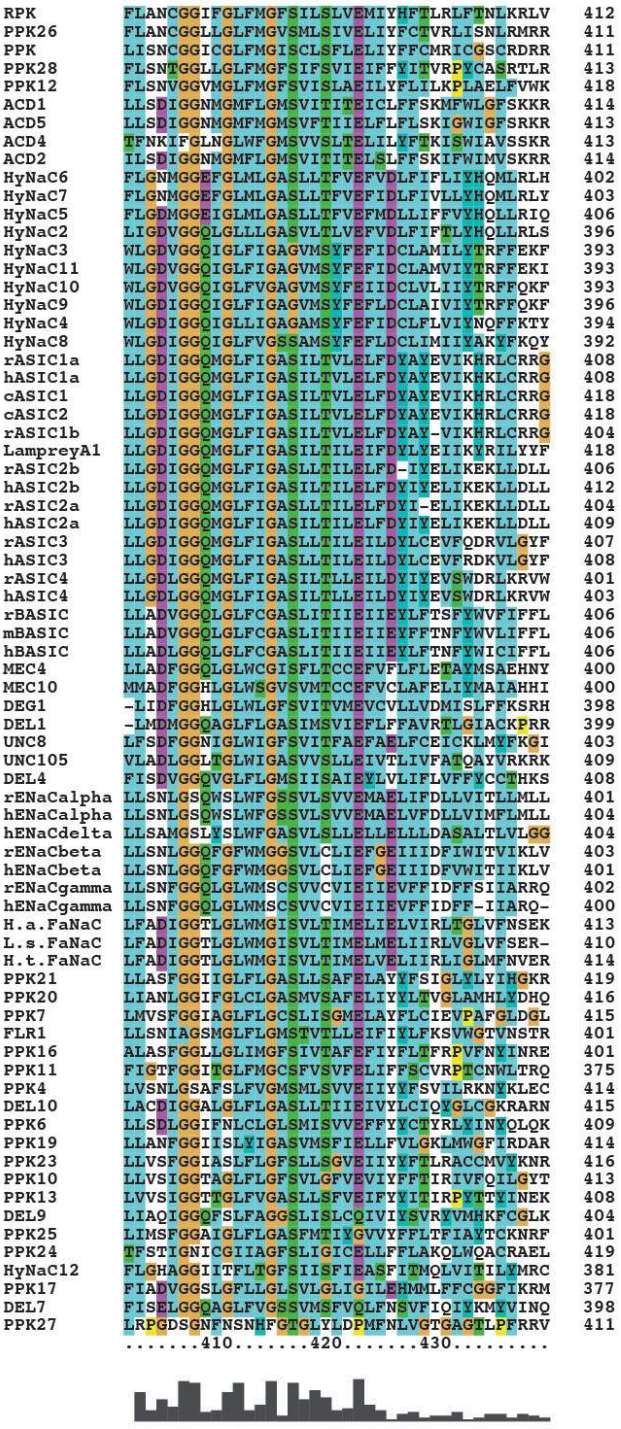

Alignment DEG/ENaC ion channel family, part 6.

A.3. Apparent affinities for diminazene, Hydra-RFamides I and II of HyNaCs

	EC_{50} **RF I** ± **SEM** [μM]	**Hill coeff.** ± **SEM**	**n**	EC_{50} **RF II** ± **SEM** [μM]	**Hill coeff.** ± **SEM**	**n**
HyNaC2/3/5	3.48 ± 0.55	1.2 ± 0.1	9	1.61 ± 0.27	0.9 ± 0.1	14
HyNaC2/11/5	13.8 ± 1.9	0.9 ± 0.1	12	0.95 ± 0.16	1.1 ± 0.2	7
HyNaC2/3/6	0.29 ± 0.06	1.2 ± 0.2	10	0.29 ± 0.04	1.0 ± 0.1	8
HyNaC2/4/6	0.70 ± 0.08	1.3 ± 0.1	12	1.05 ± 0.11	1.2 ± 0.1	10
HyNaC2/3/7	0.19 ± 0.04	1.6 ± 0.4	14	0.15 ± 0.02	2.2 ± 0.6	8
HyNaC2/9/7	0.04 ± 0.01	1.5 ± 0.3	9	0.04 ± 0.01	1.4 ± 0.1	8
HyNaC2/10/7	≥ 30	n.d.	12	≥ 30	n.d.	7

Table A.2.: **HyNaC apparent ligand affinities for Hydra-RFamides I and II.** EC_{50} values for Hydra-RFamides I (RF I) and II (RF II) were calculated with Igor Pro, version 6 Wavemetrics, from data as shown in figure 3.8 and 3.9. Mean EC_{50} values as well as Hill coefficients for different HyNaC heterotrimers are indicated ± standard error of the mean (SEM). n = number of experiments.

	IC_{50} **Dimi.** ± **SEM** [μM]	**Hill coeff.** ± **SEM**	$I/I_{100\mu M\,Amil.}$ ± **SEM**	**n**
HyNaC2/3/5	0.45 ± 0.09	0.70 ± 0.09	0.5 ± 0.1	10
HyNaC2/11/5	31.4 ± 9.4	0.91 ± 0.28	0.7 ± 0.1	8
HyNaC2/3/6	0.09 ± 0.02	0.30 ± 0.02	0.3 ± 0.1	9
HyNaC2/4/6	0.05 ± 0.02	0.57 ± 0.03	0.3 ± 0.1	9
HyNaC2/3/7	0.16 ± 0.08	0.18 ± 0.06	0.3 ± 0.1	7
HyNaC2/9/7	1.70 ± 0.58	1.54 ± 0.78	0.3 ± 0.1	9
HyNaC2/10/7	5.40 ± 1.45	1.12 ± 0.06	0.8 ± 0.1	6

Table A.3.: **Diminazene inhibits HyNaC currents with high affinity.** *Xenopus* oocytes expressing HyNaCs were activated at EC_{50} values for Hydra-RFamide I and blocked by diminazene in increasing concentrations. 100 μM amiloride was added to compare the different inhibitor affinities. Mean IC_{50} values for different HyNaC heterotrimers are indicated ± SEM. n = number of experiments.

A.4. PCR protocols used in this work

first PCR		**second PCR**	
DNA (5, 10 or 20 ng)	x μl	amplicon 1 (50 - 200 ng)	x μl
		amplicon 2 (50 - 200 ng)	x μl
dNTP (10 mM each)	1 μl	dNTP (10 mM each)	1 μl
forward primer (125 ng)	1,5 μl	5' primer (125 ng)	1,5 μl
reverse primer (125 ng)	1,5 μl	3' primer (125 ng)	1,5 μl
5x Buffer KAPA HiFi	10 μl	5x Buffer KAPA HiFi	10 μl
KAPA HiFi	0,5 μl	KAPA HiFi	0,5 μl
H_2O	to 50 μl	H_2O	to 50 μl

first PCR

Step	Temp.	Time	number of cycles
Initial denaturation	98 °C	60 - 90 sec	1
Denaturation	98 °C	15 - 30 sec	
Annealing	55 - 65 °C	30 sec	35
Elongation	72 °C	0,5 - 1 min/kb	
End	4 °C	pause	

second PCR

Step	Temp.	Time	number of cycles
Initial denaturation	98 °C	60 - 90 sec	1
Denaturation	98 °C	15 - 30 sec	
Annealing	45 °C	45 sec	35
Elongation	72 °C	0,5 - 1 min/kb	
End	4 °C	pause	

Table A.4.: **PCR protocol for recombinant PCR**

Pipette Scheme

cDNA	2.5 μl
dNTP (10 mM each)	1 μl
5' primer (125 ng)	1.5 μl
3' primer (125 ng)	1.5 μl
5x Taq Buffer	20 μl
Taq DNA Polymerase	0.5 μl
H_2O	to 100 μl

PCR protocol

Step	Temp.	Time	number of cycles
Initial denaturation	95 °C	60 - 90 sec	1
Denaturation	95 °C	30 sec	
Annealing	70 °C	30 sec	5
Elongation	70 °C	0.5 min/kb	
Denaturation	95 °C	30 sec	
Annealing	65 °C	30 sec	5
Elongation	72 °C	0.5 min/kb	
Denaturation	95 °C	30 sec	
Annealing	60 °C	30 sec	30
Elongation	72 °C	0.5 min/kb	
End	4 °C	pause	

Table A.5.: **PCR Protocol for RACE PCR (touchdown PCR).**

A.5. Oligonucleotides, DNA vectors and restriction/cloning sites

Product	**Vector**	**Cloning site**	**linearized by**
HyNaC2	pRSSP6009	SacI, BstEII	MluI
HyNaC3	pRSSP6009	BamHI, KpnI	MluI
HyNaC4	pRSSP6009	SacI, KpnI	MluI
HyNaC5	pRSSP6009	SacI, KpnI	MluI
HyNaC6	pRSSP6009	SacI, KpnI	EcoRI
HyNaC7	pRSSP6009	BamHI	MluI
HyNaC8	pRSSP6009	BamHI	MluI
HyNaC9	pRSSP6009	BamHI, BstEII	MluI
HyNaC10	pRSSP6009	BamHI, BstEII	MluI
HyNaC11	pRSSP6009	BamHI, BstEII	MluI
HyNaC12	pRSSP6009	BamHI, BstEII	MluI
Primers flanking MCS of vector pRSSP6009			
PSP3	TATGTAGCTTAGAGACTC		
SP6	GATTTAGGTGACACTATAG		

Table A.6.: **Cloning vectors, restriction sites and sequencing primers.**

RACE PCR primers for cloning new HyNaCs	
HyNaC11GSP2	GCTGCATTTGCCTATGCGATGCAAAAAG
HyNaC11GSP1	CCCAGGTGGAACTGTTAAACCACTC
HyNaC11GSP1 2.0	CTTTTTGCATCGCATAGGCAAATGCAGC
HyNaC11GSP1 3.0	CGACTGCATCATCAACAATTGTACCATTC
HyNaC12GSP2	GAATTATACGAAAAATCTCCTACGTTCCC
HyNaC12GSP1	GAAGTTTTGAGTATACTTTGTTATCAAGGG
HyNaC12GSP1 2.0	CTGGGAACGTAGGAGATTTTTCGTATAATTC
Primers for full length amplification of new HyNaCs	
HyNaC9 fw	ATGTCTGAAGAAGATGAGAAAAAGATTAAAAG
HyNaC9 re	TCATGAGGAAGTAAACTTCTGAAAAAACC
HyNaC10 fw	ATGGCAAAAGTTGAAGACAAAATCAAAAG
HyNaC10 re	TTATAAAGAGTGATTTCTTATAGAATTTATCG
HyNaC11 fw	ATGCTCAACTTTAAAGATATAGCACAAATTAC
HyNaC11 re	TCATACAGTTGTAGGATTTTTTAAACTAATTTTTTC
HyNaC12 fw	GAGCTCATGGATTACCTAAATCTTTTAGAAAGAATCCG
HyNaC12 re	GGTACCTTAAACTTCTAACGAGGCTTGACAAGTAAC
Primers for DEG mutations of HyNaCs.	
HyNaC2DEGR fw	GATTTTTACAAGCTTATTCGAGATGTCGGAGGTC
HyNaC2DEGR re	GACCTCCGACATCTCGAATAAGCTTGTAAAAATC
HyNaC3DEGR fw	CATTGGTGTGGCTACGAGATGTTGGTGGTC
HyNaC3DEGR re	GACCACCAACATCTCGTAGCCACACCAATG
HyNaC5DEGR fw	CGATTTTTATCAGTTTCTTCGAGATATGGGAGGTG
HyNaC5DEGR re	CACCTCCCATATCTCGAAGAAACTGATAAAAATCG
HyNaC12G436T fw	GGCGGAGTTTTTAACTCACGCTGGTGG
HyNaC12G436T re	CCACCAGCGTGAGTTAAAAACTCCGCC
Primers for several point mutations of HyNaC 5 and 7	
Hy5D437N fw	TTTATCAGTTTCTTGGTAATATGGGAGGTGAAATTG
Hy5D437N re	CAATTTCACCTCCCATATTACCAAGAAACTGATAAA
Hy5I442F fw	GATATGGGAGGTGAATTTGGTCTTATGTTAGGTG
Hy5I442F re	CACCTAACATAAGACCAAATTCACCTCCCATATC
Hy5M457I fw	GCTTACGTTTGTCGAATTTATCGACTTGCTTA TTTTTTTTGTG
Hy5M457I re	CACAAAAAAAATAAGCAAGTCGATAAATTCGA CAAACGTAAGC
Hy7F448I fw	GTAACATGGGTGGTGAGATTGGATTGATGTTGGGTG
Hy7F448I re	CACCCAACATCAATCCAATCTCACCACCCATGTTAC
Hy7I463M fw	GCTAACTTTTGTGGAGTTTATGGATTTATTTATTGTGTTGC
Hy7I463M re	GCAACACAATAAATAAATCCATAAACTCCACAAAAGTTAGC

Table A.7.: **List of oligonucleotides used in this work.**

A.6. *Curriculum Vitae*

Marc Christopher Assmann

Eynattener Straße 56-58
52064 Aachen

Tel.: +49 (0) 176 99638590
marcassmann@unitybox.de

Akademischer Werdegang

seit 10/10	**Promotion (Dr. rer. nat.)** Institut für Physiologie, Universitätsklinikum RWTH Aachen University Arbeitsgruppe von Herrn Prof. Dr. Stefan Gründer
09/2010	**Master of Science Biologie (Note 1,4)** Justus-Liebig-Universität Gießen
10/2008 - 09/2010	**Aufbaustudium der Biologie** Justus-Liebig-Universität Gießen *Schwerpunkte: Genetik, Tierphysiologie, Immunologie*
08/2008	**Bachelor of Science Biologie (Note 2,0)** Justus-Liebig-Universität Gießen
10/2005 - 08/2008	**Studium der Biologie** Justus-Liebig-Universität Gießen *Schwerpunkte: Genetik, Tierphysiologie, Ökologie*

Schulische Ausbildung

04/2004	**Abitur (Note 2,2)**

Wehrdienst

10/2004 - 06/2005	**Grundwehrdienst** 3.ArtAufklBtl/131 Stadtallendorf

Veröffentlichungen

D. Wiemuth, **M. Assmann**, S. Gründer. The bile acid-sensitive ion channel (BASIC), the neglected cousin of ASICs and ENaC. *Channels*, 2013.

M. Assmann, S. Dürrnagel, A. Kuhn, T.W. Holstein and S. Gründer. The comprehensive analysis of DEG/ENaCs in *Hydra* reveals a large variety of peptide-gated channels, potentially involved in neuromuscular transmission. *In Vorbereitung.*

Vorträge

M. Assmann, S. Dürrnagel, A. Kuhn, T.W. Holstein, S. Gründer. Cloning and functional characterization of seven novel members of the peptide-gated Sodium Channel family (HyNaC) from *Hydra magnipapillata*. *Physiologisches Kolloqium*, Institut für Physiologie, RWTH Aachen University, 2013.

M. Assmann, M. Fronius, W. Clauss. Effect of shear stress on DEG/ENaC ion channel family members. *Master Seminar*, Institut für Tierphysiologie, Justus Liebig Universität Gießen, 2010.

Posterpräsentationen

M. Assmann, S. Dürrnagel, S. Kuhn, T. W. Holstein und S. Gründer. S. Gründer. The peptide gated Na^+ channel from the freshwater polyp *Hydra* - Insights into ancient ion channel characteristics. *Evolution of the First Nervous Systems II*, St. Augustine, Florida, USA, 2014.

M. Assmann, S. Dürrnagel, A. Kuhn, M. Schultz, TW. Holstein und S. Gründer. The second transmembrane domain and adjacent amino acids determine the apparent ligand affinity of a peptide-gated *Hydra* Na^+ Channel. *BPS Annual meeting of the Biophysical Society*, San Francisco, Kalifornien, USA, 2014.

M. Assmann, S. Dürrnagel, A. Kuhn, M. Schultz, TW. Holstein und S. Gründer. Three new subunits expand our understanding of the function and biophysical properties of the peptide-gated *Hydra* Sodium Channel (HyNaC). *FENS Forum for Neuroscience*, Barcelona, 2012.

Aachen, den Marc Christopher Assmann